ÅBO AKADEMI UNIVERSITY
FACULTY OF SCIENCE AND ENGINEERING

Characterization of different tannins for possible industrial resin production

Master's thesis
by
Shujun Liang

10.06.2022

Carried out at the Laboratory of Natural Materials Technology at Åbo Akademi University under the supervision of Docent Andrey Pranovich, Professor Chunlin Xu, Docent Anna Sundberg, and MSc Luyao Wang at Åbo Akademi University.

Abstract

Shujun, Liang	Characterization of different tannins for possible industrial resin production.
Master's thesis	Laboratory of Natural Materials Technology, Faculty of Science and Engineering, Åbo Akademi University 2022, 61 pages, 35 figures, 16 tables
Supervisors	Docent Andrey Pranovich, Professor Chunlin Xu, Docent Anna Sundberg at Åbo Akademi University Suvi Pietarinen, Heidi Suomela-Uotila, Sanna Valkonen at UPM-Kymmene Oyj
Keywords	Tannins, extract, SEM-EDS, TGA, DSC, ASE, GPC, acid hydrolysis, methanolysis, GC, GC-MS, pyrolysis GC-MS, NMR.

Tannins are the fourth most abundant component in plant material after cellulose, hemicellulose, and lignin, and have received extensive attention due to their high content of phenolic and carboxyl groups. The earliest use of tannins can be traced back to the Neolithic Age for leather making. Although many researchers have tried to describe tannins in detail, the properties obtained from different sources by different analytical methods vary greatly. In order to tailor the commercial use of tannins, it is very important to characterize tannin samples before commercial applications.

In this thesis, six kinds of tannins were extensively characterized with various methods to explore the differences between different industrial processed tannins, and their feasibility as a substitute for petroleum-derivative phenol in the production of resins.

First, the physical properties of the tannins were determined, including pH, moisture content, ash content and elemental analysis. The elemental analysis was performed on crude tannins and tannin ash using SEM-EDS. In this thesis, DSC and TGA characterization of crude tannins were performed to provide thermogravimetric information. In addition, GPC and FT-IR methods were used to determine the molar mass and functional groups of tannins, respectively.

Secondly, in order to investigate the composition of tannins in addition to moisture and ash content, ASE with six solvents of increasing polarity was used to sequentially extract the crude tannins, and the extracts were analyzed by SEC-MALS. Acid hydrolysis and methanolysis combined with GC analysis techniques were used to determine the composition of cellulose and non-cellulosic polysaccharides in crude tannins and short column GC combined with GC-MS was used for qualitative and quantitative analysis of the extracts.

Finally, pyrolysis-GC MS and different NMR analysis techniques including ^{13}C, HSQC and ^{31}P NMR were used to determine the structure of the tannin molecules.

The results show that the different methods described above can effectively characterize the obtained tannin samples and provide information for their possible industrial application.

Acknowledgment

Firstly, I would like to express my gratitude to UPM-Kymmene Oyj and Chunlin Xu for their trust in giving me this precious opportunity to participate in and complete this project. Most importantly, I discovered my passion for research in this project. Although there are many challenges along the way, the happiness of overcoming them always motivates me to keep going.

I would also like to thank all my supervisors for giving me advice and comments during these eight months, including Andrey Pranovich, Chunlin Xu, Anna Sundberg from Åbo Akademi University, and Suvi Pietarinen, Heidi Suomela-Uotila, and Sanna Valkonen from UPM-Kymmene Oyj. A special thank you to Andrey. The successful completion of this project is inseparable from his patient guidance to me, whether from lab work or result discussion. Also, I would like to thank my colleagues at the Laboratory of Natural Materials Technology. Luyao Wang, Jarl Hemming, Rui Liu, and Jiayun Xu shared their experiences in analyzing data and gave me many useful suggestions.

Finally, I would like to express my deep gratitude to my parents, who have supported me financially and spiritually during the years of study and encouraged me to continue my studies all the time.

Turku, 10.06.2022

Shujun Liang

Abbreviations

ASE	Accelerated Solvent Extraction
BSTFA	N, O-bis-(trimethylsilyl)trifluoroacetamide
Cl-TMDP	2-Chloro-4,4,5,5-tetramethyl-1,3,2-dioxaphospholane
CoTs	Complex tannins
CTs	Condensed tannins
Đ	Dispersity
DMSO	Dimethyl sulfoxide
DSC	Dissolved solid content
EI	Electron ionization
FTIR	Fourier Transform Infrared spectroscopy
GC	Gas chromatography
GC/MS	Gas Chromatography–Mass Spectrometry
GPC	Gel Permeation Chromatography
HHDP	Hexahydroxydiphenoyl
HPSEC	High-Pressure Size Exclusion chromatography
HTs	Hydrolysable tannins
IEA	International Energy Agency
MDR	Maximum degradation rate
Mn	Number average molar mass
Mw	Weight average molar mass
Mw/Mn	Polydispersity index
NMR	Nuclear magnetic resonance
PGG	Pentagalloyl glucose
Py-GC/MS	Pyrolysis–Gas Chromatography-Mass Spectrometry
SE	Steryl esters
SEM/EDS	Scanning Electron Microscopy with Energy Dispersive Spectroscopy
SEC/MALS	Multi-angle light scattering coupled with size exclusion chromatogra
SN_2	Bimolecular nucleophilic substitution reaction
Td	Decomposition temperature
TDR	The temperature in the maximum degradation rate
Tg	Glass transition temperature
TGA	Thermogravimetric
THF	Tetrahydrofuran
TMCS	Trimethylchlorosilane

Contents

1. Introduction

The occurrence of petroleum improves life and industry greatly. Petroleum and petroleum-derived products are found everywhere. However, more effortless living and faster economic development mean more petroleum consumption. According to International Energy Agency (IEA), during those years that the economy is developing typically without the impact of COVID 19 (1971-2019), the global petroleum consumption shows a rising trend in general (IEA, 2021). In addition, the uncertainty of the actual reserves of petroleum, the severe environmental pollution, and the national defense-security problem caused by over-reliance on fossil energy have sounded the alarm for us (Speirs et al., 2015; CNA, 2009; Pagani et al., 2009). As an important renewable material, biomass has received much attention and has been extensively studied in many fields (Jansone et al., 2017). Refining renewable, abundant biomass is a crucial step in moving from petroleum-based to bio-based products. Phenolic resins are representative of petroleum-based products, and the search for substitutes for raw materials is continuing. Tannins, as one of the rich phenol-containing raw materials, have been proved to have development potential in the manufacture of phenolic resins (Sarika et al., 2020).

Tannins are the fourth most significant source of compounds after cellulose, hemicelluloses, and lignin, present in all plants cells and containing carboxyl groups and many phenolic groups (Liao et al., 2019). The rich phenolic structure and chemical reaction's characteristics have laid a good foundation for the extensive utilization of tannins. Humans have a long history of using tannins, with the oldest leather applications dating back to the end of the Neolithic periods (Falcão and Araújo, 2018). Then, with the improvement of people's awareness of environmental protection and living standards, the natural product tannins to replace the petroleum product phenol in phenolic resin has also received extensive attention. Compared with traditional phenolic resins, using the widely sourced, abundant and biodegradable tannins can reduce harmful substances produced during production and use, which means it is beneficial to the environment and also the human health. An example of a successful tannin resin production was in South Africa at the end of the 20th century (Zhou and Du, 2019). Today, the utilization and optimization of tannins in the resin industry is continuing, the search for more suitable and economical types of tannins is ongoing.

In this thesis, six tannins samples were extensively characterized with various methods, aiming to explore the possibility of their possible resin production.

2. Theory

In the theory part, tannins and applications of tannins will be introduced. In the introduction section, the source, classification, structure, acquisition methods and utilization statutes of tannins will be described. In the application part, the use of tannins in resin manufacturing, and potential areas such as medicine and food fields, other applications such as adsorbents and tanning are discussed.

2.1 Introduction of tannins

2.1.1 Sources of tannins in nature

Tannins are the fourth most abundant component in the plant world after cellulose, hemicelluloses and lignin (Liao et al., 2019). It is the most abundant secondary metabolite in plants, with a biosynthetic potential of over 160,000 tons/year (Martins et al., 2011; Arbenz and Avérous, 2015). In addition to the abundant reserves, tannins are widely distributed in the plant kingdom. Tannins are present in all vascular plants, especially in gymnosperms, angiosperms and even in some sea plants (Mole, 1993; Cuong et al., 2019) Tannins are found in roots, stems, leaves, bark, fruits and seeds (Das et al., 2020a). However, the tannin content of different parts varies considerably; in some soft tissues, such as leaves, the content of tannins can reach up to 25% of dry weight and thus exceed the content of lignin (Hernes and Hedges, 2004).

Tannins in plants mainly play a defensive role and function primarily to resist predators such as mammals and herbivores; parasitic organisms such as fungi and harmful pathogens and competitors such as plants that grow in the same area. In addition, they are also involved in the composition of plant cell structures, such as cell walls, and play an essential role in the formation of fertilized eggs in some marine organisms (McInnes et al., 1984; Maria Furlan et al., 2010).

2.1.2 Classification and structure of tannins

Tannins are phenolic compounds with high molar mass, ranging from 500 to 20 000 Daltons (Krzyzowska et al., 2017). There are many ways to classify tannins, but the two most widely known are structure-based classification and plant morphology-based classification. According to the difference in structure characteristic, tannins can be divided mainly into hydrolysable tannins (HTs), condensed tannins (CTs), and complex tannins (CoTs) that contain the structural characteristics of both HTs and CTs, seen in ***Figure 1***. Hydrolysable tannins can further be subdivided into gallotannins and ellagitannins.

As for morphology-based classification, tannins are divided into terrestrial and sea plant tannins. Terrestrial tannins include all the HTs, CTs, CoTs mentioned before; sea plant tannins exist as oligomers or polymers of phloroglucinol, also named phlorotannins (PTs) (Cuong et al., 2019), seen in ***Figure 2***. Some typical examples of different types of tannin are also shown in ***Figure 2***, more detailed information of them will be introduced in later in this thesis.

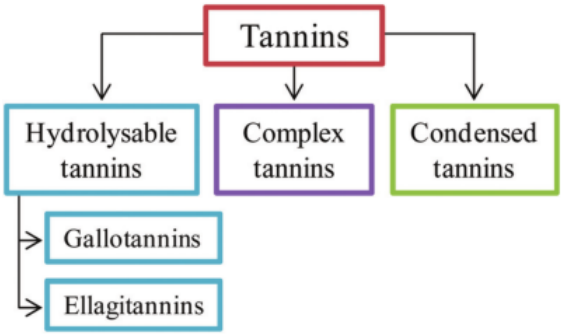

Figure 1: *Classification of tannins based on structure difference (Adapted from* Arbenz and Avérous, 2015).

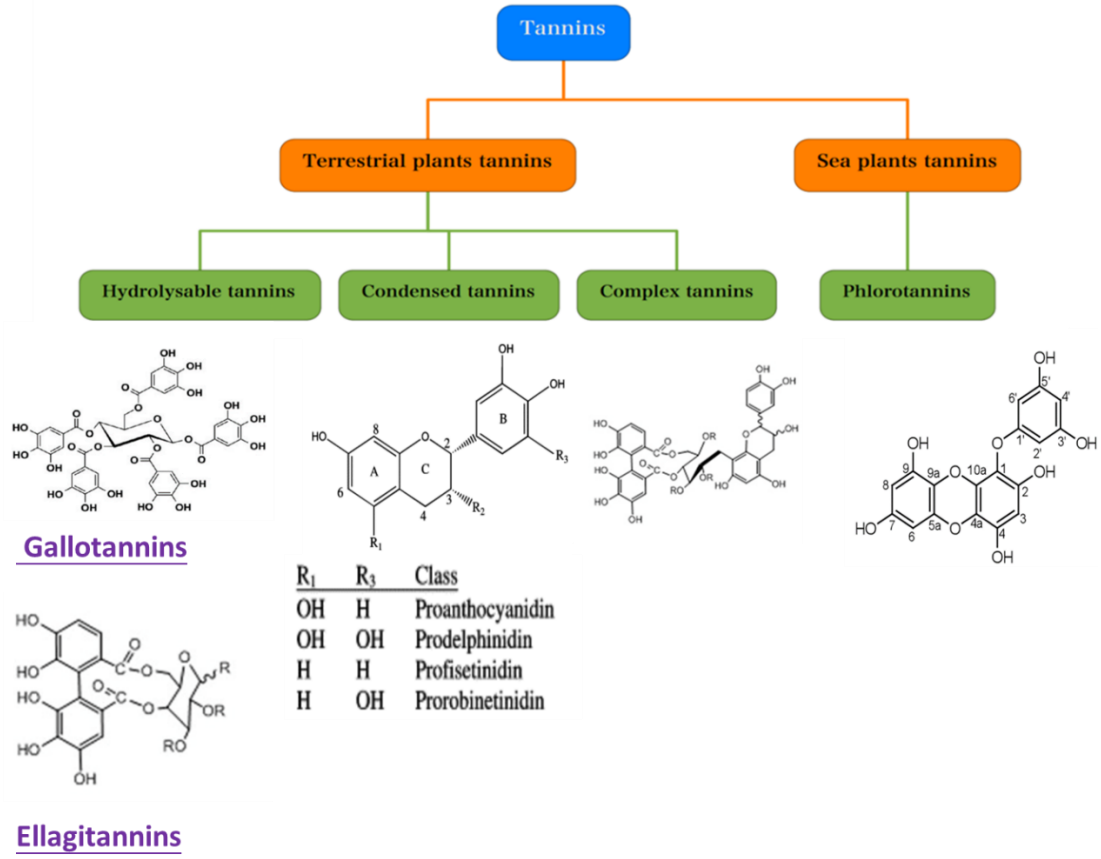

Figure 2: *Classification of tannins based on plant morphology and structure characteristics. (Modified from* Aguilar et al., 2007; Fraga-Corral, Otero, Cassani, et al., 2021).

Hydrolysable tannins (HTs)

HTs are polyphenolic compounds that can be hydrolyzed into corresponding phenolic acids and polyols under acidic, alkaline, or enzymatic conditions (Shahat and Marzouk, 2013). In other words, HTs are complex molecules formed by a sugar core (mainly D-glucose) or polyols combined with gallic acids (3,4,5-trihydroxybenzoic acid) or ellagic acids (hexahydroxydiphenic acid) units (Okuda et al., 1990). Ellagic acids are formed by polymerizing the C-C bond of the gallic acids, which means ellagic acids are the dimeric derivative of gallic acids (Malinda et al., 2017). The structure of gallic acids and ellagic acids are shown in ***Figure 3***.

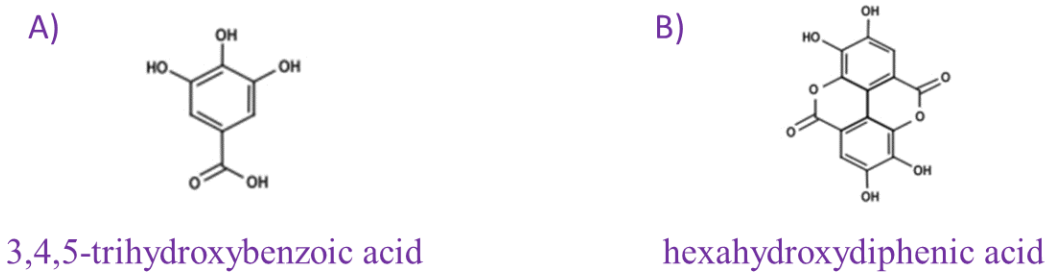

Figure 3: *Structure of gallic acid (A) and ellagic acids (B).*

Gallotannins are one of subclassifications of HTs; they can be obtained by partially or fully substituting the hydroxyl groups (-OH) in D-glucose. The most common one is named pentagalloyl glucose (PGG) formed by gallic acids replacing the -OH bond in the 1,2,3,4,6 position in D-glucose. It is worth noticing that PGG is not only a type of gallotannins and an important precursor of other complex gallotannins (Mueller-Harvey, 2001), but also an essential synthetic precursor of complex ellagitannins (seen in ***Figure 4***). In addition, gallic acids in gallotannins are connected by the depside bond, as shown in ***Figure 5***. The esterification of these aromatic hydroxyl groups to form the condensation bonds is an important structural feature that distinguishes gallotannins from ellagitannins (Smeriglio et al., 2017).

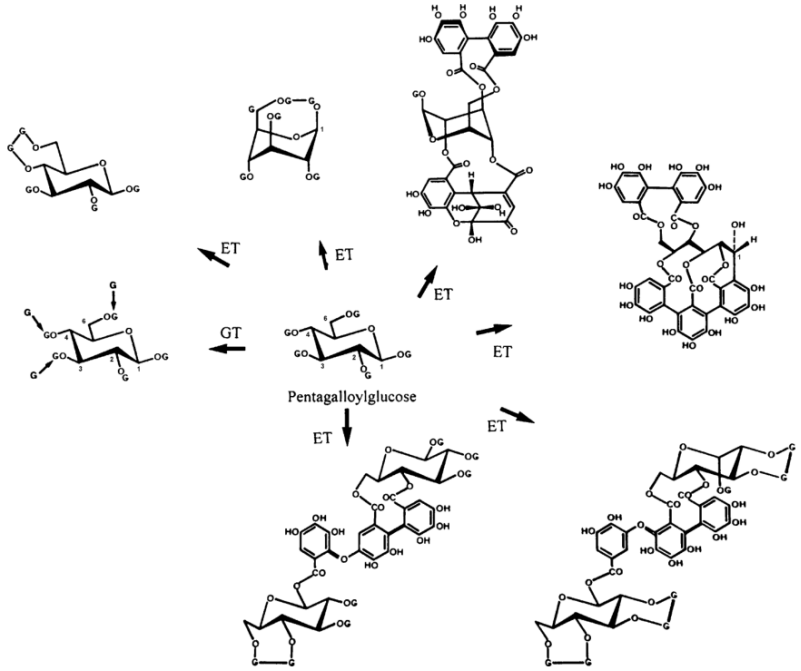

Figure 4: *Examples of complex gallotannin and ellagitannin with pentagalloyl glucose as precursor, where G=gallic acids, GT=gallotannin, ET= ellagitannin. (Adapted from* Mueller-Harvey, 2001).

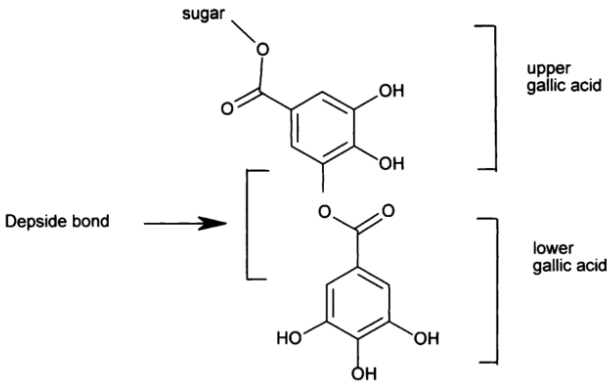

Figure 5: *Examples of depside bond between two gallic acids. (Adapted from* Mueller-Harvey, 2001).

Compared to gallotannins, ellagitannins are more dominant in the market because of their availability. Almost 1000 different forms of ETs (monomeric-, dimeric, oligomeric-, C-glycosidic-molecules) have been isolated and identified, while GTs are barely found in the plant kingdom (Smeriglio et al., 2017; Yamada et al., 2018). However, for some historical reasons, some ellagitannins in which the polyphenolic hydroxyl group is further coupled to a polyol are also classified as hydrolysable tannins, even though they cannot be hydrolyzed (Khanbabaee and van Ree, 2001). Ellagitannins contain one or more hexahydroxydiphenoyl

(HHDP) or HDDP ester, the galloyl units of HHDP through oxidizing C-C bonds instead of depside bonds (Yamada et al., 2017).

Figure 6 shows the relationship between HHDP and ellagic acid. The HHDP groups usually have axial chirality characteristics, the residues of them with glucose moieties can have different linkages and are prone to form dimer derivatives, which are the reasons that make ellagitannins in board structure diversity and more isomers can be formed (Niemetz and Gross, 2005).

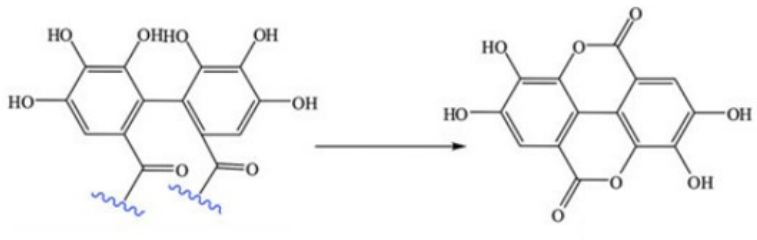

Figure 6: *HHDP derivatives lactonize into ellagic acid spontaneously in aqueous solution. (Adapted from Smeriglio et al., 2017).*

Based on the discussion above, important features to distinguish gallotannins and ellagitannins are:

- ✓ Hydrolyzates: under hydrolysis conditions, gallotannins are hydrolysed into gallic acids, while ellagitannins form ellagic acids.
- ✓ Bond connection: the galloyl units of gallotannins are connected through depside bond, while ellagitannins have an oxidative C-C bond.
- ✓ Hydrolyzation-resistant: gallotannins are easier to hydrolyze because they do not have an additional C-C bonds of polyphenol residues with glucose moieties

Condensed tannins (CTs)

CTs also named proanthocyanidins, are a natural phenolic compound, second only to lignin and the most abundant flavonoid in nature. They can easily yield anthocyanidins under oxidative cleavage conditions (Niemetz and Gross, 2005). With more than 4000 compounds having been identified, CTs are undoubtedly the most promising among the four types of tannins and account for 90% of approximately 200,000 tons of commercial tannins produced each year (Kemppainen et al. 2014; Das et al., 2020b).

Unlike HTs, CTs do not contain sugar residues in their structure and have stronger resistance to hydrolysis (Ismayati et al., 2017a). They are composed of oligomers or polymers of flavonoid units containing two phenolic rings (A-ring and B-ring) and one pyran ring (C-ring)

(seen in ***Figure 7***). The precursor flavonoids of CTs are flavan-3-ol, repeated ranging from 2 to 50 subunits (Shahidi and Ho, 2005; Soldado et al., 2021). The basic structure of CTs is monoflavonoids, and the different combinations between A-ring (resorcinol or phloroglucinol type) and B-ring (catechol or pyrogallol type) make the monoflavonoids building blocks of CTs diverse (Seen in ***Figure 7***). In other words, the different substitution possibilities of the hydroxyl groups at the C5 and C5' position allow the CTs to form different blocks named profisetidin, procyanidin prorobinetinidin, and prodelphinidin. In some cases, the B-ring may also be a phenol, such as one of the representatives of *Pine* tannins (Zhou and Du, 2019).

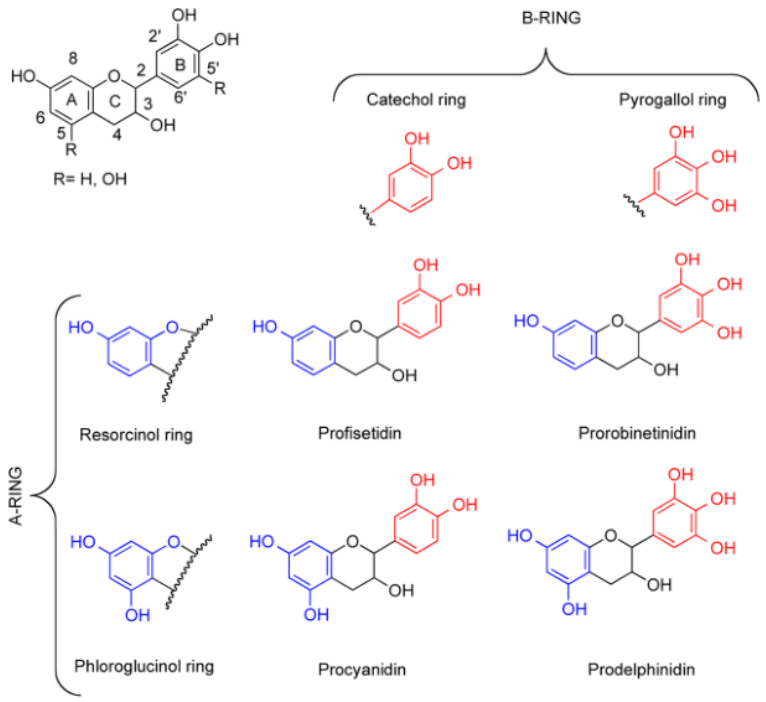

Figure 7: *Structure of monoflavonoids and different building blocks of CTs. (Adapted from* Crestini et al., 2016).

Procyanidins, mainly from Mimosa, are the most abundant of CTs in vegetables, while prodelphinidins are the least abundant among these four types (Smeriglio et al., 2017). Not only are they different in number of hydroxyl groups in the B-ring, but also the stereochemical structure in the C3 position of C-rings. For procyanidins, the subunits are catechin and epicatechin, and gallocatechin and epigallocatechin are subunits of prodelphindins (seen in ***Figure 8***). The -OH at C3 position of catechin and epicatechin differ only in stereochemistry, while gallocatechin and epigallocatechin also differ in spatial orientation. In addition, the C2 in C-rings of catechin and gallocatechin shows the trans structure, whereas epicatechin and epigallocatechin have cis structure (Soldado et al., 2021). Those structure features have a significant influence on the chemical properties of CTs.

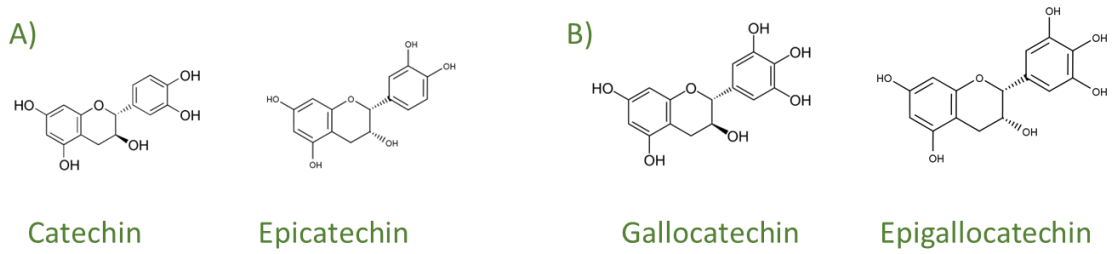

Figure 8: *Subunits of procyanidins (A) and prodelphindins (B).*

The linkage between monoflavonoids is another important feature of CTs; thus, it is also another common way of classification. Proanthocyanidins can be classified into either A-type CTs or B-type CTs depending on their linkage. The interflavan bonds of B-type CTs are C4 in the upper unit connecting to C6 or C8 in the lower unit, while A-type CTs are further bounded with either C2-O-C5 or C2-O-C7 (Girard et al., 2020). ***Figure 9*** shows the examples of A-type CTs with different interflavan bonds. Furthermore, the B-type CTs are more common and the C4-C6 linkage is prevalent in tannins mainly containing resorcinol A-ring (profisetidin and prorobinetinidin), while C4-C8 linkage is prevalent in tannins mainly containing phloroglucinol A-ring (procyanidin and prodelphinidin) (Arbenz and Avérous, 2015). In other words, the linkage of tannin molecules is influenced by the type of A-ring.

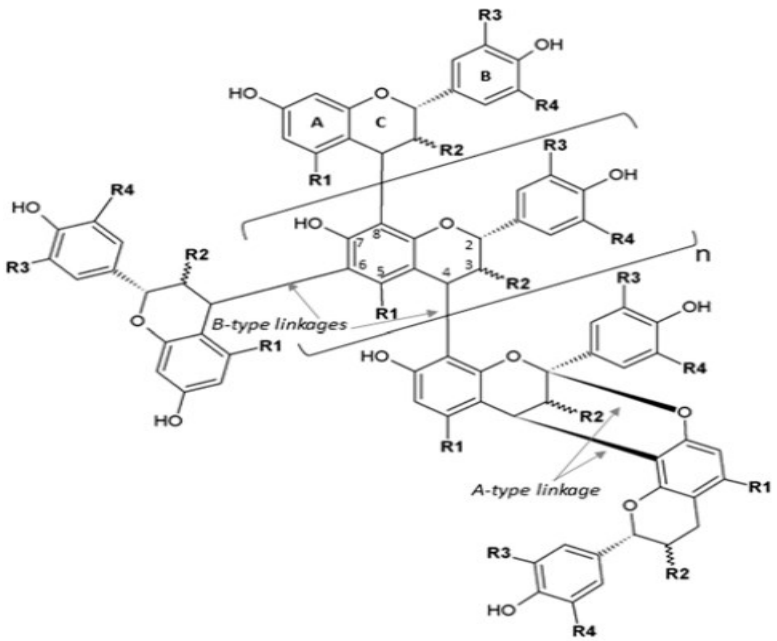

Figure 9: *The interflavan bonds of A-type CTs. R_1, R_2, R_3, R_4 represent -OH or -H (Adapted from* Girard and Bee, 2020).

Finally, from the above introduction, significant structural differences between the HTs and CTs have been shown. Most plants contain either HTs (gallotannins, ellagitannins or a mixture of them) or CTs. However, some species such as *Fagaceae, Acacia pravissima,* can have both HTs and CTs (Mueller-Harvey, 2001).

Complex tannins (CoTs) and phlorotannins (PTs)

CoTs and PTs will be introduced only briefly, because they are not explored further in this thesis and have fewer industrial applications so far. CoTs are high-molar-mass tannins, because their flavan-3-ols (catechin units) bond with gallotannins or ellagitannins through a C-C bond. It is very difficult to identify their chemical structure, thus, only a few CoTs have been found until now. Typical examples of CoTs are *acutissimins A* and *B* from *Castanea* and *Quercus* (Okuda and Ito, 2011).

PTs are different from the tannins of terrestrial plants. They are widely found in marine brown algae, which can account for ~30% of the dry weight of the algae. Phloroglucinol (PG) is the basic structure of PTs, condensed from acetic and malonic acids with special enzyme in marine plants. Based on the connection bond between PG units and the way they connect with -OH groups, PTs can be subdivided into four groups: Fuhalols and phlorethols (ether bonds); Fucols (phenyl bonds); Fucophlorethols (ether and phenyl bonds); Ekols and Carmalols (Dibenzo-p-dioxin links). The molar mass of PTs is in the range from 126 to 65 000 Da. The more PG units, the higher molar mass and the more complex PTs (Rahman et al., 2014; Arbenz and Avérous, 2015; Fraga-Corral, Otero, Echave, et al., 2021).

In recent years, the antioxidative, antibacterial, and anti-HIV properties of PTs have attracted widespread attention, especially in the medical field. However, due to the uncertainty of the function mechanism, research is still in an initial stage. What is more, high cost in harvest, shorter storage time because of the strong respiration of algae and high salinity of sea water, also make it difficult to be selected by the market (Gupta and Abu-Ghannam, 2011).

2.1.3 Extraction of tannins

Tannins are widespread in the plant kingdom and can be found in different plants such as fruit, bark, roots, and leaves. However, to obtain commercial tannins for industry application, tannins are usually extracted from bark, especially bark residues from paper mills or sawmills, and heartwood with different solvents. Compared to the traditional treatment (wastes, horticulture uses, heat power generation), it is undoubtedly more attractive to use the tannins in industrial application, since the theoretical annual production of bark in Europe alone reaches 25 million cubic meters(Feng et al., 2013). The sources of commercial CTs vary by region. In America tropical species such as *Quebracho*, *Black wattle*, *Mimosa*, or *Mangrove* are preferred, while

softwoods such as *Pine* and *Spruce* are popular in central and northern Europe (Bianchi et al., 2015; Das et al., 2019). Commercial HTs are mainly from the heartwood of *Oak* galls and *Chestnut* (Benaiges and Guillén, 2007; CHEBI).

The extraction procedure of tannins is relatively simple. Tannins can be extracted from ground or chipped wet/dry/frozen plant materials, by water or by other solvents at different temperatures. However, tannins are complex phenolic substances, which means they have a high risk of reacting with other components from harvesting to extraction. Therefore, efficient preservation and extraction methods are essential to obtain tannins of high quality. The freeze-dried method is so far one of the best ways to keep the phenolic substances at a high level and preserve the natural structure (Ferreira et al., 2004). Hot water is one of the most popular solvents for traditional extraction in industry. Moreover, acetone, ethanol, ethyl acetate and other organic solvents have been studied, and these can also be added to water to improve the extraction efficiency. Acids or enzymes as additives have also been studied in the production of tannins, but with low efficiency. However, boiling water is still dominant, whether on a lab or an industrial scale because of the lower cost and requirement of equipment. Finally, the tannin-containing solution should be evaporated under vacuum conditions to avoid oxidation until the desired concentration is reached. Otherwise, stabilizing agent should be added to avoid reaction during storage (Arbenz and Avérous, 2015; Das et al., 2020; Fraga-Corral et al., 2020).

It is worth noting that there is no standard formula for extracting tannins, although many advanced methods have been proposed, such as using supercritical fluids, infrared-assisted extraction, and ultrasonic methods (Hoyos-Martínez et al., 2019). In addition to the source of raw materials, there are many parameters which will affect the quality and yield of tannins. The higher the temperature and longer residence time usually result in a higher yield of tannins, while the quality will be decreased due to the amount of impurities that are extracted simultaneously (Petchidurai et al., 2019; Dentinho et al., 2020).

2.1.4 Impurities in tannins

Similar to other refining processes, it is not possible to obtain pure tannins just through simple extraction processes. Non-tannin impurities are mainly inorganic acids, lipophilic extractives, carbohydrates, and other tannin-related components (Ferreira et al., 2004; Benaiges and Guillén, 2007; Bianchi et al., 2015). The content of impurities in tannin samples can be as high as 35% (Mittal, 2021).

The main impurities that might exist in crude tannins are listed below:

- Inorganics: some minerals associated with soluble salts or amino and amino acids.

- Lipophilic extractives: fatty acids including saturated acids with 8-24 C atoms, resin acids (mainly abietic acids and their derivatives) with tricyclic skeleton structure and triglycerides.
- Carbohydrates: monosaccharides (i.e., pentose and hexoses), oligosaccharides (i.e., stachyose), and polysaccharides (i.e., pectin-like components, hydrocolloid gums, hemicelluloses) are the major impurities of tannin samples
- Complexes: tannins tend to form complexes with proteins and polysaccharides, sometimes even metal ions (i.e., Fe^{3+}, Ca^{2+}), and the complexes formed are persistent.

These impurities are extracted along with the tannins during the extraction process because of the similar solubility and high temperature. Their presence has a significant impact on industry application, and it is also the major obstacle to the successful development of tannins as substitutes for petroleum phenols.

2.1.5 Reactivity and industrial treatments of CTs

Before introducing sulfonation of CTs, it is necessary to understand the reactivity at different position in the CTs. Compared to HTs, the chemical structures of condensed tannins are more complex, because they contain three rings with various activities. The number and the position of hydroxyl groups on the rings are also different. Therefore, the chemical modification is more complicated in CTs than in HTs in the industrial fields. According to the different chemical structure, CTs have mainly three reactivity sites (seen in ***Figure 10***): the nucleophilic site, the heterocyclic C-ring and the hydroxyl groups (Arbenz and Avérous, 2015). Different types of CTs can be obtained based on various modifications to these active sites.

The reactivity of three sites is summarized as follows:

- Nucleophilic rings are vigorously activated due to the electron density contribution of oxygen atom to the ring. Thus, they are highly reactive towards electrophilic aromatic substitution.
- Heterocyclic C-ring can be opened and alter chemical structure and properties of the CTs, thus achieving the modification purpose.
- Hydroxyl groups are active groups; different modifications can obtain CT derivatives with other properties (more active or higher solubility in solvents).

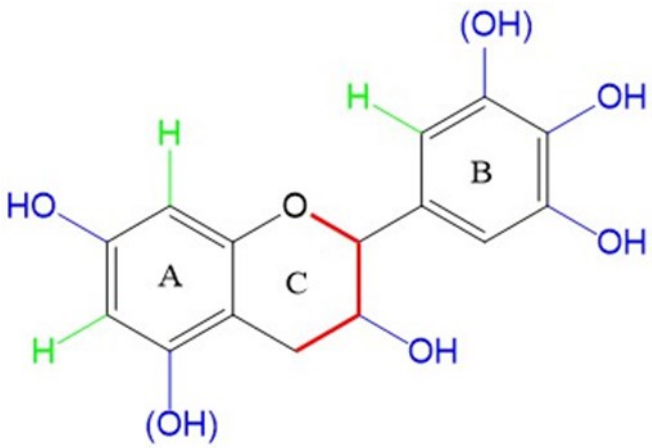

Figure 10: *Reactive sites of CT: nucleophilic site (in green), heterocyclic C-ring (in red), hydroxyl groups (in blue).*

Sulfonation is one of the traditional modification methods, used for more than 100 years, is based on the reactivity of heterocyclic rings. It is mainly applied in the leather and resin field (Hoong et al., 2009; Kuruppu and Karunanayake, 2019). There are two ways to obtain sulfonated tannins. One is to add sodium bisulfite ($NaHSO_3$) or sodium sulfite (Na_2SO_3) after obtaining the extract with traditional boiling water methods. The other is to directly treat homogenized plant material with boiling bisulphite or sulphite solution. The latter usually has higher extract yields. Extracts with sulfonation treatment can be directly dissolved in cold water, while the extract obtained by the traditional water extraction method are only soluble in warm water (Timell, 1975; Venter, Senekal, et al., 2012; Venter, Sisa, et al., 2012). The changing of solubility is due to the opening of the heterocycle during the extraction, shown in ***Figure 11***. The C-ring opening results from the sulfonated hydrolysis. The introduced phenolic hydroxyl groups, which are polar groups, lead to an increase in the water solubility and decrease of the viscosity of the extract. In addition, the sulfonation treatment also showed the advantage of reducing the average chain length, which is also the reason for the low molar mass of the extracted tannins (Venter, Senekal, et al., 2012).

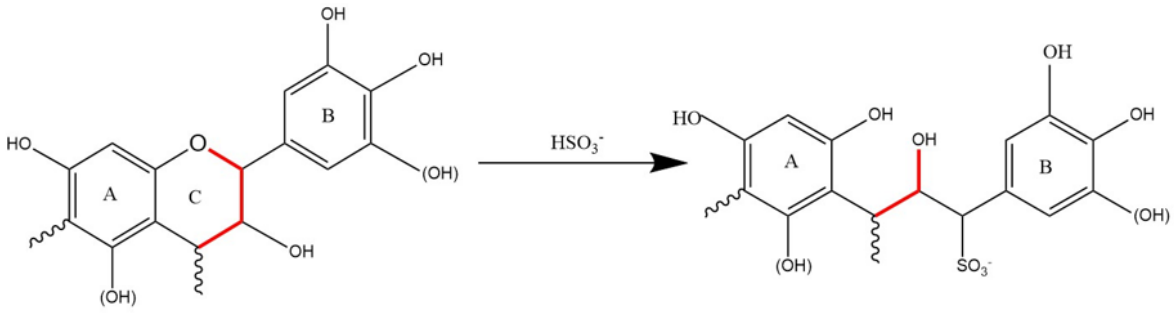

Figure 11: *Sulfonation reaction of flavan-3-ol tannin.*

Although the ring opening has advantages in many respects, introducing the sulfonic group will also have drawbacks in some fields, such as resin manufacturing. Its presence increases the resin sensitivity to water if they are not sufficiently cross-linked. Therefore, the sulfonic group needs to be replaced by the hydroxide groups through SN_2 substitution reaction at strongly alkaline conditions. The mechanism is shown in ***Figure 12***. In conclusion, the tannins will be more active due to introducing the -OH groups and the opening heterocycle ring in each flavonoid unit, especially the activity of the A-ring in the resin production (Timell, 1975). Finally, the auto-condensation reaction should also be noted under alkaline conditions or in the presence of metabisulfite (seen in ***Figure 13)***. The result is some higher molar mass tannins would be obtained (Pizzi, 1994a).

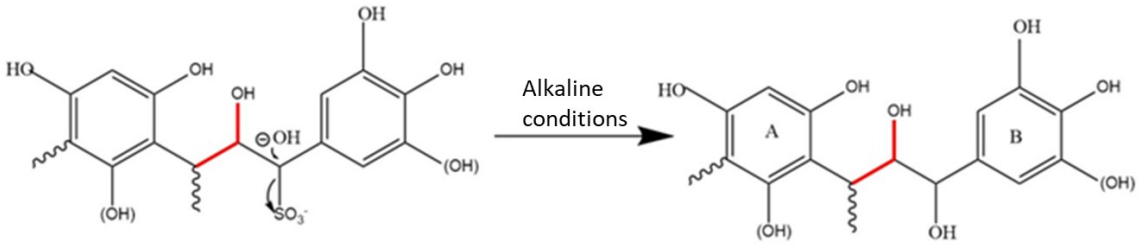

Figure 12: *Desulfonation reaction at alkaline condition.*

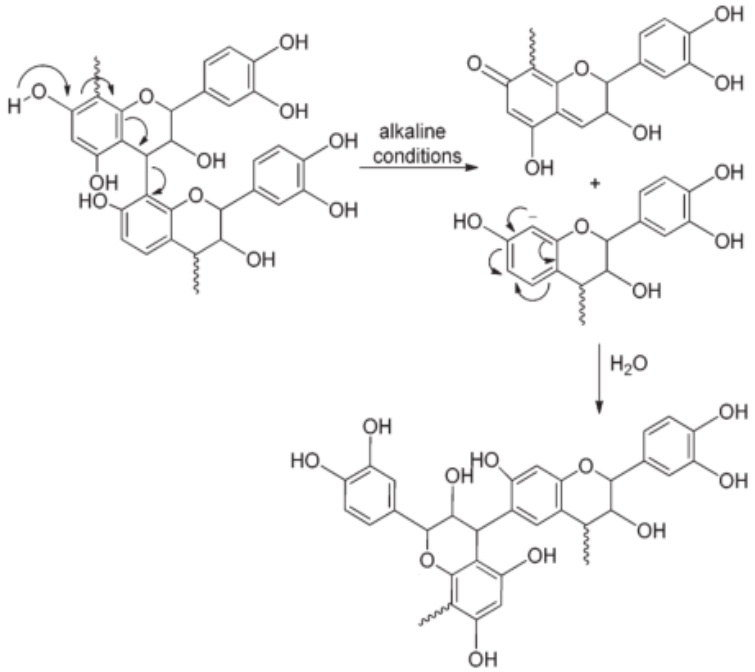

Figure 13: *Auto-condensation in alkaline condition and the presence of metabisulfite. (Adapted from* Arbenz and Avérous, 2015).

2.2 Application of tannins

Humans have a long history of using tannins, dating back thousands of years to ancient Egypt. Today, with uncertain reserves of fossil resources and serious environmental pollution, tannins are still a research hotspot. This is because they are abundant in natural reserves, comprehensive in origin, and exhibit renewable, degradable, and chemically active characteristics. This section will highlight applications of tannins in phenol-free resins production and in the medical field.

2.2.1 The application of tannins in phenol-free resin production

Background of phenolic resin

Phenolic resin is a traditional synthetic product that started in Germany in the 19th century (Xu et al., 2019). It was dominant worldwide in different fields due to the low cost and excellent mechanical and chemical properties. However, with the deepening of research, the shortcomings of the phenolic were exposed. Firstly, the raw materials for producing phenolic with the traditional method are derived from fossil raw materials. Phenol is derived from coal tar, while formaldehyde is derived from petroleum, and these fossil resources are not sustainable. Secondly, both phenol and formaldehyde have biohazardous properties, e.g., mutagenic and carcinogenic, which raise higher requirements for the protection of workers' safety and health. Thirdly, excessive or residual formaldehyde also threatens the health of the consumers. These reasons have made finding natural alternatives to phenol and formaldehyde popular. Tannins and other natural polyphenolic products rich in phenolic structures, as lignin and cardanol, have recently become popular candidates to replace petroleum-derived phenols (Sarika et al., 2020).

Phenolic resin can be divided into resole resin-based and novolac resin-based on the reaction conditions. Resole types are carried out at alkaline conditions with excess formaldehyde (molar ratio). In contrast, the novolac type is done at acidic conditions, and the ratio of formaldehyde to phenol is less than 1. Resole resin does not need curing agents, because the existing reactive hydroxymethyl (-CH_2OH) can condense into macromolecules during the reaction. Compared to novolac resin, resole resin products are more environmentally friendly, since most of the curing agents are toxic, but have a short shelf life (less than 1 year). For novolac type resin, the addition of the curing agents makes them more stable. Despite the controversies associated with environmental pollution, it has a longer shelf life (infinite) (Sarika et al., 2020).

Tannins in phenol-free resin production

As phenolic compounds, both HTs and CTs can react with formaldehyde at alkaline and acidic conditions to form resole or novolac resins. The resole type is the dominant one so far (Peña et al., 2006; Jaramillo et al., 2022). However, the simple phenolic structure and less modified methods limit the use of HTs in the resin industry. In other words, CTs with three rings are more advantageous in resin production, although not all rings are involved in the reaction. The A-rings in CTs contain the more reactive nucleophilic center, while the B-ring's general activation results from the vicinal hydroxyl substituents in B-rings (Dotan, 2014; Dunky, 2021a). Even at neutral conditions, aldehydes can rapidly react with the A-ring. C6 and C8 are the specific reaction sites of tannins. C6 is often the reactive site of tannins with C4-C8 linkages, such as *Pine* tannins, while the C8 occurs in those with C4-C6 linkages, such as tannins found in *Mimosa*. The polymerized products are linked by either the methylene bridges or methylene-ether bridges, seen in ***Figure 14***. The B-ring in CTs only tends to react with formaldehyde at pH $\geqslant$ 10 or when the divalent or trivalent metal ions are added at pH 4–5.5. However, such an approach is not worthwhile, because the reactivity of the A-ring is too strong at such high pH, resulting in a shorter pot life of the resin product (Braghiroli et al., 2019).

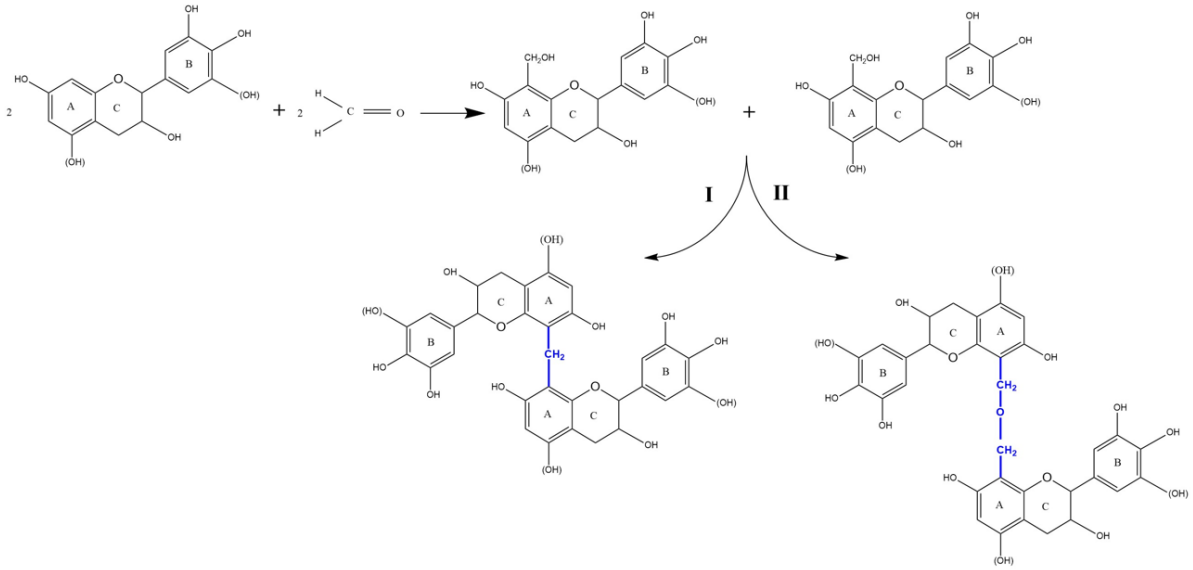

Figure 14: *CTs monomer reacts with formaldehyde: methylene bridges line (I) and methylene-ether bridges line (II).*

The reactions mentioned above are detailed descriptions of CTs when reacting with aldehydes, but practical resin production is more complex. Different kinds of tannins show different reactivity but still offer a significant advantage compared with industrial phenols. *Pine* and *pecan* tannins are representatives for tannins containing a phloroglucinol A-ring, and their reactivity with formaldehyde is increased by more than 50 times, while tannins from *Mimosa* and *Quebracho*, which are tannins dominated by resorcinol A-ring, only increased the reactivity 8–9 times (Zhao and Umemura, 2014).

Although tannins resin shows excellent advantages in terms of environmental friendliness and higher reactivity, the quality of the products just through simply mixing is unsatisfactory. This is because the resulting product is three-dimensional, which means less liquidity than phenolic products. Furthermore, the low degree of condensation generally results in a brittle product, with low strength, and poor water resistance (Pizzi, 2017). However, the degree of condensation can be increased by adding a small number of intermediates to react with the active sites on the tannins. The typical intermediates include urea-formaldehyde resins, phenolic resins, or isocyanates. Additionally, replacing formaldehyde with furfural is another feasible method to increase the degree of polymerization. On the one hand, furfural effectively cross-links with tannin, which improves the resin stress distribution, and on the other hand, furfural decreases the risk of releasing formaldehyde from the product (Pizzi and Scharfetter, 1978).

Large or branched tannin molecules will exhibit poor flowability and flexibility at low curing degrees. The larger the Mw of tannins the higher the speed of the curing at low temperature, which will make it more difficult to polymerize tannin molecules. This would result in a fragile resin. Different curing agents (hexamethylenetetramine, paraformaldehyde, polyisocyanate) are usually added to improve the mechanical properties of the product and decrease the amount of formaldehyde released, and the adhesives produced have been used in artificial panels to meet the requirements of indoor and outdoor use (Ping et al., 2011).

Viscosity is a complex issue in resin synthesis, and maintaining proper viscosity helps to improve tannin flow and resin synthesis. The initial tannin viscosity is affected by the tannin's nature and type of extraction. *Pine* tannin with a degree of polymerization of 6–7 are more viscous than *Mimosa* and *Quebracho* tannin with a degree of polymerization of 4–5. However, the branched structure of *Mimosa* tannins makes this tannin more viscous than straight-chain *Quebracho* tannin. The concentration of tannin resin is affected by impurities and hydrogen bonds. The interaction between high-molar-mass carbohydrates and tannin-tannin, tannin-gum, and gum-gum will make tannin resin show high viscosity characteristics compared to phenolic resins. Degradation of carbohydrates, sulfonation to open heterocyclic rings and dilution (enhancing fluidity) are commonly used methods to reduce initial tannin viscosity. Sulfonation is the most widely used method for industrial resin preparation, this was described in section ***2.1.5***. In addition to lowering viscosity, sulfite-treated tannins also exhibit better cross-linking characteristics and longer pot life of the product (Dunky, 2021b).

The self-condensation reaction of tannin is another interesting phenomenon. Tannins tends to self-condensate under acidic or basic conditions even without adding any curing agent. No release of volatile organic compounds is the main feature of tannin self-condensation adhesives, but the self-condensation polymerization reaction is slow, and the adhesive reaction

is not effective enough to achieve waterproof adhesion. More research is still needed to improve the quality of the product (Pizzi, 2012).

Finally, the realization of industrialization is affected by many factors as cost, origin of raw materials, and purification method. Due to geographical advantages, the first country to commercialize tannin resin was South Africa. Currently, tannin resins are used in applications most in Chile, New Zealand, Australia. So far, there is only a small market scope in the European region (Zhou and Du, 2019).

2.2.2 The applications of tannins in other fields

Medicine

Tannins with various biological activities have been proven to have great development potential in the field of medicine. Antioxidant effect, inhibiting growth of tumor and cancer cells, antibacterial and antiviral effects, preventing diabetes, and anti-inflammatory effects make the development of tannins attract much attention. However, in clinical medicine, most of the applications are still in the stage of in *vitro* experiments, and research needs to be continued (Zhanget al., 2021).

- **Antioxidant:** Tannins are an excellent free radical scavenger. Its function mechanism blocks the free radical chain reaction by releasing hydrogen ions and competitively combining them with free radicals. The antioxidant properties of CTs in *Cranberry* are ten times than that of ascorbic acid, and ellagitannin show good anti-lipid oxidation activity. The antioxidant properties of tannin depend on their chemical structure, and higher antioxidant tannin are associated with higher degrees of polymerization (Kaczmarek, 2020).

- **Inhibition of growth of tumor and cancer cells:** Tannins can promote the apoptosis of tumor cells by regulating the expression of signaling molecules in tumor cells and cancer cells. Ellagic acid has been reported to inhibit rat tumors as early as the 1860s (Duan et al., 2020), and the anticancer properties of condensed tannin have also been extensively studied and confirmed. However, these studies are still in their infancy and have not yet been applied to treatment (Nagesh et al., 2020; Zhang et al., 2021).

- **Antibacterial and antiviral:** Tannins can coagulate the protoplasm of microorganisms, so they have apparent inhibitory effects on bacteria and viruses. The antibacterial and antiviral mechanism of action is based on the property of tannins (especially ellagitannins) to inhibit the metabolism of pathogens, the more active the chemical properties, the stronger the inhibitory effect (cytotoxicity) (Shahidi and Ho,

2005; Molino et al., 2020). Common pathways include crossing the cell wall to the inner membrane, binding to the cell resulting in the inability of the bacteria to attach and inhibiting the uptake of sugars and amino acids by the bacteria. There are already kinds of toothpaste in Japan that utilize the antibacterial properties of HTs to prevent dental caries and promote clean teeth. Some low-molar-mass HTs exhibit significant antiviral and anti-HIV activity, and antiviral activity is generally related to total galloyl residues (Kaczmarek, 2020).

- **Prevention of diabetes:** Diabetes is caused by disorders of fat and carbohydrate metabolism in the body, and tannins have the potential to treat non-insulin diabetes by inhibiting lipogenesis and enhancing glucose uptake. *Acacia* tannin showed the effects of lowering blood sugar and improving cholesterol in diseased rats (Kooti et al., 2016).

- **Anti-inflammatory and hemostasis:** The anti-inflammatory mechanism of tannins *in vivo* is not precise, and it seems to have a non-specific effect on cells through its astringency. In rat studies, tannins oppress the entry of inflammatory mediators into rat cells. Tannins are also used to remedy localized burns and as an additive to toothpaste to prevent gum inflammation. Recent clinical studies have shown that tannins have pain relief and blood flow stabilization properties (Fikru et al., 2012; Zhang et al., 2021).

Food

Tannins are also widely used in food. Fruits and vegetables rich in tannins are often accompanied by astringency. When the number of hydroxyl groups in the molecule is within 1-5, the astringency will increase with the number of hydroxyl groups. Excessive intake of tannins can, however, negatively affect a person's health. Animal food additives and food packaging are currently hot research on tannins in the food field (Molino et al., 2020; Xindi Zhang et al., 2021).

- **Animal food additives:** Tannins have antimicrobial properties and are natural products that can replace antibiotics in animal feed and effectively control parasites in the gut (Lillehoj et al., 2018). Moreover, studies have shown that adding *Quebracho* tannins and *Chestnut* tannins to dairy cows' feed can improve the quality of protein in milk and reduce nitrogen content in urine, reducing the environmental pollution (Aguerre et al., 2020).

- **Food packaging:** As natural compounds, tannins with antibacterial, antioxidant, and UV-absorbing properties are preferred over traditional packaging materials (polyethylene and polypropylene). Products with tannins combined with different raw materials, as chitosan and cellulose, show outstanding advantages such as high thermal

stability, prolonging food shelf life, anti-ultraviolet, anti-oxidation, and preventing microbial growth (Molino et al., 2020).

Others

In addition to the applications mentioned above, the traditional applications based on tannins are tanning and adsorbents. These are examples of mature commercial applications of tannins today. Tanning is one of the oldest applications of tannins. It mainly uses the binding ability of tannins and proteins to change the protein structure of leather permanently. The tanned leather products have the advantages of high quality, less odor, and long storage time (Pinto et al., 2013). The preparation of adsorbents is based on the characteristic that tannin is easy to chelate with metal ions, making tannins good materials for the preparation of adsorbents for wastewater. Since tannins are water-soluble compounds, they need to be immobilized to make adsorbents. Typical forms include tannin resin, tannin gum, and tannin foam. The curing agent of tannins shows strong adsorption capacity for various common heavy metals (chromium, copper, lead, nickel) in electroplating industrial wastewater and tannins are also used to absorb surfactants in sewage (Bacelo et al., 2016).

In short, although people have used tannins for a long time, the applications are not limited to some specific fields. The exploration of the applications of tannins in different areas is still ongoing today.

2.3 Hypothesis and objective

The theoretical part of this thesis expounds on the basic situation of tannins, including the source, classification, different extraction methods, industrial applications, and the potential for other applications. Although the description of tannins in literature has been very detailed, the properties of tannins of different types, from different parts of the plants, and applying different extraction methods are very different. In addition, decreasing the unavoidable impurities in tannins has become a hot topic in tannins research, so it is significant to characterize the differently treated tannins. In this thesis, six types of tannins were extensively characterized with high-level analytical methods, mainly to explore the feasibility of these different tannins as petroleum-derived phenolic substitutes.

The hypotheses of this thesis are:

- Condensed tannins can be obtained from *Spruce* and *Quebracho*. *Spruce* is found in Europe while *Quebracho* is found in South America. If the quality of *Spruce* tannin is comparable to that of *Quebracho*, production costs can be saved by taking advantage of the geographical location.

- *Quebracho* that has undergone various industrial treatments, including partially sulfonated (Q1), sulfonated (Q2), and purified (Q3), should theoretically have fewer impurities than the untreated *Quebracho*. However, the sulfonation process will introduce some sulfides and the specific purification steps are unknown. Extensive characterization will reveal the differences between the treatments.

- After different industrial treatments of *Quebracho*, the linkage between monoflavonoids may change, and the reactive sites may be increased due to the heterocycle opening. However, the self-condensation reaction under sulfonation conditions increases the degree of polymerization of tannin. These two different reactions make it difficult to speculate on the linkage of *Quebracho* for further treatments.

- *Chestnut tannin*, as the only hydrolyzed tannin, analysis of phenolic content and impurities will be emphasized.

- Due to the structural differences between CTs and HTs, CTs are theoretically more stable than HTs, so thermal stability and glass transition temperature would be higher.

- Impurities in tannins theoretically include acids and lipids, sugars (free sugars, cellulose and hemicelluloses), and some inorganics (amino acids). Therefore, comprehensive characterization will be included in the analysis.

The objectives of this thesis are:

- Sequential extraction of different tannins using six solvents with gradually increasing polarity was used to fractionate the tannin samples. Each fraction was thoroughly characterized to explore the content and differences of components in this thesis.

- Differences between CTs and HTs were explored, including quantitative and qualitative components analysis, especially regarding impurities and phenolics.

3. Experimental

3.1 Material and methods

3.1.1 Crude tannins samples

In this study, six crude tannins were used. Basic information about those samples is given in ***Table 1***. All tannins were brown powder and were kept in brown bottles in the cold room to prevent degradation of phenolic compounds (Makkar, 2003).

Table 1: *Summary of tannin samples.*

Classified of tannin	Types of tannin	Industry treatment	Code
Condensed tannins	*Quebracho*	-	*Q*
		Partially sulfonated	*Q1*
		Sulfonated	*Q2*
		Purified	*Q3*
	Spruce	-	*S*
Hydrolysable tannins	*Chestnut*	-	*C*

3.1.2 Sequential extraction of tannins with Accelerated Solvent Extraction (ASE)

Accelerated Solvent Extraction (ASE) was used with six different solvents with increasing polarity to fractionate the tannin samples, the solvents used can be seen in ***Table 2.*** The instrument used was an Accelerated Solvent Extractor 350 (ASE 350, Dionex, USA). Crude tannins were dried in a vacuum freeze dryer for 48 hours and approximately 2.5 g of each dried crude tannin was mixed well with quartz sand (1:16, w: w). The mixture was added to a 33 mL stainless steel ASE-cell and extracted in inert atmosphere at 90 ℃ and 10 Mpa for 25 min (5 min × 5 times). ***Figure 15*** shows the flow chart. All extracts were collected and kept in a dark and cold room.

Table 2*: Solvent used in sequential ASE extractions.*

Solvent list	Purity
Hexane	⩾97%
Methyl tert-butyl ether (MTBE)	⩾99.8%
Dichloromethane (DCM)	⩾99.9%
Acetone	⩾99.8%
Ethanol (EtOH)	⩾94%

Water	Deionized water

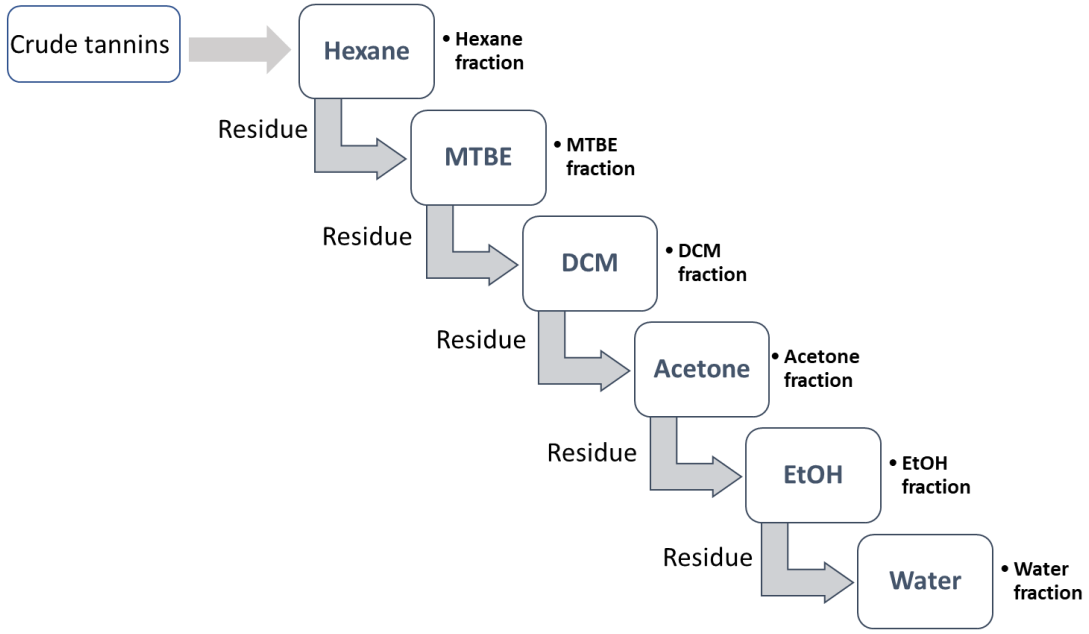

Figure 15: *Flow chart of sequential ASE extraction.*

To calculate the total dissolved solids in each extract, the collected extracts of each different tannin were first diluted into the desired volume in a measure cylinder. 10 mL of the adjusted extract was taken, and the solvent was evaporated with flow of nitrogen. After the solvent was removed, the samples were placed in a vacuum desiccator at 40 °C until constant weight. The percentage of the total dissolved solids in extract was calculated as follows:

Equation 1: $$Extract\ percentage(w\%) = \frac{w_1 - w_2}{w} * 100\%$$

where:
W_1=Weight of bottle and dried extract
W_2=Weight of bottle
W= Total weight of all extracted materials from each tannin

3.2 Characterization

3.2.1 Moisture content and pH of crude tannins

The moisture content of each crude tannin was determined according to ***Equation 2*** after they dried in the vacuum freeze dryer for 48 hours.

Equation 2: $$Moisture\ content\ (\%) = \frac{W_1 - W_2}{W_1} * 100\ \%$$

where:
W_1= Total weight of crude tannin and bottle before drying
W_2= Total weight of crude tannin and bottle after drying

1% aqueous suspension of each crude tannin was prepared based on the dry content, and the pH value was measured at room temperature.

3.2.2 ATR-FTIR analysis

Attenuated Total Reflection Fourier Transform Infrared (ATR-FTIR) spectroscopy was performed to determine the functional groups in crude tannins and their corresponding extract. The Thermo Scientific Nicolet IS50 FTIR spectrometer was used to analyze crude tannin and obtained extract in absorbance mode. The spectral range collected by ATR was 4000-400 cm^{-1}, the resolution was 4 cm^{-1}, and the cumulative scans were 64 (Xu et al., 2018).

3.2.3 Ash content

The ash content of tannin was determined gravimetrically (TAPPI T 211 om-02, 2002; Sameni et al., 2014a), After the complete combustion of the sample, the remaining ash is mainly composed of inorganic elements and some trace metals (ADAA, 2022). Approximately 0.5 g of each dried crude tannin were weighted into dried and clean crucibles and kept in the muffle furnace at 525 °C overnight until constant weight. Three parallel samples were done. The ash content percentage are calculated follow ***Equation 3***.

Equation 3: $$Ash\ content\ (w\%) = \frac{W_{ash+crucible} - W_{crucible}}{W_{crude\ tannins}} * 100\%$$

3.2.4 Elemental analysis

The organic elemental carbon (C), hydrogen (H), nitrogen (N), sulfur (S) were determined in weight percentage content by an Organic Elemental Analyser (Thermal Scientific), and the oxygen (O) was calculated by subtracting the sum of the above elements from 100% (Liu et al., 2021).

To elucidate the elemental composition of the ash, Scanning Electron Microscopy with Energy Dispersive X-ray Spectroscopy (SEM/EDS) was applied. Operation equipment of SEM/EDS is Thermo Scientific Apreo S and Oxford Instruments Ultim Max 100, respectively. The obtained tannin ashes were spread on the double-sided carbon tape of SEM, the acceleration voltage was set to 15 kV. Several areas of each different sample are selected for analysis.

3.2.5 Thermal-gravimetric properties of crude tannins

Decomposition temperature (Td)

The thermal stability of crude tannins was determined by thermogravimetric analysis (TGA). The decomposition was performed by a SDT 650 (TA Instruments). Crude tannins were placed at a constant temperature oven at 100 ℃ overnight. Approximately 7 mg of each tannin was analyzed in a nitrogen gas atmosphere (100 mL/min). The temperature was set from 25 ℃ to 700 ℃ with a heating rate of 10 ℃/min. The higher the Td, the higher the thermal stability of the tannin. Result of maximum degradation rate (MDR), temperature of tannins in the maximum degradation rate (TDR), and the remaining weight (w%) after 700 ℃ was be obtained. The result was analyzed by the software *TRIOS 5.2*.

Glass transition temperature (Tg)

Tg determination of crude tannins is more difficult and complex than that of traditional synthetic polymers (Lisperguer et al., 2016). Crude tannins were dried overnight in a constant temperature oven at 100 °C to prevent damage to the instrument from volatiles. Approximately 5.6 mg of each crude tannin was placed in a Tzero pot and later covered with a Tzero cup (TA Instruments, Switzerland). The equipment was a DSC 250 (TA Instruments), heated from room temperature to a specific temperature at a rate of 20 °C/min. The Td determines the specific temperature. It is usually lower than the Td to avoid tannin melting and damage to the equipment. In addition, the Tg generally occurs earlier than the Td, so this setting can determine the Tg. The results were analyzed also by the software *TRIOS 5.2*.

3.2.6 Molar mass analysis

Size exclusion chromatography (SEC) is an efficient method to obtain the molar mass distribution (*Đ*) and molar mass information based on the size exclusion. The Đ of crude tannin and their solvent extract, and the molar mass of crude tannin were analyzed with different eluents, the different eluents selected associated to their solubility.

The SEC-MALS analysis for crude tannin and obtained extracts were carried out on a High-Pressure Size Exclusion chromatography (HPSEC) (Agilent 1100/1200/1260 Serious, USA) equipped with a refractive index detector (Optilab High Concentration Differential Refractometer, Wyatt Technology, USA) and a multiangle light scattering detector (SEC-MALS, Wyatt Technology, USA) (WYATT, 2022). The series column connected with the system were a Jordi Gel GBR Mixed bed column (250 mm length, 10 mm inner diameter) and a Jordi Gel Glucose Mixed bed guard column (50 mm length, 10 mm inner diameter). Freeze-dried crude tannin and corresponding tannin extracts were dissolved in dimethyl sulfoxide (DMSO)/0.05 M LiBr solution to obtain 10 mg/mL sample, the sample was filtered on a 0.2 µm nylon filter before injection. The operation conditions were DMSO/0.05 M LiBr as the

eluent at 0.5 mL/min flow rate, injection volume of samples was 100 µL, and column temperature was 60 ℃. The obtained data were analyzed with software ASTRA, version 7.3.2 (Liu et al., 2021).

Molar mass characteristics for acetylated crude tannins including the weight average molar mass (Mw), the number average molar mass (Mn) and Mw/Mn, can be obtained from GPC analysis using tetrahydrofuran (THF) as eluent. The system was equipped with a HPLC pump LC-40D, an auto sampler SIL-20A $_{HT}$ (SHIMADZU), a column oven CTO-10AC (SHIMADZU) and a detector SEDEX-100 $_{LT\text{-}ELSD}$ (SEDERE). The series columns were two Jordi Gel DVB 500A columns (300 mm length, 7.8 mm inner diameter) coupled with a guard column (50 mm length, 7.8 mm inner diameter). The operation conditions were as follows: THF as the eluent at 0.8 mL/min flow rate, The temperature of the column was 40 ℃ and the pressure was 3.4 bar. 5 mg of freeze-dried tannin was acetylated by 1 mL pyridine-acetic anhydride (1:1 v: v), agitated in a shaking basket for one week in the dark and at room temperature. Extended acetylation time is needed to ensure dissolution of the crude tannin (Makino et al., 2011a). The acetylation solution was evaporated with flow of nitrogen and the acetylated sample was dried in a vacuum desiccator at 40 ℃ overnight. Dried acetylated sample was dissolved in THF to 1 mg/mL and filtered with 0.2 µm polytetrafluoroethylene syringe filters before performing the GPC analysis.

3.2.7 Gas chromatography

Gas chromatography (GC) of the obtained extracts was used to analyze the composition in detail. Short-column GC was used to analyze high-molar-mass extractives as triglycerides and steryl esters and long-column GC were used to analyze extractives as resins acids and fatty acids (Örså and Holmbom 1994).

The extracts were prepared according to the following process: 1 mg of dried extracted material was added to a test tube and 2 mL betulinol (0.02 mg/mL) was added as internal standard. The extracts were evaporated in a flow of nitrogen and placed in a vacuum desiccator for 2 hours. The dried samples were silylated with 50 µL pyridine, 80 µL N, O-bis-(trimethylsilyl) trifluoroacetamide (BSTFA) and 40 µL trimethylchlorosilane (TMCS). The samples were then placed in an oven at 70 ℃ for 45 min and moved to the fume hood at room temperature overnight. The completely dissolved part of samples was transferred to vials and analyzed first by short-column GC, then by long-column GC, and finally by GC-MS.

The short-column system was a GC-instrument Perkin Elmer Clarus 500, the capillary column is HP-1 (6 m length, 0.53 mm inner diameter). The long-column system was a GC-FID (Perkin Elmer Auto System XL), and the capillary columns are HP-1-channel A and HP-5-channel B (25 m length, 0.20 mm inner diameter). Then, the individual components were identified by

gas chromatography coupled with mass spectrometry (GC-MS) by comparing the obtained chromatographic peaks with the Nist Spectral Library (Mazri et al., 2021). GC-MS is also long-column instrument equipped with the HP-1 capillary column. The performed condition is same as that of GC-FID instrument.

Alkaline hydrolysis of samples was performed to confirm the presence of triglycerides, as the grouping of triglycerides and steryl esters was not classified clearly in the short-column analysis. Triglycerides are be hydrolysed into fatty acids at alkaline conditions (Chandra et al., 2020). 10 mg of dried extracted materials were placed in a test tube and hydrolyzed with 2 mL 0.5 M KOH in EtOH/H_2O (9:1) at 70 ℃ for 4 h. 1 mL of hot liquid phase was transfer to a new test tube. The samples were acidified with 0.25 M ortho-phosphoric acid and with bromocresol green as the indicator (color changes from green to yellow at pH=3.8). 2 mL betulinol (0.02 mg/mL) was added as the internal standard to the test tubes, and the content was extracted with MTBE three to four times. The collected extracts were combined, and the trace acids were washed out with 1 mL of deionized water twice. MTBE was evaporated with nitrogen and the samples were silylated with pyridine: BSFTA: TMCS (1:4:1, v: v) at a 70 ℃ for 45 min and kept them in the fume hood overnight. Long-column GC analysis and GC-MS were carried out as described above.

3.2.8 Py-GC MS

The structural analysis of crude tannins and their extracted fractions was performed with pyrolysis/gas chromatography-mass spectrometry method (Py/GC-MS) (Galletti and Reeves, 1992). Approximately 100 µg of the sample was pyrolyzed at 650 °C for 2 seconds. The Pyrola 2000 pyrolyzer was connected to an Agilent 7890B gas chromatography system and an Agilent 5977B mass selective detector. The gas chromatography system was equipped with a 30 m long, 0.25 mm inner diameter ZB-35 column. The electron ionization (EI) mode of the mass selective detector was 70 Ev (Liu et al., 2021).

3.2.9 Carbohydrates analysis and GC

Only free sugar monomers can be analyzed by GC after direct silylation of dried extracted samples as it was described in **3.2.4**, but oligo- and polysaccharides are not volatile at these GC conditions. Both acid methanolysis and acid hydrolysis can be used to cleave the bonds of the sugar units. Acid hydrolysis is a total carbohydrates hydrolysis method for crystalline carbohydrates such as cellulose, while acid methanolysis is specific for amorphous carbohydrates as hemicelluloses and pectins (Sundberg et al., 1996; Willför et al., 2009). Both acid hydrolysis and methanolysis products were prepared and followed by GC analysis, processes as described by Sundberg (1996).

Acid methanolysis and GC

Acid methanolysis was used to analysis the non-cellulosic carbohydrates in crude tannins and in the obtained extract. Approximately 10 mg of freeze-dried samples and 1 mL of calibration solution were prepared in separated pear-shaped flasks and dried in nitrogen flow. The calibration solution contains equal amounts of 0.1 mg/mL monosaccharides (glucose, galactose, mannose, xylose, rhamnose, arabinose, glucuronic and galacturonic acid). 2 mL of 2 M HCl in MeOH was added to the samples in the hermetically close flasks and the samples were kept at 105 °C for 3 h. After the mixture was cooled to room temperature, 200 µL of pyridine was added to neutralize the samples and they were dried in a flow of nitrogen. 150 µL of pyridine, 150 µL of hexamethyldisilazane and 70 µL of TMCS were added to the flasks and then they were left at room temperature overnight. The silylated samples were transferred to GC vials. A GC-FID (PerkinElmer Clarus 500) equipped with HP-1 and HP-5 (25 m length, 0.2 mm inner diameter) was used for analysis of the methanolysis products.

The calculation of content of the different monosaccharides is based on the internal standard methods with correction factor from calibration solution. The sugar composition was calculated according to ***Equation 4***.

Equation 4: $Amount\ of\ the\ sugar\ in\ sample\ (mg/g) = A * B * C * D$

where:

A: $Correction\ factor = (\frac{Area_{Individual\ sugar\ monomer}}{Area_{Standard(resorcinol)}})^{-1}$

B: $Ratio\ = \frac{Area\ _{Individual\ sugar\ monomer}}{Area_{Standard(resorcinol)}}$

C: Weight of the dried sample, mg

D: Anhydrosugar coefficient. The anhydrosugar coefficient is 0.88 for pentose and 0.91 for hexose and uronic acids.

Acid hydrolysis and GC

The cellulose content of crude tannins was determined by acid hydrolysis combined with GC. Approximately 20 mg of freeze-dried crude tannin was weighed in a test tube with a screw cap, and one glass ball was put in each test tube. 6 mL of calibration solution of monosaccharides and uronic acids was added, and the sample was evaporated with nitrogen gas in separate test tube. 0.2 mL 72% sulfuric acid was added while keeping the samples in an ice bath. Then 0.5 mL of deionized water was added to each tube. After waiting for four hours, 6 mL of deionized water was added. The samples were left overnight at room temperature. The samples were then agitated in a shaking basket to ensure sufficient reaction. Afterward, the samples were autoclaved at 125 °C for 90 minutes and cooled down to room temperature. 1-2 drops of bromocresol green were added as an indicator before neutralizing the samples with barium

carbonate (yellow to green). It is worth noting that color changing is not the only criterion for complete neutralization. For some tannins, the solution always remains brown during the neutralization process. However, it is known that the upper limit amount of barium carbonate required to neutralize all the sulfuric acid is 2.4 g, so the whole process must be carried out on a balance. After complete neutralization, 4 mL of resorcinol (0.1 mg/mL) as internal standard was added to the sample and then the sample was centrifuged for half an hour. 2 mL of the supernatant was transferred to a new test tube and the solvent was evaporated with nitrogen flow. The dried components were silylated follow by GC analysis. The GC result calculation were similar as described in the methanolysis part; cellulose content calculated after subtracted of glucose content obtained from acid methanolysis result.

3.2.10 Nuclear magnetic resonance (NMR) analysis

^{13}C NMR

The information about the linkages between units can be obtained by ^{13}C NMR analysis. About 100 mg of freeze-dried *Q tannin* and *Q2 tannin* were weighed, dissolved in 650 µL of DMSO-d6, and 3 mg of chromium (III) acetylacetonate was added as the relaxation delay reducer. The mixture was kept in the dark and stirred for three hours to ensure full dissolution of the solid. The spectra were collected on a Bruker 500 MHz spectrophotometer with 15,000 scans and a delay of 2 s. The acquisition time was 1.8 s (Duval and Avérous, 2016). Results were analyzed on the software *TopSpin 4.1.4.*

Heteronuclear Single Quantum Coherence (HSQC) NMR

S tannin, Q tannin, and *C tannin* were analyzed by HSQC NMR method. 80 mg of sample was dissolved in 750 µL of DMSO-d6. The analysis was performed with a Bruker 500 MHz instrument with a probe (5mm-z gradient Broadband Observe). The relaxation delay was 2.0 s in 256 increments of 80 scans each. The spectral widths are 8012 Hz (from -3.3-16 ppm) and 20750 Hz (from -7.5-157.5 ppm), corresponding to ^{1}H and ^{13}C, respectively. Results were analyzed on the software *TopSpin 4.1.4* (Wang et al., 2020).

^{31}P NMR

The hydroxyl groups (-OH) of tannins can be identified and quantified by ^{31}P NMR analysis. The procedure followed the standard protocol (Meng et al., 2019). 15.03 mg of freeze-dried *Q tannin* was dissolved in 400 µL of pyridine/$CDCl_3$/DMF (2:1:1) solvent. The mixture was stirred for 2 hours, 0.01 mmol cholesterol was used as an internal standard, dissolved in 100 µl $ClCl_3$/pyridine (1:1.6, v: v). Then stirred it 10 min then transferred it to an NMR tube. The spectra were measured on a Bruker 500 MHz spectrophotometer with 64 scans. The acquisition time and relaxation delay were 1.6 s and 15 s, respectively. The spectrum was centered at 140 ppm. The strong calibration signal at 132.2 ppm is the result of the reaction product of water with Cl-TMDP, and the integral of the strong standard signal near 152 ppm used for the calculation was set to 0.66 mmol/g. Results were analyzed on the software *TopSpin 4.1.4.*

4. Results and discussion

Unless otherwise stated, all calculations in this thesis are based on the oven-dried mass of crude tannin as (mg/g) or w % of crude tannin. Equivalently, 1 mg/g = 0.1 w % of dried crude tannin.

4.1 Characterization of crude tannins

4.1.1 Moisture content, pH and ash content

The moisture content, pH and ash content of crude tannins are shown in ***Table 3***. All obtained tannin samples exhibited acidity, ranging from 3.7 to 4.8 and HTs (i.e., *C tannin)* are more acidic than CTs. In the Q group tannins, the pH difference was not significant between industrially treated *Quebracho* and untreated *Quebracho* tannins. The moisture content in obtained tannins varies widely, from 2.7% to 7%, probably related to their transportation and storage conditions. The ash content of crude tannin ranges from 0.84% to 6.15%. *S tannin* has the lowest ash content while *Q2 tannin* has the highest. *Q1* and *Q2 tannins* with sulfonation treatment have increased the ash content due to the introduction of sulfur compounds. The ash content of the purified *Q3* was the lowest in the Q group tannins.

Table 3: *Moisture content, pH, and ash content of crude tannins.*

Types of tannin	pH	Moisture content[w%]	Ash content[w%]
Q	4.8	7.00	2.33
Q1	4.8	6.22	3.18
Q2	4.7	5.81	6.15
Q3	4.4	4.85	0.87
S	4.3	5.50	0.84
C	3.7	2.70	2.07

4.1.2 Elemental analyses

Elemental analysis of crude tannins

The results of elemental analysis of crude tannins are shown in the ***Table 4***. The lowest content of C element is found in *C tannin*, 48%, while the other tannins contained 53–60% C. The possible resources of C content are from impurities or tannin itself. All tannins contain trace amounts of N, ranging from 0.20 to 0.91%, and the highest content was found in *S tannin*. The presence of N can be related to the protein in tannins. Therefore, its existence is inevitable in the elemental analysis of plants. In the Q group tannins, both sulfonation and purification

reduced the N content. 0.62% S element was found in *Q2*, which was due to sulfonation. The tannin sample with the highest O content was *C tannin*, reaching 47.29 %. High O content is usually associated with a high content of carbohydrates. At the same time, it has been mentioned that the core structure of HTs is glucose (seen in ***Figure 4***), which means it is logical that HTs has a high O content compared to the CTs.

Table 4: *Elemental analysis result of crude tannins.*

Types of tannin	C [%]	H [%]	N [%]	S [%]	O [%]
Q	56.63	5.21	0.74	-	37.43
Q1	55.24	4.81	0.27	-	39.68
Q2	53.73	4.68	0.37	0.62	40.60
Q3	59.34	5.20	0.20	-	35.26
S	60.81	6.14	0.91	-	32.51
C	48.03	4.41	0.28	-	47.29

SEM/ EDS of ash

The elemental analysis of ash samples from tannins are shown in ***Figure 16***. All tannin ash samples exhibited typical plant ash elements (Sameni et al., 2014). It should be noted that all elemental contents (w%) are based on ash and not crude tannins. The dominant metal element was Ca or Na. As it can be expected, the sulfite treated *Q1* and *Q2* tannins exhibited a relatively high amount of S. In the SEM/EDS ash analysis, particles with high content of Si were observed only in *Q* and *Q2* tannins (seen in ***Figure 17***), i.e., 15.7 % and 17 % (w% of the selected square area), respectively. The possible sources of the introduction of silica are industrial processing.

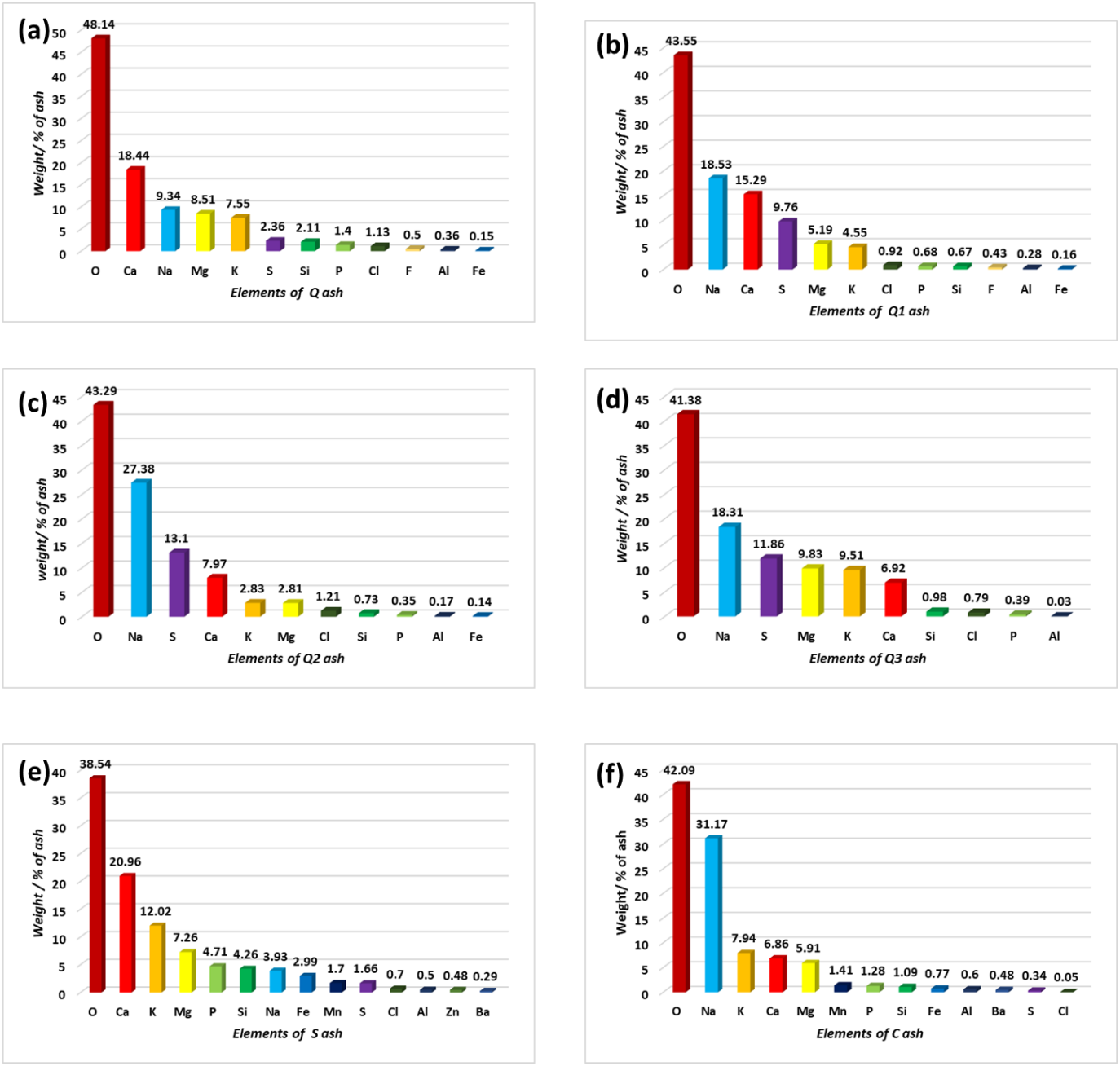

Figure 16: *SEM/EDS of ash from Q tannin(a), Q1 tannin (b), Q2 tannin (c), Q3 tannin (d), S tannin (e), C tannin (f), results are based on weight % of ash.*

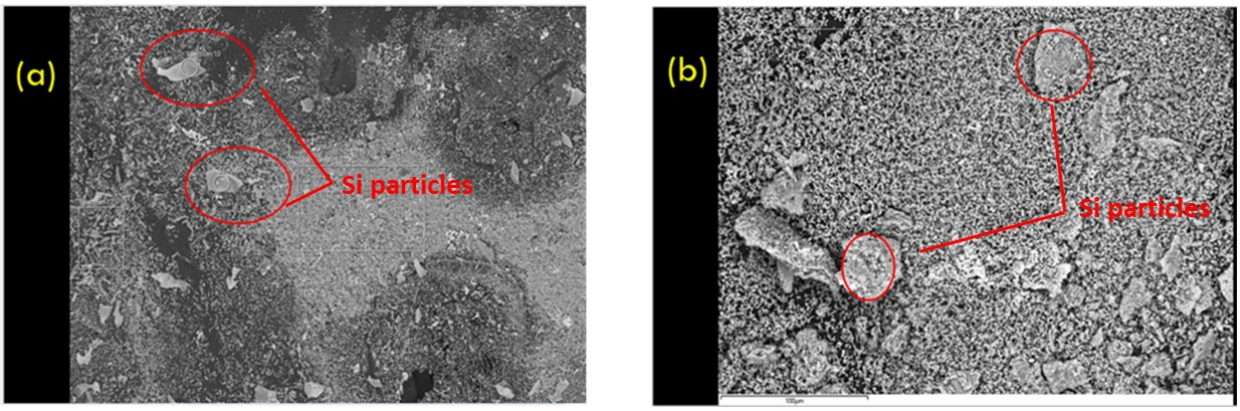

Figure 17: *Particles in SEM/ EDS images of ash from crude tannins: Q tannin (a) and Q2 tannin (b).*

4.1.3 Thermal-gravimetric properties of crude tannins

The TGA analysis curves of crude tannins are shown in ***Figure 18*** and the corresponding results are summarized in ***Table 5***. After removing moisture and low temperature-boiling impurities, the start state of tannins is stable at 100 w%. The *Q1 tannin* has the highest Td (229 °C), and *S tannin* has the lowest (186 °C). The Td of sulfite treated *Q1* and *Q2 tannins* are higher than the untreated *Q tannin*, possibly due to the high degree of polymerization (auto-condensation). The TDR of CTs is higher than that of HTs and the MDR of HTs is higher because the structure of CTs is more complicated than that of HTs. The monoflavonoids of CT consists of three different rings. However, for HTs, only one sugar core linked to ellagic acids or gallic acids (seen in ***Figure 4*** and ***Figure 7***). It is worth noting that at 700 °C, the remaining residues is the least in *S tannin*, with only 37.7% solid remaining. N_2 is also injected as protection gas at high temperature, so the residue can also be regarded as carbon. On the other hand, the C content of *S tannin* in the elemental analysis was as high as 60%. The explanation of the phenomenon can be due to the sample proportion classification, i.e., low boiling temperature acids or alcohols. The tannin samples in elemental analysis were freeze-dried crude tannins, while the tannin samples in TGA were dried at 100 °C overnight at a constant temperature. Based on different drying conditions, the C content in *S tannin* at 100 °C was reduced, which means that the main source of C element in *S tannin* is from those volatile components.

TGA analysis

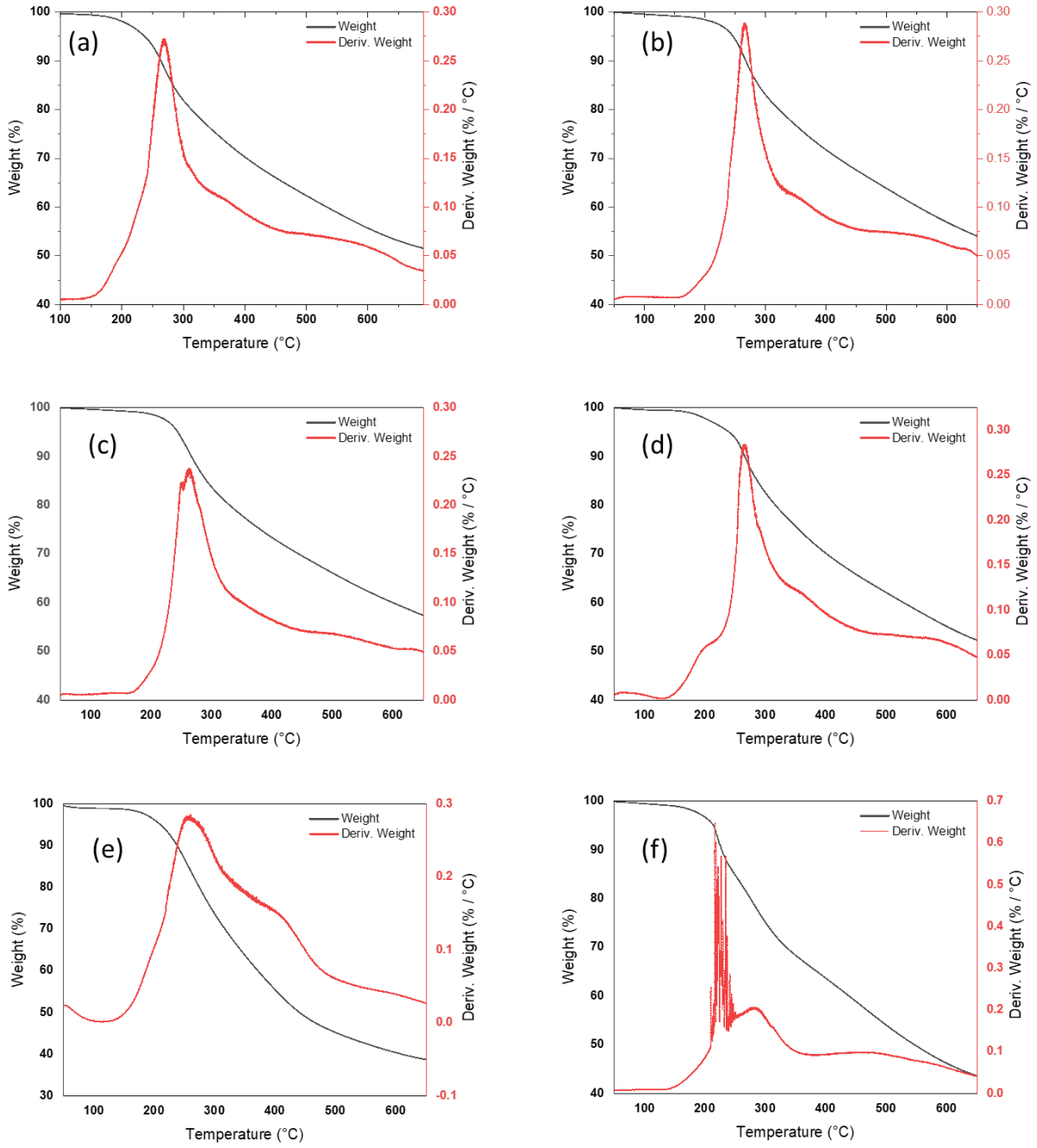

Figure 18: *TGA analysis of crude tannins: Q tannin (a), Q1 tannin (b), Q2 tannin (c), Q3 tannin (d), S tannin (e), C tannin (f).*

Table 5: *Summary of TGA analysis*

Types of tannin	Td [°C]	TDR [°C]	MDR[w%/°C]	Remaining weight at 700°C [%]
Q	200	269.21	0.273	51.4
Q1	229	265.28	0.289	52.1
Q2	226	263.6	0.238	55.5
Q3	188	265.9	0.284	50.5
S	186	260.46	0.285	37.7
C	204	216.62	0.647	42.1

DSC analysis

The Tg is described as the lowest temperature at which the molecular chain segments move. The higher the Tg, the greater the rigidity of the molecular chain. Tg was determined based on the heat flux of the tannin samples during the heating process. Due to the amorphous structure of tannins and the error of manual operation, the Tg was obtained within a certain range but not accurately. All DSC spectra are shown in ***Appendix I***. The results of DSC analysis of crude tannins are shown in ***Table 6***. Similar to the previous conclusion for TGA, sulfonation treatment increased the Tg. *Q2 tannin* with a high degree of sulfonation had the highest Tg, reaching 105 °C. In other words, the sulfonation treatment result in a decrease in the flexibility of the tannin molecules. On the other hand, a high Tg may also affect the viscosity of the final resin synthesis (Hesekamp et al., 1996).

Table 6: *Summary of Tg and Td* for crude tannins. * From TGA analysis*

	Q	Q1	Q2	Q3	S	C
Tg[℃]	85	96	105	93	96	89
Td [℃]	200	229	226	188	186	204

4.2 Fractionation of crude tannins with ASE

4.2.1 Color of extracts and total dissolved solids

Sequential ASE extraction with six solvents of increasing polarity resulted in extracts shown in ***Figure 19***. The hexane, MTBE and DCM extracts were transparent for most of the tannin samples, expect *S tannin*. The total dissolved solids shown in ***Figure 20,*** was negliable for these extrats confirming that almost no materials was extracted from *Q* and *C tannins* with low polarity solvents. The MTBE and DCM extract from *S tannin* were yellowish and significant

amounts of total dissolved solids also were found in the three first extract. Thus, *S tannin* contain more components soluble in low polarity solvents compared to the other tannins samples.

The extracts from all tannins showed yellow or brown color using acetone, EtOH, and H_2O (***Figure 19***). The yields of the total dissolved soluble confirmed that, except for *S tannin*, the yield of extracted material from other tannins was high mainly in the last three extracts. In the Q group tannins, high TDS was found in EtOH extract from *Q2 tannin*, i.e., 73.0 %. In contrast, the yield of extracted materials from *Q, Q1, and Q3 tannins* were the highest in acetone extract, i.e., 56.6%, 68.8%, and 84.3%, respectively. The solubility of tannins changes due to the heterocyclic ring opening and the introduction of hydroxyl groups (typical polar groups) which occurs during the sulfonation process (Venter, Senekal, et al., 2012). Thus, the sulfonated tannins will dissolve in solvents with higher polarity.

The extracted material from *S tannin* was mainly concentrated in acetone and EtOH extract, but both the yields were close to each other, i.e., 28.0%, and 32.6%, respectively. *C tannin*, as the only HTs, showed hydrophilicity characteristic (Fraga-Corral et al., 2020b). The extracted materials were concentrated in EtOH, and H_2O fractions, and the yields were 39.6% and 42.7%, respectively.

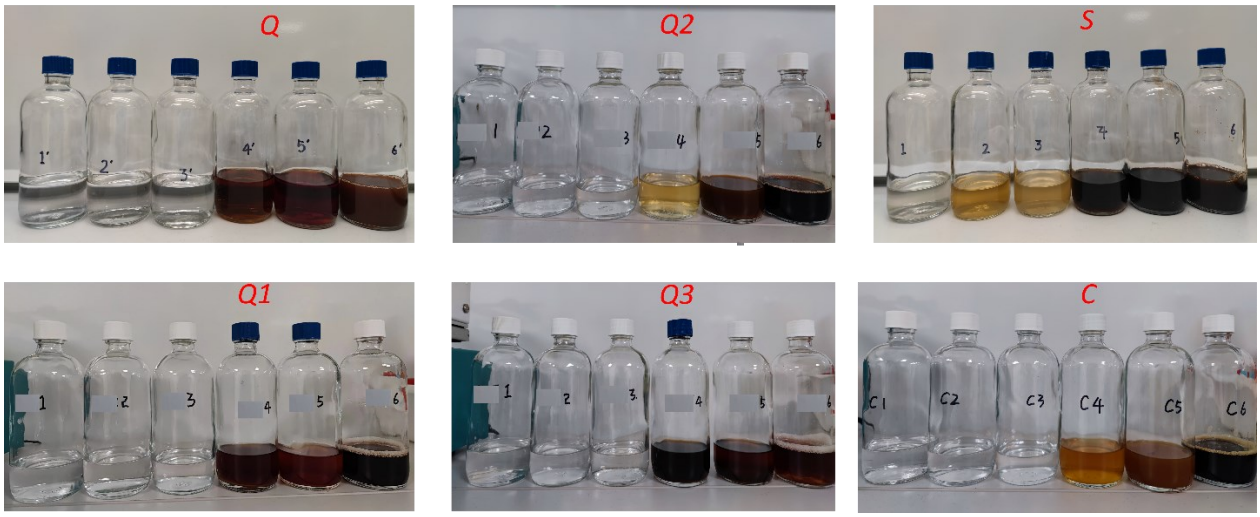

Figure 19: *Sequential ASE extracts of six crude tannins. Each tannin sample was extracted with the following solvents, from left to right, hexane, MTBE, DCM, acetone, EtOH, and H_2O.*

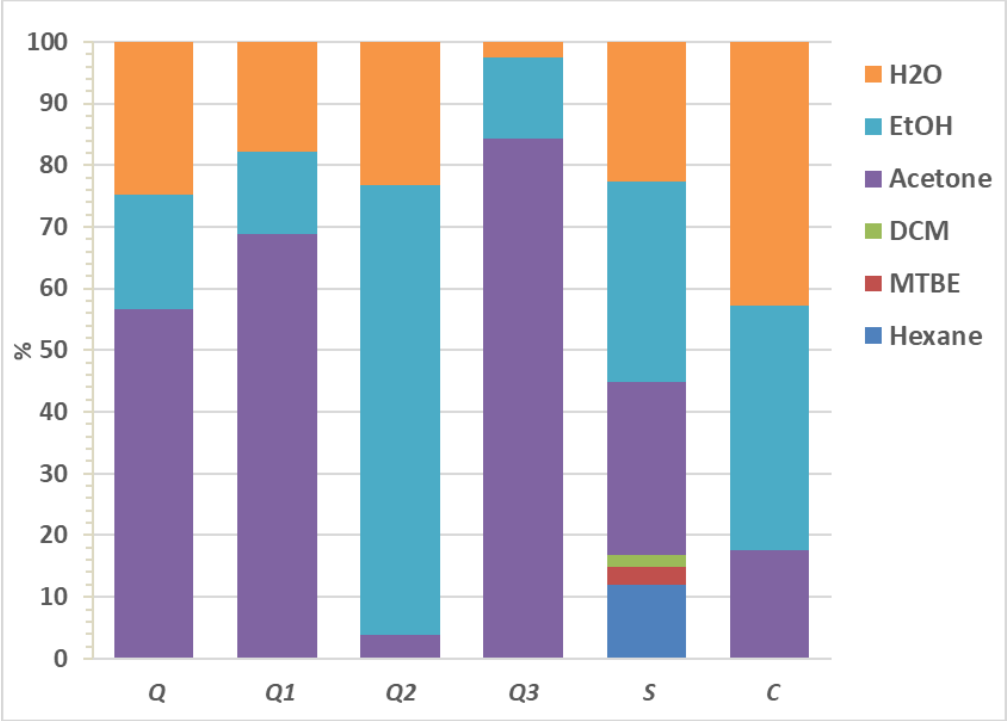

Figure 20: *Yields of extracted materials, % of total crude tannin based on total dissolved solids of extracts.*

4.2.2 Functional groups with FT-IR analysis

The FT-IR spectra for crude CTs and HTs are shown in ***Figure 21***. For *C tannin*, the broad signal at 1721cm^{-1} represents the C=O and the two intensive signals in the range of 1330-1100 cm^{-1} are aromatic structural signals of the C-O stretching of an aromatic ring of HTs. For other tannins, of CT type, the spectra show similarities. The strong signal at 1510 cm^{-1} indicates that CTs contain more aromatic rings than HTs. The signal at 1300-1100 cm^{-1} corresponds to the vibration of the phenolic ring in the CTs, where the signal at1300-1200 cm^{-1} is typical for the vibration of the B-ring and signal at 1200-1100 cm^{-1} is assigned for the band of A-ring. The band at 1115cm^{-1} is related to the C-O of the ether bridge instead of that in the aromatic ring. In addition, the aromatic torsions of CTs and HTs are also in different regions, and the C-H out-of-plane bending is 800 cm^{-1} for CTs and 750 cm^{-1} for HTs. Both CTs and HTs have obvious signal bands at 1605 and 1045 cm^{-1}, which are characteristic bands of tannins. The signal at 1605cm^{-1} is from C=C stretching aromatic, while at 1045 cm^{-1} is the C-H bend aromatic asymmetric vibration. The common representatives of C-H in 1045 cm^{-1} include glucose and ellagic acids so that band would be sharper for HTs (Tondi and Petutschnigg, 2015).

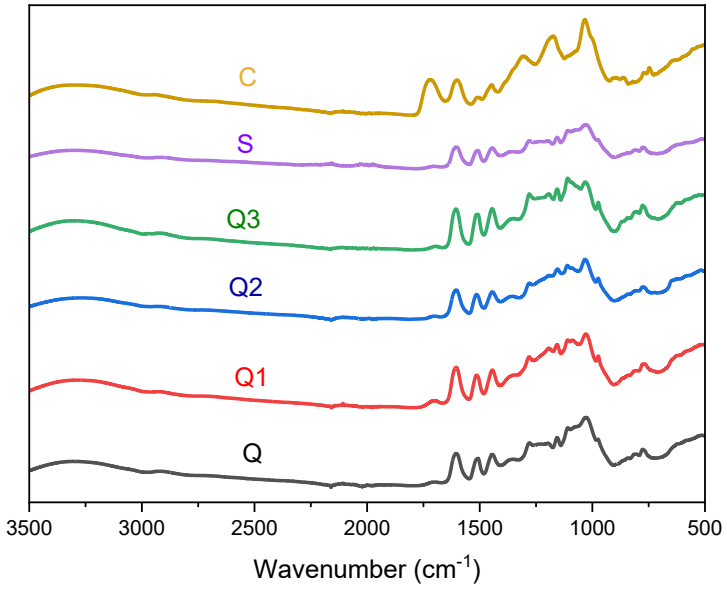

Figure 21: *FT-IR spectra of crude tannins.*

The first four obtained solvent fractions of *S tannin* could not be applied for functional group analysis because they showed an oil-like appearance. Only the dried powder-like fraction from EtOH and H_2O extract of *S tannin* were characterized by FT-IR. However, the dried fractions from acetone, EtOH, and H_2O extracts of the other tannins were all applicable for FT-IR analysis. The FTIR spectra of tannins and their extract are shown in ***Figure 22.*** Due to the higher purity, the tannin extracts had sharper signal bands in the spectra than the crude tannins.

The signal of the tannins from Q group was stronger in acetone and EtOH extract. For *Q tannin*, although the H_2O extract showed similar signal bands, the signals at 1438 and 1154 cm^{-1} corresponded to B-ring stretching C-C and vibration resorcinol-type of A-ring were significantly decreased. It means that the tannin content in the H_2O extract is low. *Q1, Q2,* and *Q3 tannins* had a similar pattern. However, due to the increased hydrophilicity of the tannins after ring-opening and purification, the H_2O extract indicated a more pronounced signal typical for the tannin structure than that of *Q tannin*. A signal corresponding to the vibration resorcinol-type of A-ring (1154 cm^{-1}) was observed in crude *S tannin* and EtOH extract, but not in H_2O extract. For *C tannin*, the signal spectra of the crude tannin and extracted factions were not significantly different.

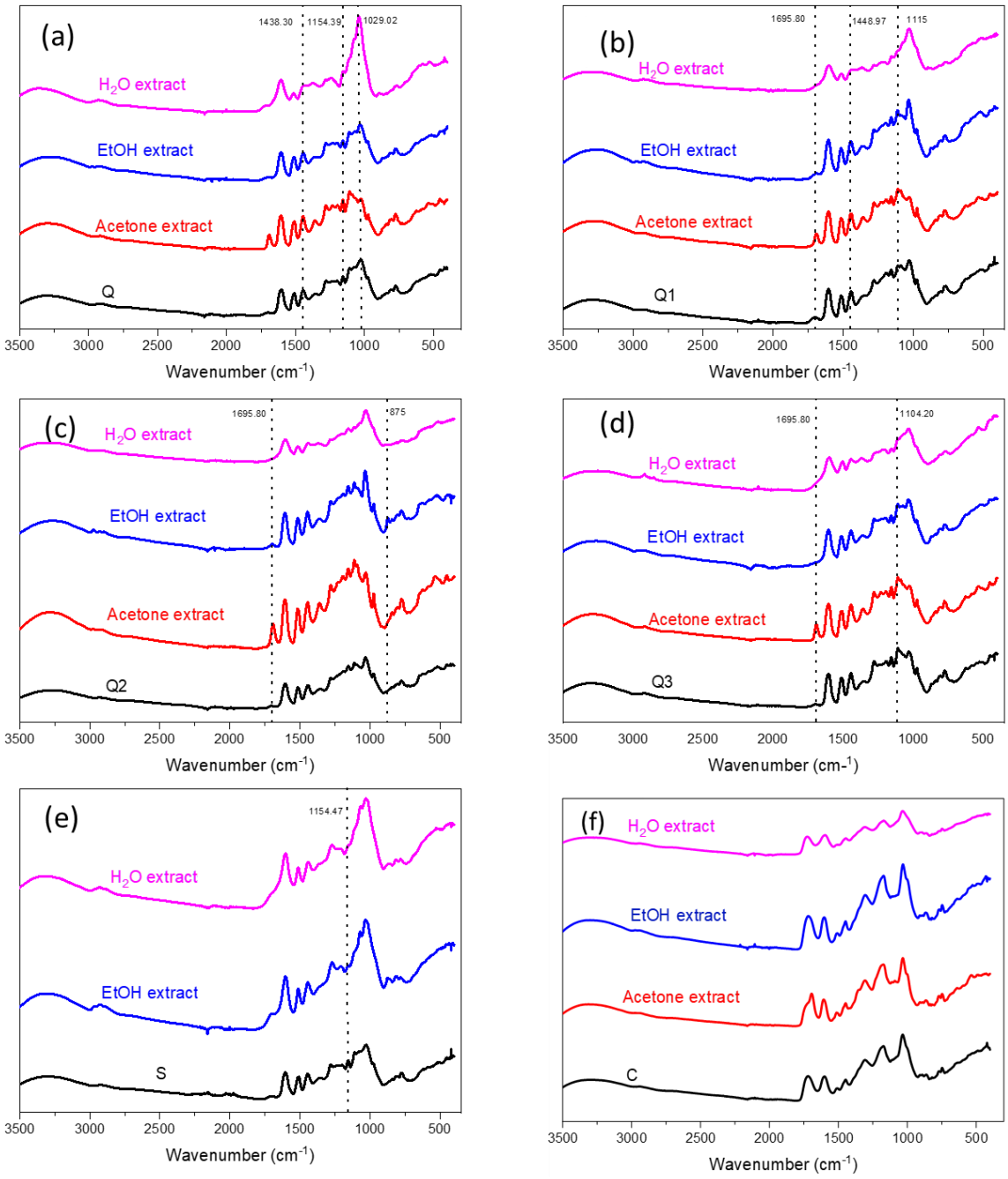

Figure 22: *FT-IR spectra of crude tannins and their corresponding extract. Q tannin (a), Q1 tannin (b), Q2 tannin (c), Q3 tannin (d), S tannin (e), C tannin (f).*

4.2.3 Molar mass determination with SEC-MALS

Figure 23 shows the SEC-MALS chromatograms of the tannins and the corresponding the isolated fractions. All samples were completely dissolved in DMSO. The chromatograms showed that the ASE extraction achieved a unimodal distribution of isolated components, as the peaks for all extracted materials are uniformly distributed and no obvious shoulders as for

the crude tannins. The peaks on chromatograms from H_2O extracted materials appeared at the shortest retention time for all tannin samples, indicating the presence of the highest molar mass components. Especially for *S tannin,* the peak corresponding to H_2O extracted material was found at the shortest retention time, indicating that the content of large molar mass components is higher. Comparing the overlap of the extract with the tannin peaks, the peaks of *Q, Q1*, and *Q3 tannins* were more similar to acetone extracts, while peaks of *Q2, S,* and *C tannins* were closer to that from EtOH extract's. In other words, the components in the obtained extracts from acetone and EtOH are the core materials in the corresponding crude tannins.

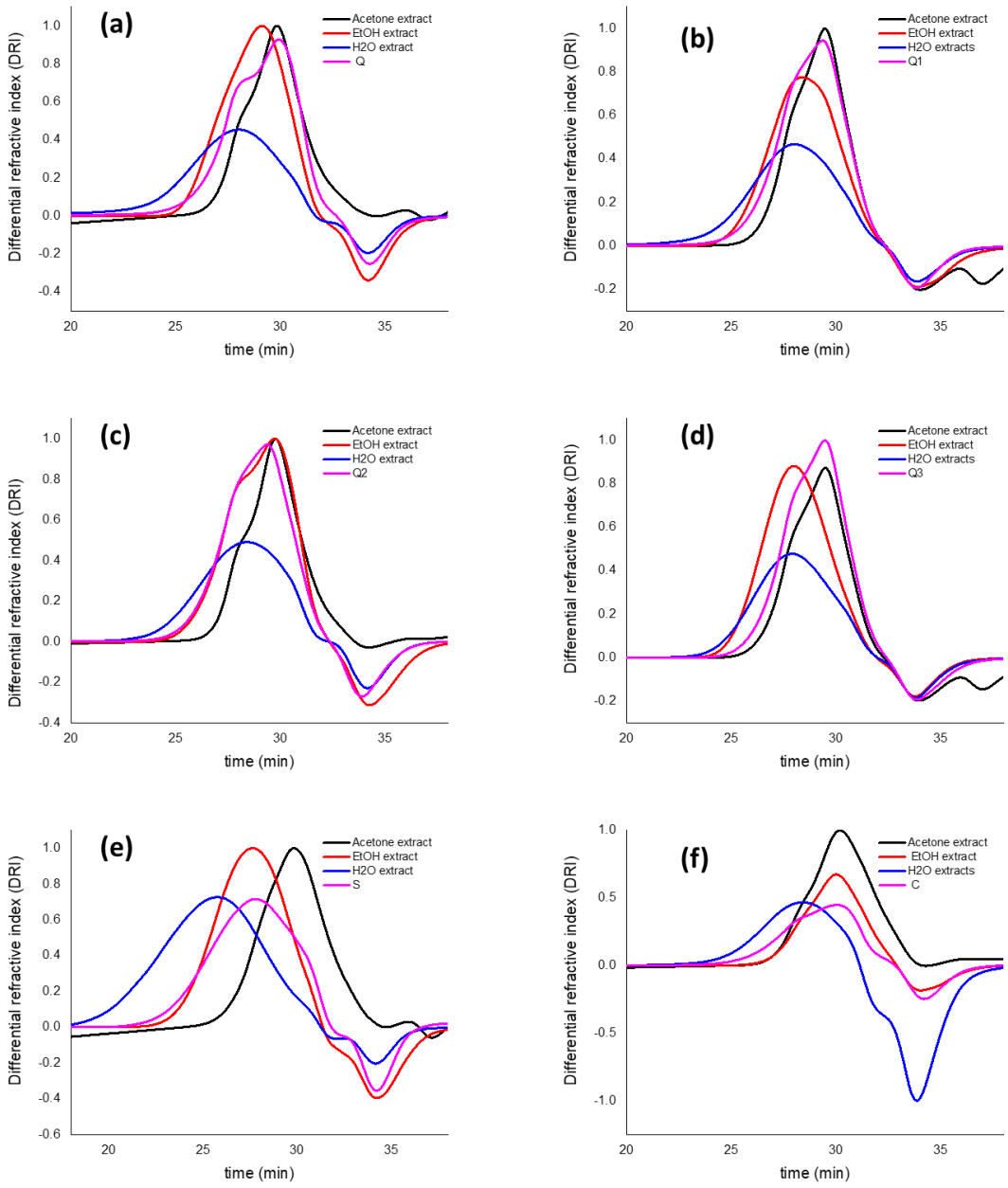

Figure 23:*SEC-MALS chromatograms of crude tannins and their extracts. Q tannin (a), Q1 tannin (b), Q2 tannin (c), Q3 tannin (d), S tannin (e), C tannin (f).*

The molar mass characteristics of crude tannins are shown in ***Table 7***. The Mw of crude tannin ranges from 1290-6790 g/mol, which is within the value form a previous study, i.e., 500 to 20 000 g/mol (Krzyzowska et al., 2017). After one week of acetylation, all tannins except *Q2* and *C tannins* were dissolved completely in the acetylation mixture. The Mw of *S tannin* was much higher than the other tannin samples at 6790 mg/mol, and the Đ was 5.80. The high *Đ* means that *S tannin* has a broad molar mass distribution, i.e., highly dispersed molar mass distribution. There was no significant difference in Mw of *Q tannins*. However, the Đ of *Q2 tannin* (*Đ* 4.65) and *Q1 tannin* (*Đ* 2.12) is significantly higher than that of untreated *Q tannin* (*Đ* 1.45), which means that the sulfonation process cleaved the bonds in the molecules, increasing the amount of lower molar mass fragments. However, the Đ of *Q3 tannin* (*Đ* 1.36) is slightly lower than that of crude *Q tannin* (*Đ* 1.45), which means that remaining impurities after the purification process results in a more uniform molar mass distribution. Similar to the *Q3 tannin*, the partially dissolved fraction of *C tannin* in acetylated mixture also exhibits a uniform molar mass distribution (*Đ* 1.55).

Table 7: *Molar mass characteristics of crude tannins.*

Types of tannin	Mw[g/mol]	Mn[g/mol]	*Đ*
Q	1900	1310	1.45
Q1	1810	850	2.12
Q2	1860	400	4.65
Q3	1830	1350	1.36
S	6790	1170	5.80
C	1290	830	1.55

4.2.4 Extractives analysis with short and long column GC

Short-column GC was used to roughly classify the extracted fractions in order to determine which of them should be subjected to long-column GC analysis and alkaline hydrolysis. The results of short column analysis are seen in ***Appendix II***. The short-column GC verified the presence of extractives in hexane, MTBE, DCM and acetone extract of S *tannin*, the indicating compounds with retention time are typical for high-boiling point steryl esters and triglycerides. While tannins in *Q tannin* and *C tannin*, the peaks in the chromatograms typical for steryl esters or triglycerides was found in acetone and EtOH fractions. However, acetone extracts contain more extractives since the obtained GC chromatograms have larger peaks.

Based on the short-column GC result it can be concluded that all the acetone extract of tannin samples showed peaks in the steryl ester /triglycerides regions. In order to verify the existence of steryl ester and triglycerides, alkaline hydrolysis was carried out. An increasing content of fatty acids after alkaline hydrolysis will be the evidence of triglycerides. Short-column GC and

GC-MS were performed for the alkaline hydrolyzed products, and the GC-MS results are shown in ***Appendix III***. The GC-MS results revealed that only a small content of fatty acids was present in the acetone extract after alkaline hydrolysis of tannins in Q groups and *C tannin*. In other words, except for *S tannin*, low amounts of steryl ester and triglycerides were present in the others crude tannin samples.

Based on the preliminary GC with short-column result, only acetone and EtOH extracts are containing extractives from Q groups and *C tannin* and thus they were analyzed further by long-column GC and GC-MS. In case of *S tannin*, the hexane, MTBE, DCM and acetone extract were selected for long-column GC and GC-MS. Long-column GC and GC-MS were used for quantitative and qualitative analyses of the volatile extractives.

The list of identified compounds from long column GC and their content information in six crude tannins can be found in ***Appendix IV***. The classification and content of extractives are summarized in ***Table 8***. *S tannin* had the highest extractive content at 104.5 mg/g, while *Q2 tannin* had the lowest at 13.4 mg/g. The dominant free sugars in all tannin extract were pentoses and hexoses.

Table 8:*Group of components analyzed by long column GC in extract from tannin samples.*

		Aldehydes **[mg/g]**	***Acids*** **[mg/g]**	***Sugars*** **[mg/g]**	***Alcohols*** **[mg/g]**	***Others*** **[mg/g]**	**Sum [mg/g]**
Q	Acetone extract	0.05	9.73	28.34	0.6	2.31	***41.03***
	EtOH extract	-	1.6	10.86	0.65	0.26	***13.38***
Q1	Acetone extract	0.28	7.45	10.02	0.62	2.25	***20.62***
	EtOH extract	-	0.97	4.62	0.67	-	***6.26***
Q2	Acetone extract	-	0.68	0.73	0.03	0.48	***1.92***
	EtOH extract	-	4.71	5.84	0.56	0.35	***11.46***
Q3	Acetone extract	-	9.21	20.74	1.5	1.55	***33***
	EtOH extract	-	1.49	0.41	0.25	0.17	***2.32***
S	Hexane extract	-	58.43	-	2.08	1.68	***62.19***
	MTBE extract	0.01	0.58	0.34	-	0.04	***0.97***
	DCM extract	0.4	1.32	1.19	0.62	0.33	***3.86***
	Acetone extract	0.46	4.86	25.62	3.63	2.94	***37.51***
C	Acetone extract	-	14.6	14.38	1.16	-	***30.14***
	EtOH extract	-	20.67	31.32	6.78	-	***58.77***

The summarized conclusion of long-column GC and GC-MS analysis result are as follows：

- In the *Q group tannins*, the dominant compounds were sugars, followed by acids. A low content of alcohols (glycerol) was also detected. It is worth noting that both the sulfonation and the purification effectively reduced the content of volatile compounds,

but the sulfonation was superior to the purification. The extractives content in untreated *Q tannin* was 54.4 mg/g, and the partially/completely sulfonated *Q tannins* contained 26.9 mg/g and 13.4 mg/g, respectively. The purified *Q3 tannin* contained 35.3 mg/g of the extractives.

- In *S tannin*, mainly lipophilic low molar mass extractives existed. For instance: fatty and resin acids were present in hexane extract, accounting for about 58% of all extractives. The second largest group in the extracts were the free sugars mainly present in acetone extract.

- *C tannin* is the only HTs, and the extracts contain a lot of sugars (pentoses and hexoses) and acids (ellagic acids and gallic acids). Since chestnut tannins are hydrolyzed tannins of the ellagic acid type (Mannelli et al., 2019), the presence of these compounds is logical. In other words, there are fewer types of volatile extractives in *C tannin* than in the other tannin samples.

4.2.5 Py-GC MS

Py-GC/MS is a powerful tool used to determine the building units of tannins and semi-quantitative content (w%) of tannins in the samples. During tannins pyrolysis, mainly C2 and C1' bonds of flavonoids cleavage occur and results in B-ring aryl groups release. However, the pyrolysis product of phloroglucinol type A-ring was difficult to detect due to its high polarity and instability. Only low intensity peaks related to phloroglucinol type A-ring moieties can be detected (Diouf et al., 2013a; Ismayati et al., 2017b).

Similar to FT-IR analysis, Py-GC/MS requires that the sample is in solid state. The first four sequentially extracted fractions of *S tannin* were not analyzed since they contain large portion of lipophilic extractives. However, other tannins and their acetone, EtOH, and H_2O extracts were analyzed by Py-GC/ MS. ***Figure 24*** to ***Figure 29*** show the pyrograms of crude tannins and their corresponding extracts. ***Table 9*** to ***Table 14*** summarize the list of main pyrolysis products and their content (w%) of crude tannins and the corresponding extracts.

Py-GC/MS results are summarized as follows:

- In the Q group tannins, resorcinol, catechol, and 4-methylcatechol are the main phenolic structural components. Most of the tannin material were found in acetone or EtOH extracts. The content of phenolic components in the H_2O extract of *Q tannin*, *Q1 tannin*, *Q2 tannin* and *Q3 tannin* were 0.2%, 3.0%, 6.9%, and 1.3%, respectively. The results indicate that the tannin content in the H_2O extract is low compared to the tannin content in acetone or EtOH extract. Resorcinol is the main products related to the A-ring of tannin, and no phloroglucinol was detected. Catechol and 4-methylcatechol are the

main products from the B-ring, and the higher content of catechol indicates that it is easier to cleave C2-C1' than the pyran ring. It is possible that there is no or little pyrogallol B-ring, since no pyrogallol was observed. The result shows that the main building block of *Quebracho* tannin was profisetidin, consisting of resorcinol A-ring and catechol B-ring, which corresponds to the previous research result (Ohara et al., 2003; Ismayati et al., 2017c).

- The pyrograms from *S tannin* were more complicated, containing many overlapping peaks. For instance: 2-methyl-1,2-propanediamine, ethyl hexopyranoside, and some resin acids were the main pyrolysis products. However, low contents were detected in EtOH and H_2O extract. Only 3.1% of catechol and 1.7% of 4-methylcatechol from the B-ring were detected, and no units related to A-ring were detected. Therefore, the building block of *S tannin* probably is profisetidin or procyanidin, However, no certain conclusion can be made from the Py-GC/MS results. What is more, compared to about 30% of the B-ring related main products (catechol and 4-methylcatechol) in the Q group, the tannin content in *S tannin* was much lower, and thus, further purification is still needed. Compared to other tannins, the relatively high amount of 4-vinylguaiacol, guaiacol, and 3-methylguaiacol may be related to lignin (Diouf et al., 2013b).

- *C tannin* is HTs, and thus, pyrogallol was the main pyrolysis product, reaching 10.8%. In addition, the high content of acetone and furfural are the main pyrolysis products originated from carbohydrates (Kaal et al., 2012), while a small amount of 4-vinylguaiacol and guaiacol are most possibly originate from lignin. The possible source of about 2% of syringol is ellagic acid ester (Varila et al., 2020).

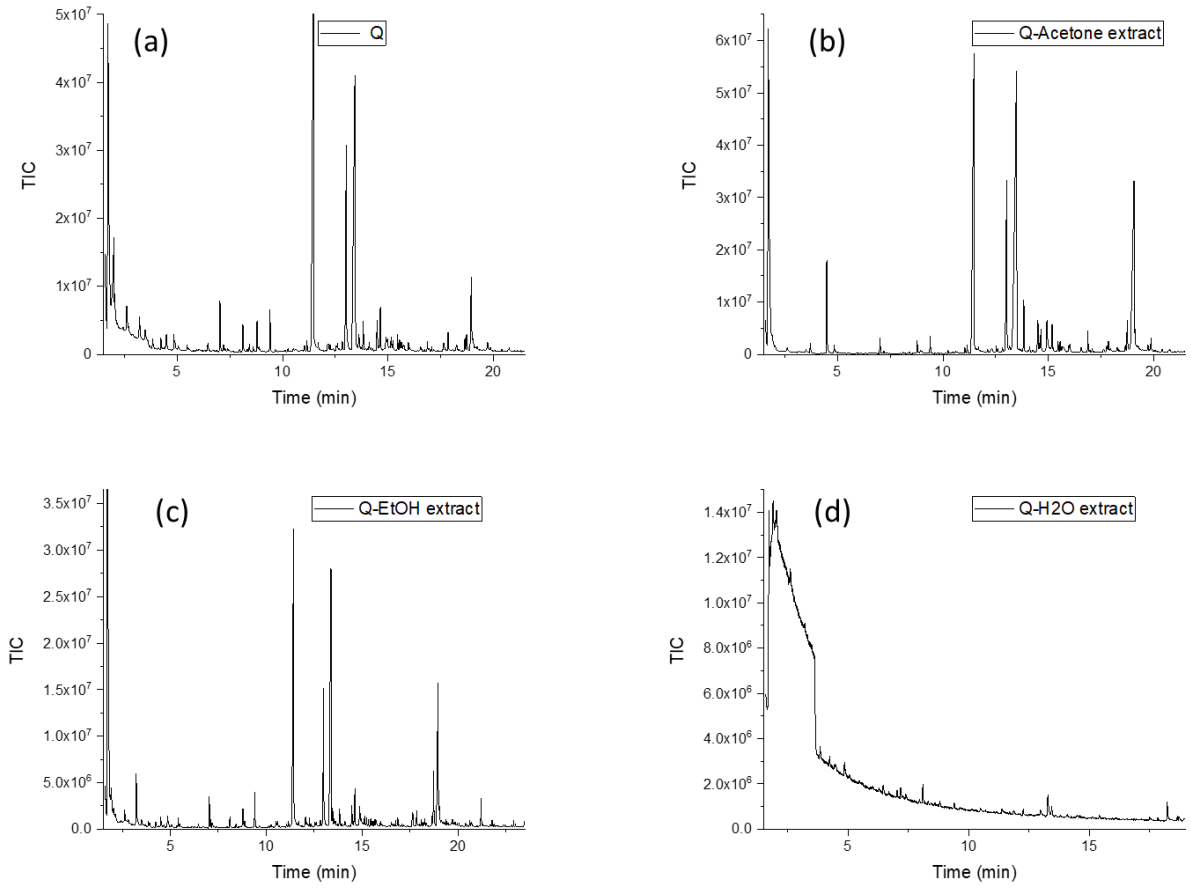

Figure 24: *Pyrograms of crude Q tannin (a) and its corresponding extracts: acetone extract (b), EtOH extract (c), H_2O extract (d).*

Table 9: *Summary of major pyrolysis products from crude Q tannin and its corresponding extracts. *Components with overlap peaks.*

Products	Retention time [min]	Q [w%]	Acetone extract [w%]	EtOH extract [w%]	H_2O extract [w%]
catechol	11.48	21.17	11.02	2.97	0.19
resorcinol	13.49	19.87	13.65	-	-
acetone + amine	1.72	18.08	-	-	-
acetone	1.72	-	9.94	4.31	10.53
4-methylcatechol	13.02	7.73	3.76	1.04	-
acetic acid	1.94	2.84	-	0.18	1.72
phenol	7.02	1.60	0.26	0.21	0.29
syringol	14.64	1.21	0.32	0.21	-
guaiacol	9.37	1.18	0.27	0.20	0.20
Resorcinol+2-methyl*	14.11	1.14	0.09	-	-
4 - hydroxy - 5,6 - dihydro -	8.10	1.03	0.03	0.08	0.69
1-methyl-1h-pyrrole	3.22	1.01	-	0.44	-
P-cresol	8.78	0.85	0.19	0.15	0.29

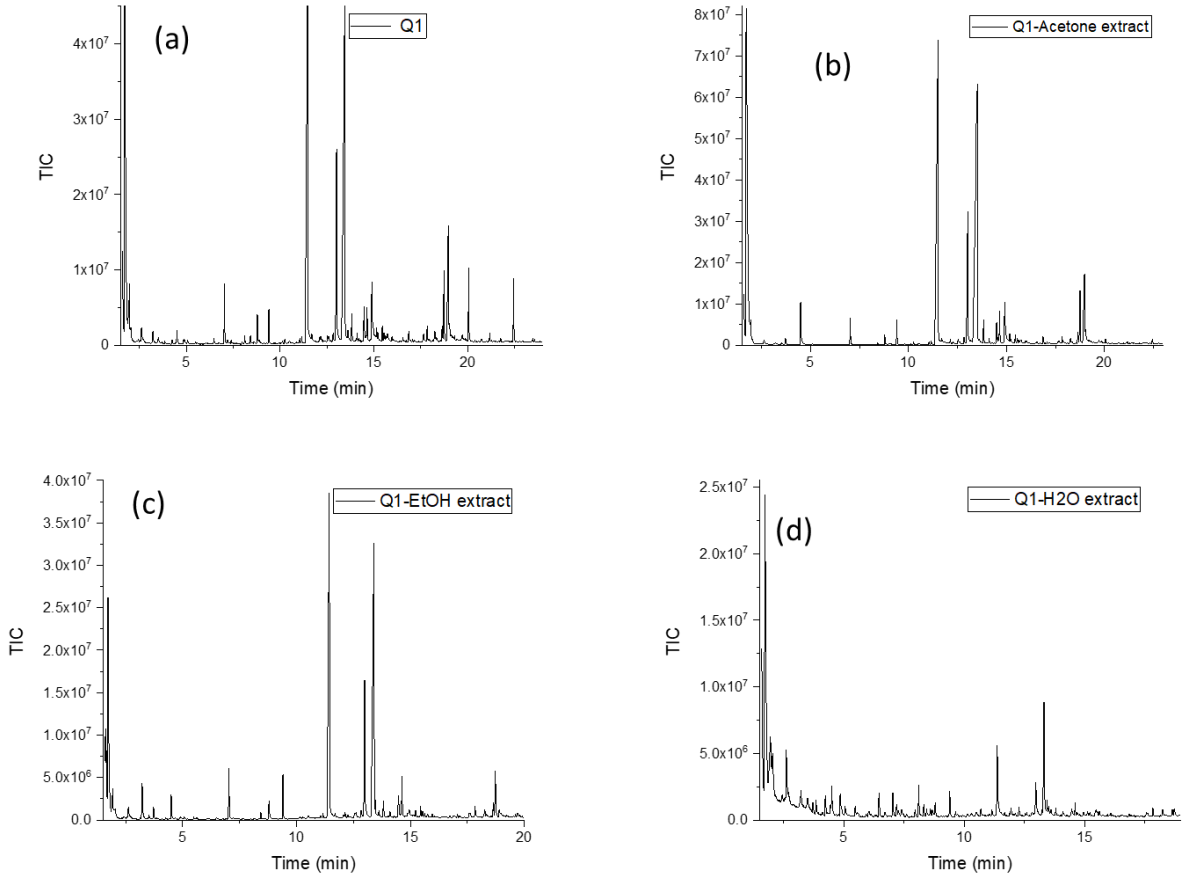

Figure 25: *Pyrograms of crude Q1 tannin(a) and its corresponding extracts: acetone extract (b), EtOH extract (c), H_2O extract (d).*

Table 10: *Summary of major pyrolysis products from crude Q1 tannin and its corresponding extracts.*

Products	Retention time [min]	Q1 [w%]	Acetone extract [w%]	EtOH extract [w%]	H_2O extract [w%]
resorcinol	13.44	21.88	17.65	3.24	1.54
catechol	11.47	19.94	16.33	3.12	0.96
acetone	1.72	15.49	16.18	-	5.20
4-methylcatechol	13.01	6.92	3.43	0.93	0.53
pyrogallol	14.90	3.13	-	0.02	-
1-hexadecanol	20.06	1.79	0.10	-	-
acetic acid	1.97	1.70	0.77	0.17	0.65
phenol	7.03	1.63	0.59	0.02	0.30
1-octadecanol	22.45	1.53	0.10	-	-
resorcinol, 2-methyl-	14.48	1.22	0.11	0.03	-
syringol	14.64	0.94	0.64	0.22	0.11
guaiacol	9.40	0.91	0.51	0.24	-
p-cresol	8.79	0.79	0.21	0.14	-

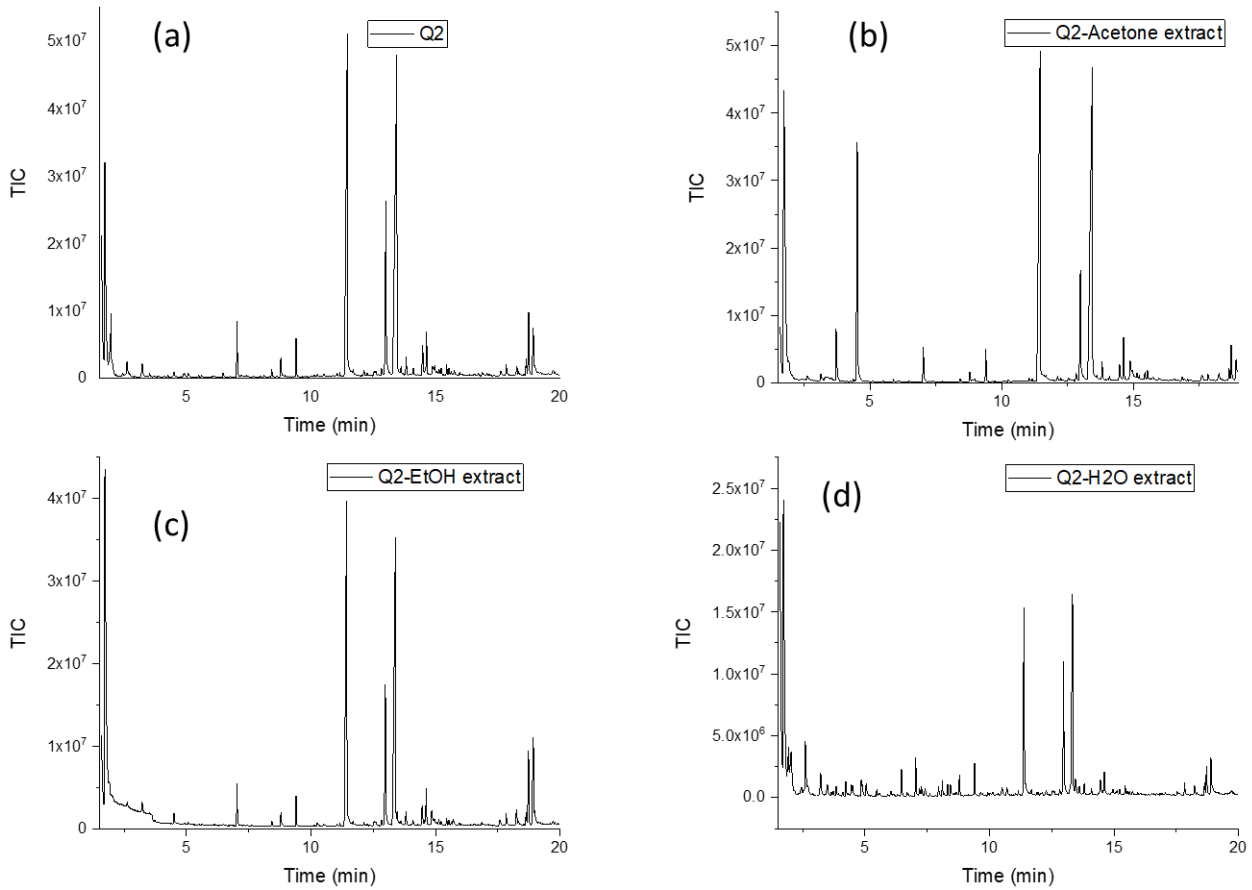

Figure 26: *Pyrograms of crude Q2 tannin (a) and its corresponding extracts: acetone extract (b), EtOH extract (c), H_2O extract (d).*

Table 11: *Summary of major pyrolysis products from crude Q2 tannin and its corresponding extracts.*

Products	Retention time [min]	Q2 [w%]	Acetone extract [w%]	EtOH extract [w%]	H_2O extract [w%]
resorcinol	13.44	28.11	1.02	16.74	2.76
catechol	11.46	24.06	0.84	15.78	2.55
acetone	1.72	12.00	0.75	-	-
4-methylcatechol	13.01	7.61	0.17	4.68	1.62
acetic acid	1.98	2.56	-	-	0.47
phenol	7.03	2.04	0.05	1.26	0.46
syringol	14.64	1.45	0.05	0.92	0.30
2-methylresorcinol	14.48	1.38	-	-	-
guaiacol	9.40	1.32	0.04	0.82	0.33
1-methyl-1h-pyrrole	2.61	0.82	-	-	-

p-cresol	8.79	0.73	0.01	0.42	0.22

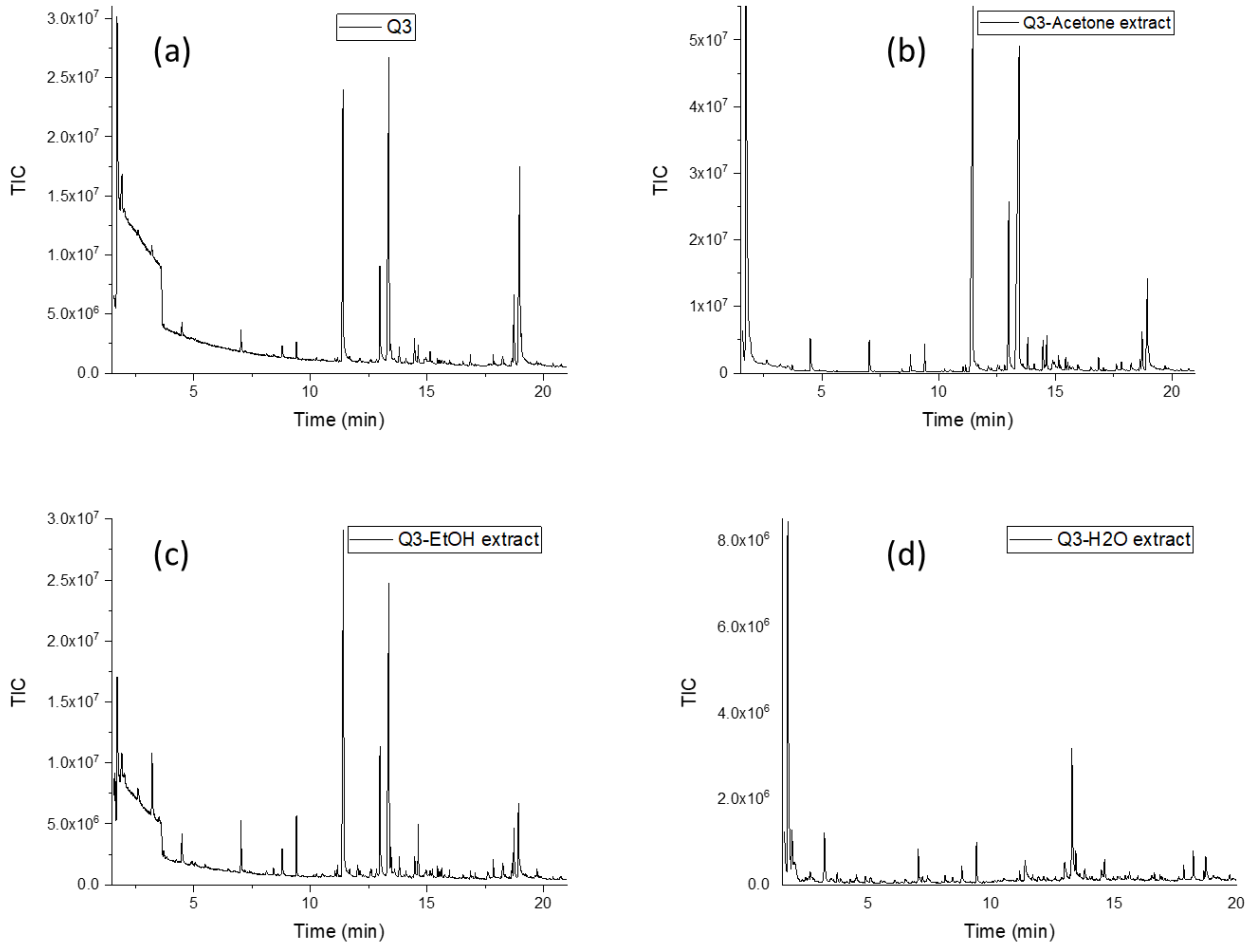

Figure 27: *Pyrograms of crude Q3 tannin (a) and its corresponding extracts: acetone extract (b), EtOH extract (c), H_2O extract (d).*

Table 12: *Summary of major pyrolysis products from crude Q3 tannin and its corresponding extracts.*

Products	Retention time [min]	Q3 [w%]	Acetone extract [w%]	EtOH extract [w%]	H_2O extract [w%]
resorcinol	13.37	22.45	19.41	2.80	0.31
acetone	1.72	19.77	21.55	1.18	0.89
catechol	11.40	14.60	19.86	2.86	0.09
4-methylcatechol	12.98	5.38	4.86	0.88	0.06
acetic acid	1.94	2.21	-	0.21	0.07
2-methyl-1,4-benzenediol	14.46	1.39	-	-	-
phenol	7.03	1.02	0.87	0.31	0.08
syringol	14.62	0.80	0.84	0.29	0.04
guaiacol, 4-vinyl	13.45	0.77	-	-	-
p-cresol	8.79	0.76	0.44	0.19	0.05

guaiacol	9.40	0.74	0.67	0.31	0.08

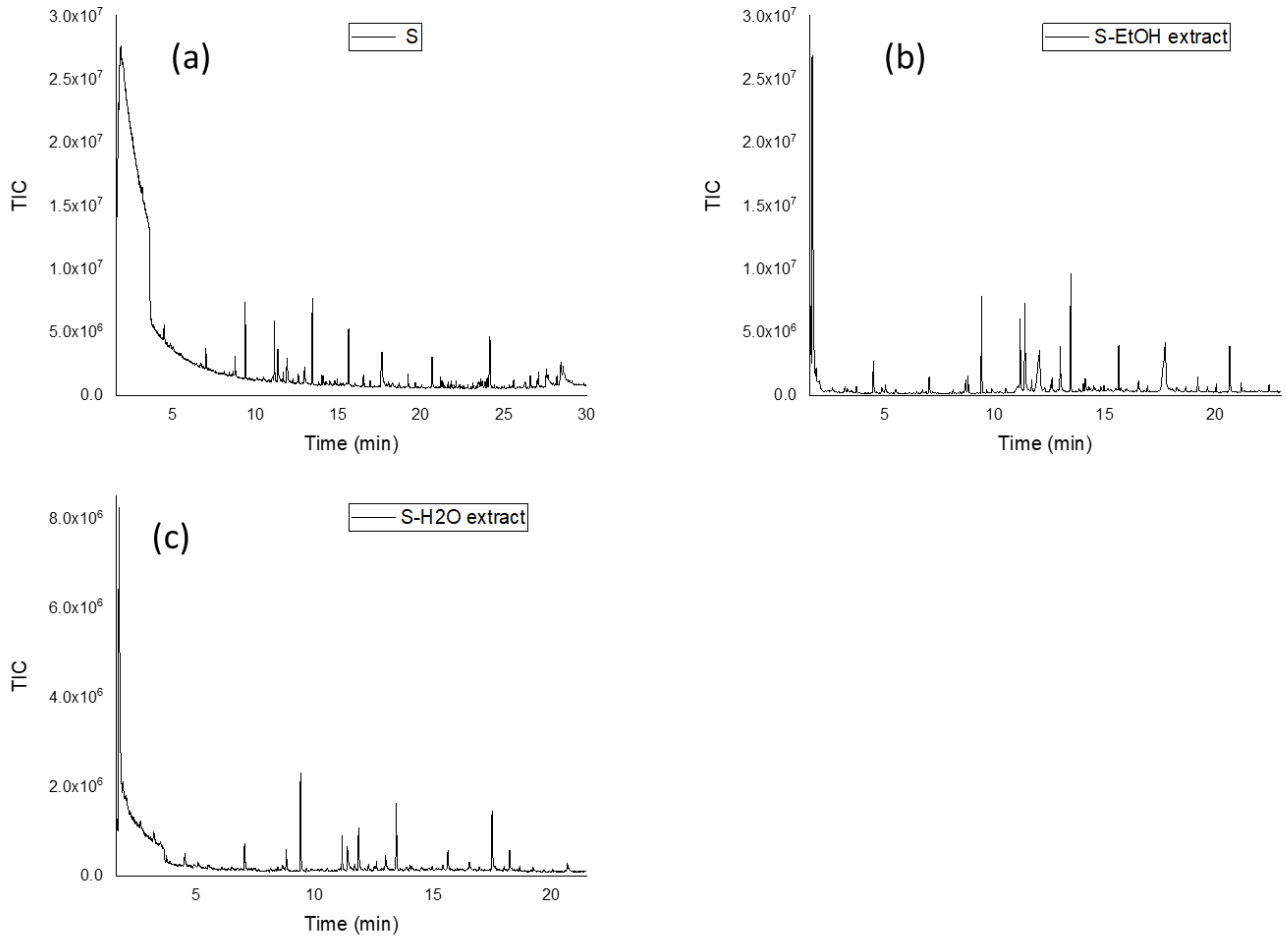

Figure 28: *Pyrograms of S tannin (a) and its corresponding extracts: EtOH extract (b), H_2O extract (c).*

Table 13: *Summary of major pyrolysis products from crude S tannin and its corresponding extracts.*

Products	Retention time [min]	S [w%]	EtOH extract [w%]	H_2O extract [w%]
2-methyl-1,2-propanediamine 2--1,2-	1.72	9.69	-	-
ethyl hexopyranoside	17.64	6.63	-	-
4-vinylguaiacol	13.44	4.99	-	1.05
guaiacol	9.39	4.72	1.48	1.68
abietic acid	28.56	4.06	-	-
3-methylguaiacol	11.15	3.80	1.12	0.56
trans-isoeugenol + vanillin	15.62	3.52	0.67	0.42
dehydroabietic acid	28.43	3.41	-	-
cytidine	11.92	3.28	-	-
catechol	11.36	3.14	1.78	0.81

7-vinyl - trimethyl - dodecahydro - phenanthrene - carboxylic acid	27.54	2.17	-	-
phenol	7.02	1.88	0.34	0.58
4-methylcatechol	12.97	1.67	0.88	-
acetic acid	1.89	1.66	-	-
p-cresol	8.78	1.50	0.32	0.39
diacetonalcohol	4.49	1.49	-	-
dihydroconiferyl alcohol	19.21	1.36	0.35	0.11
bis terephthalate	26.28	1.13	-	-
2 - hydroxymethyl - 5 - hydroxy - 2,3 - dihydro -	14.09	1.03	0.35	-
homovanillin	16.52	1.02	0.23	0.19

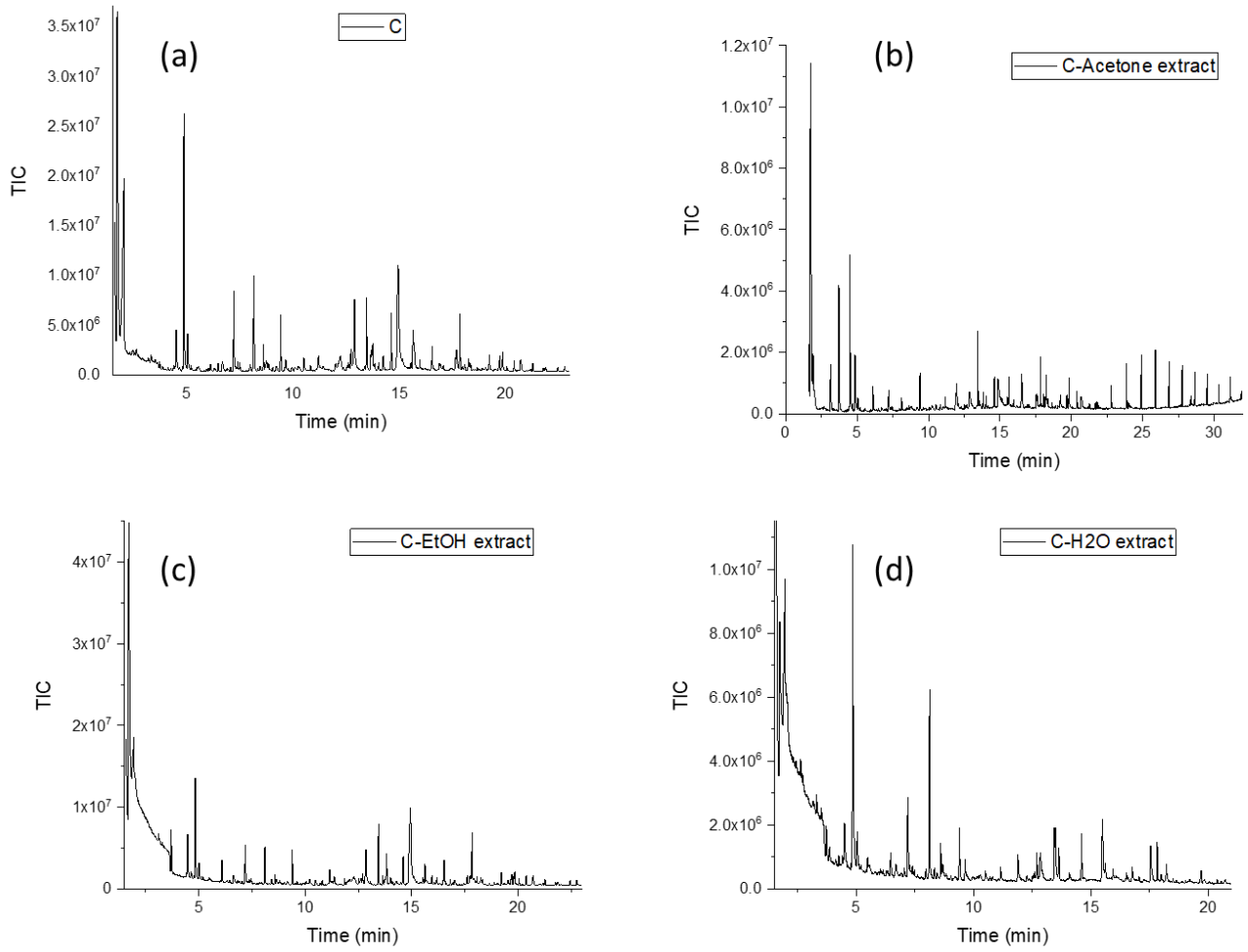

Figure 29: *Pyrograms of crude C tannin (a) and its corresponding extracts: acetone extract (b), EtOH extract (c), H_2O extract (d).*

Table 14: *Summary of major pyrolysis products of crude C tannin and its corresponding extracts.*

Products	Retention time [min]	C [w%]	Acetone extract [w%]	EtOH extract [w%]	H2O extract [w%]
acetone	1.73	18.04	4.28	-	5.85
pyrogallol	14.87	10.81	0.78	4.71	-
furfural	4.85	9.01	0.55	2.17	6.17
acetic acid	1.96	8.94	0.43	1.64	3.04
4 - hydroxy - 5,6 - dihydro -	8.13	4.03	0.11	-	3.50
5-hydroxymethylfurfural	12.84	3.81	-	-	0.68
trans-isoeugenol + vanillin+hexose	15.58	2.87	-	-	-
5-methyl-2-furfural	7.19	2.77	-	-	-
4-vinylguaiacol	13.45	1.96	0.46	1.02	0.84
furan - 3 - one - 3	4.49	1.68	-	-	-
guaiacol	9.40	1.68	0.28	0.59	0.88
syringol	14.61	1.66	0.22	0.53	0.70
4-vinylsyringol	17.83	1.60	0.31	0.82	0.56
anhydro-pentofuranose	12.20	1.58	-	-	-
cyclopent-2-en-1,4-dione	5.02	1.49	-	0.37	-
ethyl hexopyranoside	15.50	1.33	-	-	0.43
guanosine	13.49	1.18	-	0.71	1.26

A further comparison of Q group tannins is shown in ***Table 15.*** In Q group tannins, the content of resorcinol-derived products from profisetidin (resorcinol, 4-methylcatechol, resorcinol+2-methyl-) is high. It is important to note that resorcinol is the main reaction site for resin production. The content of resorcinol-derived products from profisetidin from *Q2 tannin* (complete sulfonated) was the highest, reaching 35.72%, followed by *Q1 tannin* (28.8%), *Q tannin* (28.74%), and *Q3 tannin* (27.83%). Sulfonation improves the quality of *Quebracho* tannins, which may have advantages in the subsequent resin production. The total content of about 2% of syringol and guaiacol were found in the Q group tannins, implying the presence of lignin and lignin-related substances. The possible resources of these substances are profisedin polymers or lignin. Lastly, about 0.8% of p-cresol implies the presence of p-hydroxyphrenyl B rings (Diouf et al., 2013b; Varila et al., 2020).

Table 15: *Comparison of pyrolysis GC/MS products for Q group tannins. *Components with overlap peaks.*

	Retention time [min]	Q [w%]	Q1 [w%]	Q2 [w%]	Q3 [w%]
catechol	11.48	21.17	19.94	24.06	14.60
resorcinol	13.49	19.87	21.88	28.11	22.45
acetone + amine	1.72	18.08	-	-	-
acetone	1.72	-	15.42	12.00	19.77
4-methylcatechol	13.02	7.73	6.92	7.61	5.38
acetic acid	1.94	2.84	1.70	2.56	2.21
phenol	7.02	1.60	1.63	2.04	1.02
syringol	14.64	1.21	0.94	1.45	0.80
guaiacol	9.37	1.18	0.91	1.32	0.74
Resorcinol + 2-methyl- *	14.11	1.14	-	-	-
4 - hydroxy - 5,6 - dihydro	8.10	1.03	0.27	-	0.15
1-methyl-1h-pyrrole	3.22	1.01	-	-	-
p-cresol	8.78	0.85	0.79	0.73	0.76

4.2.6 Carbohydrates with acid hydrolysis and acid methanolysis and GC

The results of acid methanolysis and GC of crude tannins are shown in ***Figure 30***. The non-cellulosic carbohydrates contents in crude tannins are summarized in ***Table 16***. *C tannin* contains the highest total amount of non-cellulosic carbohydrates of the crude tannins (162 mg/g), followed by *Q tannin* (103 mg/g), and the lowest content was found in purified *Q3 tannin* (20 mg/g). Galactose (Gal), xylose (Xyl), and glucose (Glc) were the major sugar moieties of *C tannin* and *Q tannin*, originating from galactoglucomannan and glucuronoxylan, which are typical for hemicelluloses in wood (Willför et al., 2009; Becker et al., 2021). In all tannin samples, there were more galacturonic acids (GalA) than glucuronic acids (GlcA). Relatively, the presence of high amount of GalA indicates the presence of pectin. A small content of neutral sugars, arabinose (Ara), and rhamnose (Rha) can also be present in the side chains (Liu et al., 2021; Mazri et al., 2021). The sulfonation and purification treatments exhibited excellent non-cellulose removal capacity in the Q group tannins. The total non-cellulosic carbohydrates content of *Q1 tannin*, *Q2 tannin*, and Q3 *tannin* were 37, 29, and 20 mg/g, respectively. The results show that the purification treatment is more effective for hemicellulose removing from crude tannins, compared to the sulfonation treatment.

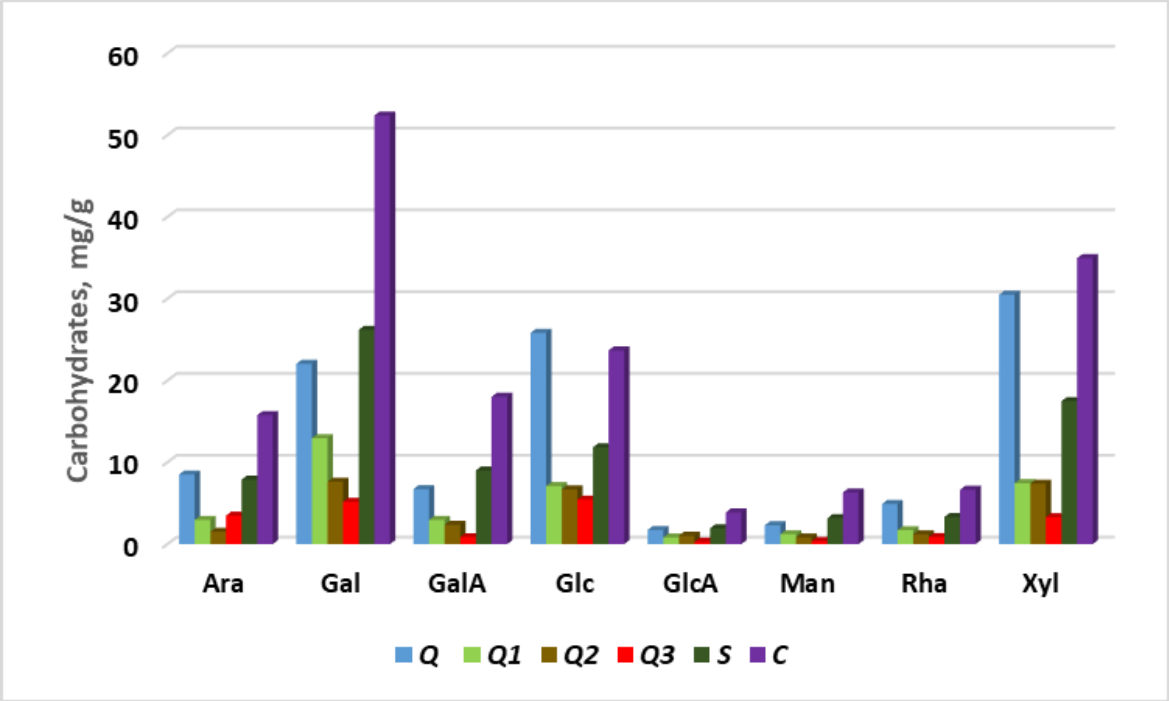

Figure 30: *Sugar units in non-cellulosic carbohydrates in tannins samples, analyzed by acid methanolysis and GC.*

The summary of acid methanolysis of crude tannins and the obtained extracts are shown in ***Figure 31***. All extracts contain non-cellulosic carbohydrates, which means that the extraction processes of tannins will inevitably include carbohydrates. However, the proportion of sugar units' content in solvents is not evenly distributed along the fraction (seen in ***Figure 20***). The non-cellulosic carbohydrates of the tannin samples were widely distributed in the H_2O extract, except for the Q3 tannins (mainly found in the acetone extract) The main sugar moieties in *S tannin* were Ara and Glc, consistent with the results described in previous studies, i.e., *Spruce* is a tree species rich in arabinose and glucose-containing hemicellulose (Normand et al., 2012).

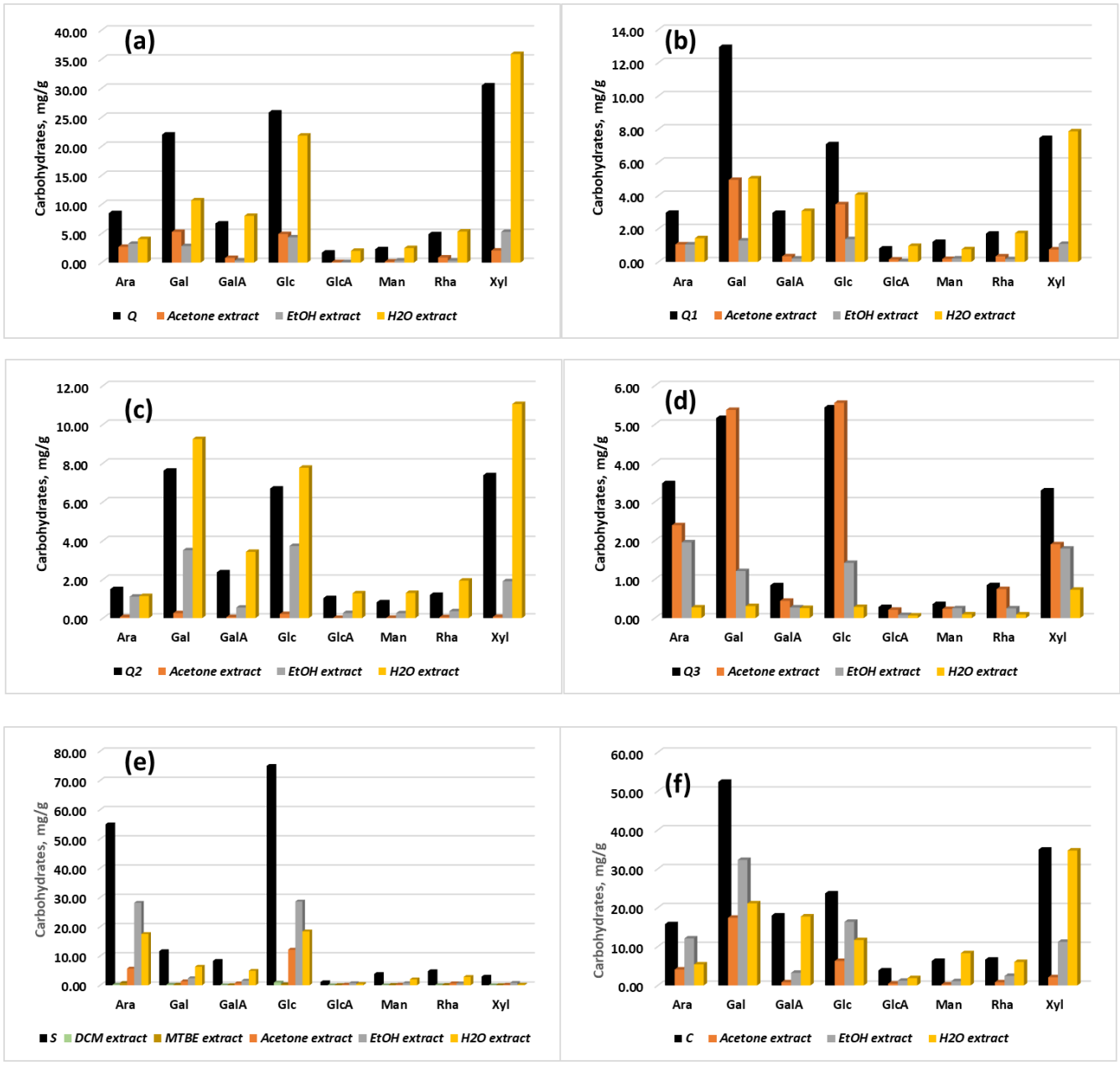

Figure 31: *Sugar units in non-cellulosic carbohydrates in tannin samples and corresponding extract from Q tannin (a), Q1 tannin (b), Q2 tannin (c), Q3 tannin (d), S tannin (e), C tannin (f).*

The results of the acid hydrolysis-GC of crude tannins are also summarized in ***Table 16***. *Q tannin* contains the most cellulose and *C tannin* the least. Similar to the total non-cellulosic content results from acid methanolysis, both sulfonation and purification treatment resulted in effective decrease in the cellulosic carbohydrates content in Q group tannins. *C tannin* contain the highest amount of total carbohydrates, which also was seen in the elemental analysis result in **4.1.2**, where *C tannin* had the highest O content.

Table 16: *Summary of total carbohydrates in crude tannins.*

	Q	***Q1***	***Q2***	***Q4***	***S***	***C***
Total hemicelluloses [mg/g]	102.52	37.12	28.59	19.72	80.83	161.66
Total cellulose [mg/g]	55.00	9.39	29.81	23.98	16.51	15.22
Total carbohydrates [mg/g]	157.52	46.51	58.40	43.73	97.33	176.88

4.2.7 NMR analyses

^{13}C NMR of crude *Q tannin and Q2 tannin*

The ^{13}C NMR spectra of crude *Q tannin* and *Q2 tannin* were overlaid and is shown in ***Figure 32***. ^{13}C NMR is mainly used to determine the linkage (C4-C6 or C4-C8) and molecular skeleton of tannins. The signal band at 156-153 ppm is the C5 and C7 bond to -OH of the resorcinol A-ring. The distinct signal at 145-140 ppm is C3' and C4' of the catechol B-ring. There is no obvious signal in the region of the pyrogallol B-ring (135-132ppm), whereas signals at 131 ppm and 118-116 ppm indicate C1' and C5' in the catechol B-ring, respectively. The strong signal at 115-110 ppm indicates predominantly C4-C8 linkage in *Q tannin* and *Q2 tannin*, while the signal peak indicating C4-C6 linkage was weak at 107-105 ppm. The tertiary C8 of resorcinol A-ring is visible at 102 ppm. In addition, intensive peaks were observed at 95-60 ppm, which is related to -CHOH in lipophilic components and -CHOH and -CH_2OH in the polysaccharidic structure.

The results indicated that the crude tannins contained a small amount of lipophilic and polysaccharide impurities, as it has discussed in extractive analysis above. A small amount of methoxyl groups from lignin was observed at 55.8 ppm. The ^{13}C NMR results indicated that *Quebracho* tannins were the profisetidin of catechol B-ring and resorcinol A-ring, consistent with the Py-GC/MS result. The linkage is dominated by C4-C8 and less by C4-C6. According to the literature, if the signal from C4-C8 linkage is higher than that from C4-C6, then the tannins would be more branched. In other words, *Quebracho* tannin is a branched tannin. (Pizzi, 1994a; Duval & Avérous, 2016)

The ^{13}C NMR spectrum of *Q2 tannin* was similar to that of *Q tannin*. However, it is worth noting that the signal corresponding to C4-C6 linkage is more abundant in *Q2 tannin*, compared to *Q tannin*. Moreover, the content of free C4 and C6 (95-90 ppm) was decreased. This means that *Q2 tannin* has a higher degree of polymerization than Q *tannin*. It is also pointed out that the sulfonation process tends to extract high molar mass tannins (Pizzi, 1994b). Finally, the results also showed that the sulfonation treatment significantly decreased lipophilic extractives

and polysaccharide impurities (95-60 ppm). Meanwhile the signal assign to lignin was non-altered at 55.8 ppm (Zhao et al., 2013).

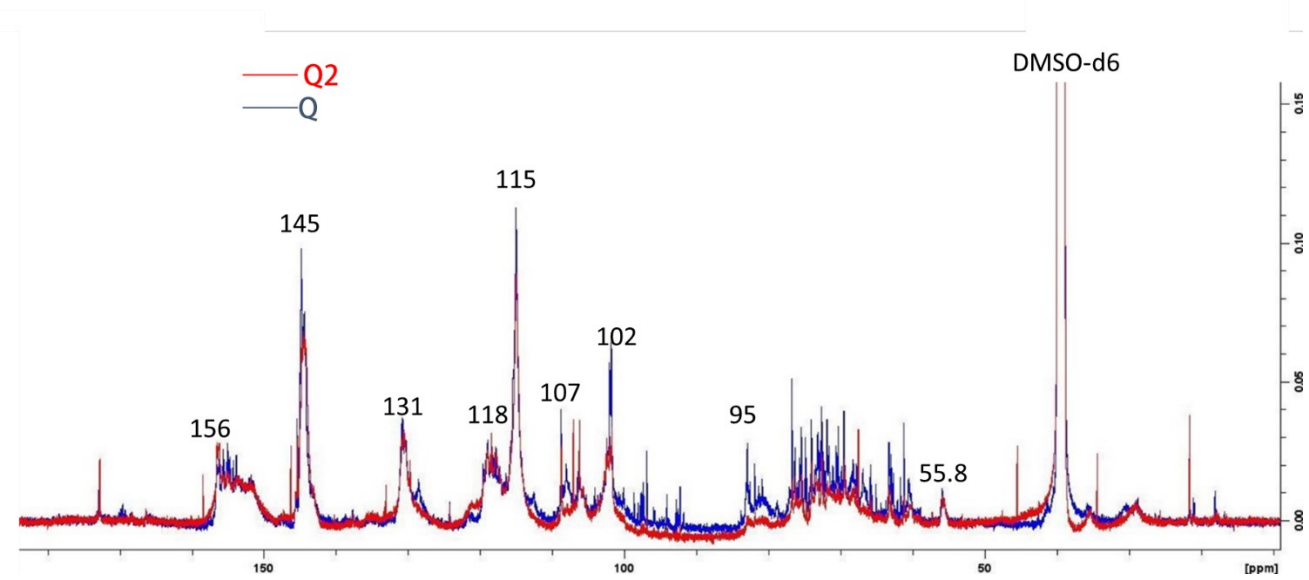

Figure 32: *^{13}C NMR spectra of Q tannin and Q2 tannin.*

HSQC NMR of crude *S, Q, C tannins*

HSQC NMR spectrum of *S tannin* is shown in ***Figure 33 (a),*** where a large amount of saturated lipophilic impurities can be seen. For the flavan-3-ol area, bond of C2'-H, C5'-H, and C6'-H assign to catechol B-ring are at (115.1, 6.90 ppm), (114.8, 6.69 ppm), and (118.6, 6.63 ppm), respectively. The C5-H, C6-H, and C8-H of resorcinol A-ring were found at (127.9, 7.2 ppm), (105-107, 6.0-6.4 ppm), (101.7, 6.12; 102.8, 6.34 ppm). The results show that the main building block of tannins in *S tannin* is also profitesidin. For carbohydrates, Ara_1 (107.9, 4.78), Ara_2 (283.9, 3.75), Glc_2 (74.7, 2.90), and Glc_3 (76.7, 3.08) were found to indicate that the sugars in *S tannin* were mainly arabinose and glucose, which corresponds to the result of acid methanolysis-GC. In addition, some lignin related components were found at (110.7, 6.94 ppm), (115.2, 6.76 ppm), (118.7, 6.76 ppm), and (83.8, 4.26 ppm), corresponding to G2, G5, G6 and β-O-4 from lignin, respectively. Besides, some resin and fatty acid corresponding esters, and stilbene were also found. Therefore, HSQC NMR results indicate that crude *S tannin* contained a large portion of different impurities (resin and fatty acids, lignin, carbohydrates), and its building block is mainly prodfisidin (Yuan et al., 2011; Girard and Bee, 2020b)

Q tannin sample represents the Q group tannins, and the HSQC NMR spectrum is shown in ***Figure 33 (b)***. The carbohydrate impurities in the area were mainly Glc (70-60.17, 3.58-3.13 ppm) and Xyl (75.7-60.17, 3.67-3.05 ppm). The signals in the flavan-3-ol area are mainly from

the resorcinol A-ring and catechol B-ring. Moreover, some lignin/tannin linkage with carbohydrates was also detected due to the spectrum signal related to Γ-ester (64.5, 4.2 ppm), -OCH_3 (55.4, 3.7 ppm), phenylglcosides (100.0, 5.1 ppm) (Yuan et al., 2011).

The HSQC NMR spectrum of *C tannin*, as shown in ***Figure 33 (c)***, which is relatively less complicated than CTs. Carbohydrates in the tannin sample corresponding to signal (76.2-68.1, 4.94-4.90 ppm) and carbohydrates impurities signal range of (74.8-70.2, 3.20-2.91 ppm), which are mainly related to glucopyranose. Therefore, the sugar components in the impurities in *C tannin* is mainly glucuronoarabinoxylan, and part of ellagic acid was also detected. The results are consistent with the described carbohydrates analysis and Py-GC/MS analysis.

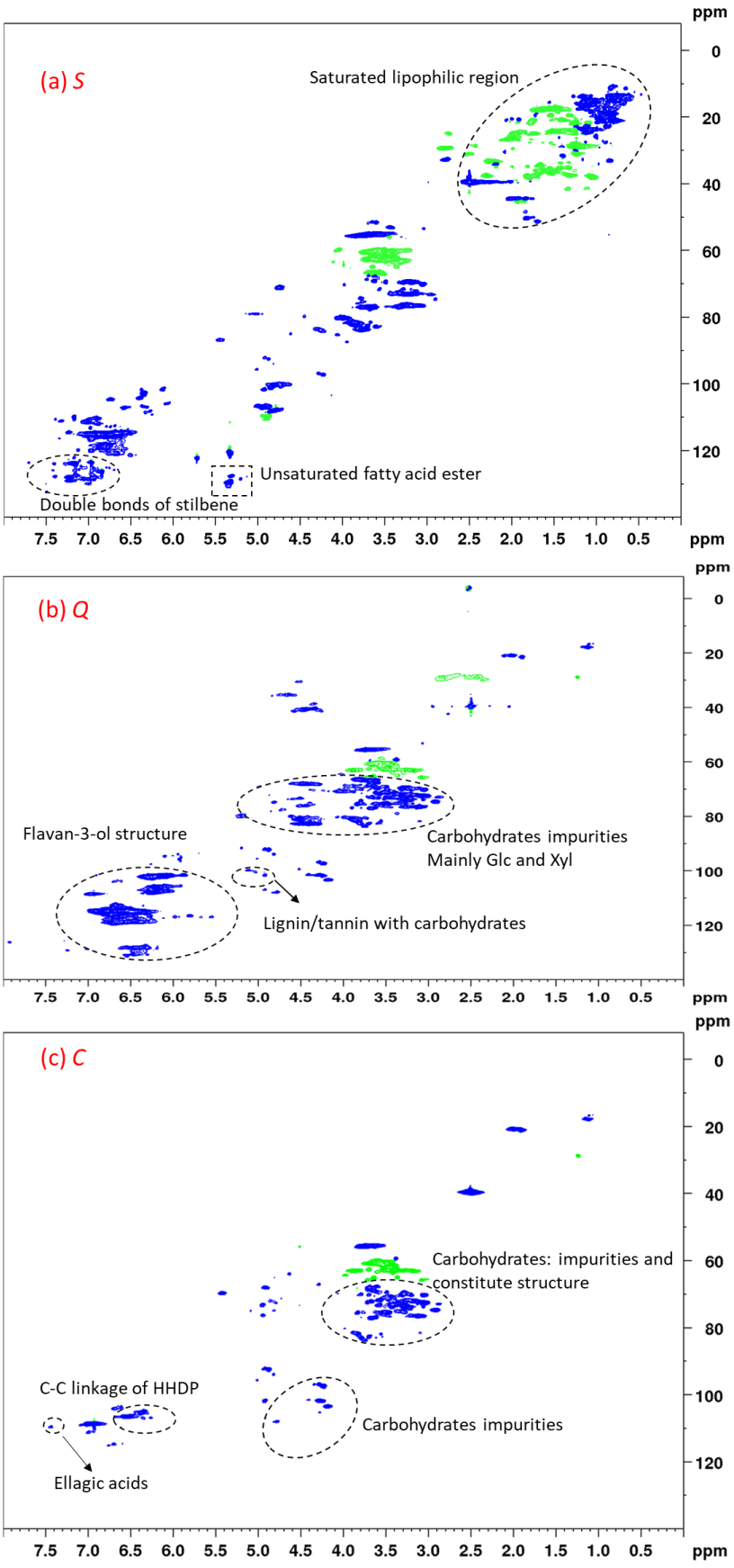

Figure 33: *HSQC spectra of S tannin (a), Q tannin (b) C tannin (c).*

^{31}P NMR of crude *Q tannin*

^{31}P NMR mainly uses the signal of -OH groups in the spectrum for their quantitative analysis (seen in ***Figure 34)***. The ^{31}P NMR spectrum was divided into aliphatic-OH, B-ring, and A-ring regions. Among them, the signal at 146-145 ppm, 140-138.8 ppm, 137.9-137.4 ppm represents -OH of C-ring, -OH of catechol B-ring, and -OH of phenolic A-ring, respectively. However, signal at range of 144-142 ppm is from pyrogallol. Using cholesterol as integration standard (IS) in 0.667 mmol/g (mmol/g crude tannin). The catechol and pyrogallol B-ring contents were 3.3 mmol/g and 0.33 mmol/g, respectively. The ratio of pyrogallol to catechol was 0.1. This corresponds with the literature value of 0 to 0.1 (Makino et al., 2011b). The resorcinol A-ring amount was about 1.21 mmol/g.

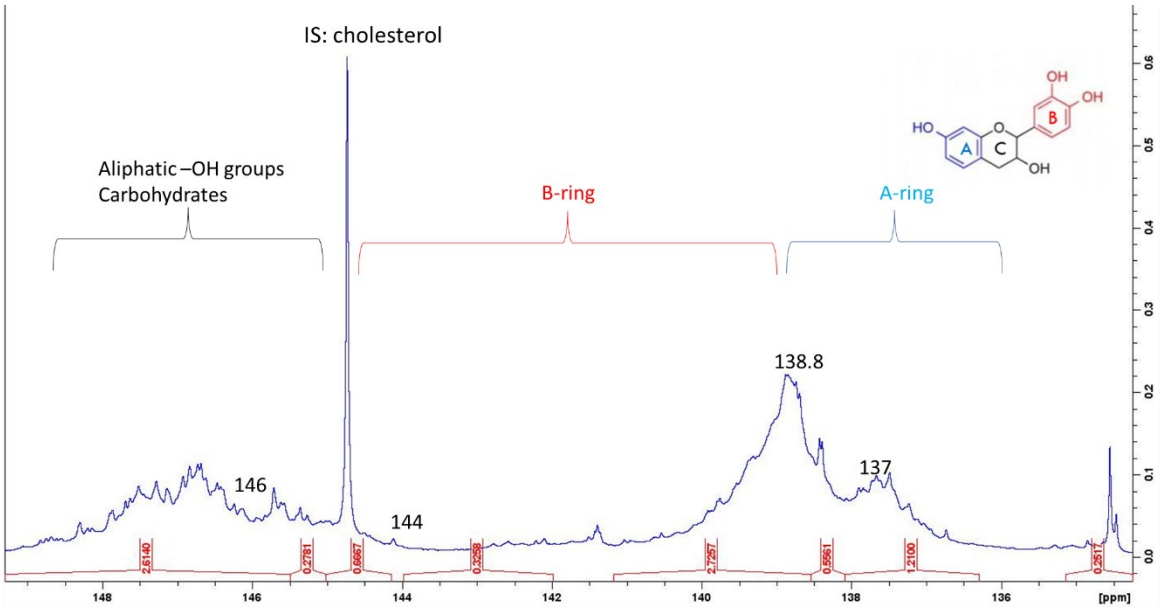

Figure 34: *^{31}P NMR result of Q tannin.*

4.3 Total chemical composition of crude tannins

A summary graph of the total chemical composition of tannins is shown in ***Figure 35***, the results are based on the w% of oven-dried tannin. The tannin content is calculated by subtracting the ash, non-cellulosic carbohydrates, cellulose and extractives content from 100%. In terms of tannin content, CTs samples were superior to HTs sample, i.e., *C tannin* had the lowest content the tannin content (71%) compared to the others. In the Q group tannins, the purified *Q3 tannin* sample had the highest tannin content, reaching 91%, followed by *Q1 tannin* (89%), Q2 tannin (87%), and *Q tannin* (76%). Both purification and sulfonation have advantages in decreasing the content of carbohydrates. The sulfonated tannins had significantly lower extractives content but higher ash content mainly due to the introduction of sulfur containing substances. In addition, *S tannin,* and *C tannin* were similar in that both have high

content of total carbohydrates and extractives. Thus, they may not have a competitive advantage among other tannins in resin production, and further purification would be required. However, according to the literature (seen in **section 2.2.2**), due to the excellent performance of HTs in the field of food or medicine, the high potential of *C tannin* in other fields should be also considered.

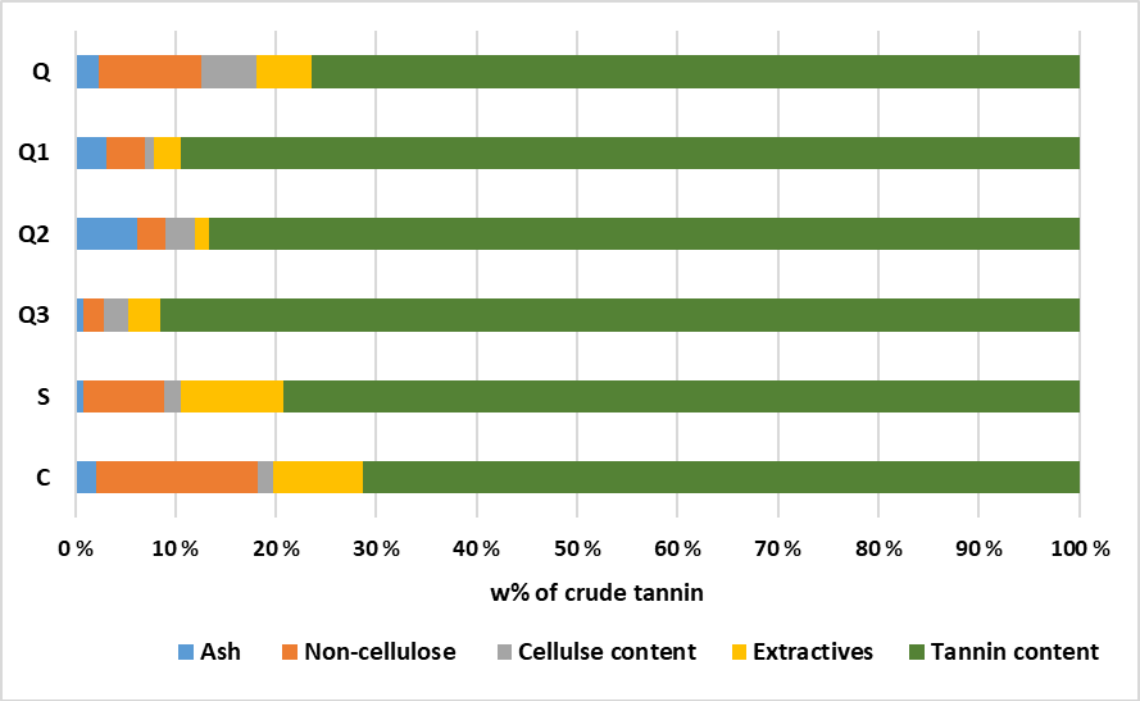

Figure 35: *Total summary of composition of crude tannins.*

5. Conclusions

In this thesis, the aim was to extensively characterize six different tannin samples to provide information on their feasibility as petroleum-derived phenol substitutes and to assess their potential for resin production or other applications. Although tannins have been well described in detail in literature, the properties of tannins obtained from different species, different sources, with different extraction methods or different industrial processes vary greatly.

The tannin samples were obtained from *Quebracho* (*Q tannin*, *Q1 tannin*, *Q2 tannin*, *Q3 tannin*), *spruce* (*S tannin*) and *chestnut* (*C tannin*). *Quebracho* is one of the well-known sources of condensed tannin, with high phenolic content and purity, mainly growing in South America. *Spruce* is main tree resource in Europe. *Chestnut* is a famous source of hydrolysable tannin, spreading all over the word.

All tannin samples were extracted by ASE with six different solvents. The SEC-MALS results confirm that after ASE extraction, the unimodal distribution was reached, which makes the extracted materials more uniform and beneficial to the accuracy of subsequent study results.

GC and GC-MS is a powerful tool to determine the composition of tannin samples. The results show that all tannins inevitably contain impurities (i.e., carbohydrates, extractives, and lignin). The purified *Q3 tannin* has the highest tannin content, followed by *Q1 tannin*, *Q2 tannin*, *S tannin, Q tannin*, and *C tannin*. The purification treatment decreased the carbohydrates content and inorganic impurities. The sulfite-treatment effectively decreased the carbohydrates and extractives content but introduced sulfur containing components, which also lead to a significant increase in the ash content. *S tannin* contains higher content of lipophilic impurities and is not competitive in purity compared to industrially treated *Quebracho*. Further impurity removal processes are essential if spruce is to be accepted as a raw material to produce phenol-free resins. Although *C tannin* has the same profile as *S tannin*, the composition is not as diverse as *S tannin,* only sugars and alcohols were found in the extractives analysis. Further purification of all tannin samples is needed since the content of carbohydrates and extractives may have a negative effect in resin synthesis.

In terms of structure, the py-GC MS and different NMR including ^{13}C NMR, HSQC NMR ^{31}P NMR have been carried out. The results have confirmed that the building block of CTs (*Quebracho* and *Spruce*) was profistdine composed of catechol A-ring and resorcinol B-ring. *Quebracho* was a branched tannin mainly linked by the C4-C8 bond. The *C tannin* consists of a sugar core and ellagic acids.

Thermal-gravimetric properties have been explored by TGA and DSC analysis. In the Q groups, the Td and Tg were increased due to sulfonation, and the thermal stability was improved. The degree of polymerization of *Q1 tannin* and *Q2 tannin* were higher than the *Q*

tannin. With the self-condensation reaction during sulfonation process, tannin molecules with high molar mass and high degree of polymerization are obtained. On the other hand, due to the opening of the heterocyclic ring, the free reactive sites (C4, C6) are increasing, which is beneficial for synthesizing phenolic resins.

C tannin as the only HTs, had the lowest tannin content. The low tannin content and low reactivity with formaldehyde make HTs less popular in the market for phenol-free resin production (Zhou and Du, 2019). However, HTs have a great potential in medical and food applications.

Finally, since there are many factors that affect actual resin production. The results of the characterization and analysis summarized above are only some of the factors. The feasibility of the tannin samples as a substitute for phenol-free resin needs to be confirmed by the various test for resin polymer. The applicability of synthetic resins needs to be further explored.

References

ADAA (2022). *Glossary Ash Development Association of Australia*. https://www.adaa.asn.au/knowledge/ccp-handbook/glossary. 16/05/2022

Aguilar, C. N., Rodríguez, R., Gutiérrez-Sánchez, G., Augur, C., Favela-Torres, E., Prado-Barragan, L. A., Ramírez-Coronel, A., & Contreras-Esquivel, J. C. (2007). Microbial tannases: Advances and perspectives. *Applied Microbiology and Biotechnology*, *76*(1), 47–59. https://doi.org/10.1007/S00253-007-1000-2

Arbenz, A., & Avérous, L. (2015). Chemical modification of tannins to elaborate aromatic biobased macromolecular architectures. *Green Chemistry*, *17*(5), 2626–2646. https://doi.org/10.1039/C5GC00282F

Becker, M., Ahn, K., Bacher, M., Xu, C., Sundberg, A., Willför, S., Rosenau, T., & Potthast, A. (2021). Comparative hydrolysis analysis of cellulose samples and aspects of its application in conservation science. *Cellulose* *28*(13), 8719–8734. https://doi.org/10.1007/S10570-021-04048-6

Benaiges, A., & Guillén, P. (2007). Botanical extracts. *Analysis of Cosmetic Products*, 345–363. https://doi.org/10.1016/B978-044452260-3/50044-9

Bianchi, S., Kroslakova, I., Janzon, R., Mayer, I., Saake, B., & Pichelin, F. (2015). Characterization of condensed tannins and carbohydrates in hot water bark extracts of European softwood species. *Phytochemistry*, *120*, 53–61. https://doi.org/10.1016/J.PHYTOCHEM.2015.10.006

Braghiroli, F. L., Amaral-Labat, G., Boss, A. F. N., Lacoste, C., & Pizzi, A. (2019). Tannin gels and their carbon derivatives: A Review. *Biomolecules*, *9*(10). https://doi.org/10.3390/BIOM9100587

Chandra, P., Enespa, Singh, R., & Arora, P. K. (2020). Microbial lipases and their industrial applications: A comprehensive review. *Microbial Cell Factories*, *19*(1). https://doi.org/10.1186/S12934-020-01428-8

CHEBI. *hydrolysable tannin (CHEBI:78689)*. https://www.ebi.ac.uk/chebi/searchId.do?chebiId=CHEBI:78689. *21/04/2022*

CNA. (2009). *Energy and the risks to national security*. 05/04222

Crestini, C., Lange, H., & Bianchetti, G. (2016). Detailed Chemical Composition of Condensed Tannins via Quantitative ^{31}P NMR and HSQC Analyses: Acacia catechu, Schinopsis balansae, and Acacia mearnsii. *Journal of Natural Products*, *79*(9), 2287–2295. https://doi.org/10.1021/ACS.JNATPROD.6B00380

Cuong, D. X., Hoan, N. X., Dong, D. H., Thuy, L. T. M., Thanh, N. van, Ha, H. T., Tuyen, D. T. T., & Chinh, D. X. (2019). Tannins: Extraction from Plants. *Tannins - Structural properties, biological properties and current knowledge*. https://doi.org/10.5772/INTECHOPEN.86040

Das, A. K., Islam, M. N., Faruk, M. O., Ashaduzzaman, M., & Dungani, R. (2020a). Review on tannins: Extraction processes, applications and possibilities. *South African Journal of Botany*, *135*, 58–70. https://doi.org/10.1016/J.SAJB.2020.08.008

Das, A. K., Islam, Md. N., Faruk, Md. O., Ashaduzzaman, Md., Dungani, R., Rosamah, E., Hartati, S., & Rumidatul, A. (2019). Hardwood tannin: sources, utilizations, and prospects. *Tannins structural properties, biological properties and current knowledge*. https://doi.org/10.5772/INTECHOPEN.86003

De Hoyos-Martínez, P. L., Merle, J., Labidi, J., & Charrier – El Bouhtoury, F. (2019). Tannins extraction: A key point for their valorization and cleaner production. *Journal of Cleaner Production*, *206*, 1138–1155. https://doi.org/10.1016/J.JCLEPRO.2018.09.243

Dentinho, M. T. P., Paulos, K., Francisco, A., Belo, A. T., Jerónimo, E., Almeida, J., Bessa, R. J. B., & Santos-Silva, J. (2020). Effect of soybean meal treatment with Cistus ladanifer condensed tannins in growth performance, carcass and meat quality of lambs. *Livestock Science*, *236*, 104021. https://doi.org/10.1016/J.LIVSCI.2020.104021

Diouf, P. N., Tibirna, C. M., García-Pérez, M.-E., Royer, M., Dubé, P., Stevanovic, T., Diouf, P. N., Tibirna, C. M., García-Pérez, M.-E., Royer, M., Dubé, P., & Stevanovic, T. (2013a). Structural elucidation of condensed tannin from picea mariana bark. *Journal of Biomaterials and Nanobiotechnology*, *4*(3), 1–8. https://doi.org/10.4236/JBNB.2013.43A001

Dotan, A. (2014). Biobased Thermosets. *Handbook of thermoset plastics*, 589–599. https://doi.org/10.1016/B978-1-4557-3107-7.00015-4

Duan, J., Li, Y., Gao, H., Yang, D., He, X., Fang, Y., & Zhou, G. (2020). Phenolic compound ellagic acid inhibits mitochondrial respiration and tumor growth in lung cancer. *Food & Function*, *11*(7), 6332–6339. https://doi.org/10.1039/D0FO01177K

Dunky, M. (2021a). Wood Adhesives Based on Natural Resources: A critical review: Part III. Tannin- and lignin-based adhesives. *Progress in adhesion and adhesives* (Vol. 6). John Wiley & Sons, Ltd. https://doi.org/10.1002/9781119846703.CH10

Duval, A., & Avérous, L. (2016). Characterization and physicochemical properties of condensed tannins from acacia catechu. *Journal of Agricultural and Food Chemistry*, *64*(8), 1751–1760. https://doi.org/10.1021/ACS.JAFC.5B05671

Falcão, L., & Araújo, M. E. M. (2018). Vegetable tannins used in the manufacture of historic leathers. *Molecules (Basel, Switzerland)*, *23*(5). https://doi.org/10.3390/MOLECULES23051081

Feng, S., Cheng, S., Yuan, Z., Leitch, M., & Xu, C. (2013). Valorization of bark for chemicals and materials: A review. *Renewable and Sustainable Energy Reviews*, *26*, 560–578. https://doi.org/10.1016/J.RSER.

Ferreira, E. C., Nogueira, A. R. A., Souza, G. B., & Batista, L. A. R. (2004). Effect of drying method and length of storage on tannin and total phenol concentrations in Pigeon pea seeds. *Food Chemistry*, *86*(1), 17–23. https://doi.org/10.1016/J.FOODCHEM.2003.08.024

Fraga-Corral, M., García-Oliveira, P., Pereira, A. G., Lourenço-Lopes, C., Jimenez-Lopez, C., Prieto, M. A., & Simal-Gandara, J. (2020b). Technological application of tannin-based extracts. *Molecules 2020, Vol. 25, Page 614*, *25*(3), 614. https://doi.org/10.3390/MOLECULES25030614

Fraga-Corral, M., Otero, P., Cassani, L., Echave, J., Garcia-Oliveira, P., Carpena, M., Chamorro, F., Lourenço-Lopes, C., Prieto, M. A., & Simal-Gandara, J. (2021). Traditional applications of tannin rich extracts supported by scientific data: Chemical composition, bioavailability and bioaccessibility. *Foods 2021, Vol. 10, Page 251*, *10*(2), 251. https://doi.org/10.3390/FOODS10020251

Fraga-Corral, M., Otero, P., Echave, J., Garcia-Oliveira, P., Carpena, M., Jarboui, A., Nuñez-Estevez, B., Simal-Gandara, J., & Prieto, M. A. (2021). By-products of agri-food industry as tannin-rich sources: A review of tannins' biological activities and their potential for valorization. *Foods 2021, Vol. 10, Page 137*, *10*(1), 137. https://doi.org/10.3390/FOODS10010137

Galletti, G. C., & Reeves, J. B. (1992). Pyrolysis/gas chromatography/ion-trap detection of polyphenols (vegetable tannins): Preliminary results. *Organic Mass Spectrometry*, *27*(3), 226–230. https://doi.org/10.1002/OMS.1210270313

Girard, M., & Bee, G. (2020). Invited review: Tannins as a potential alternative to antibiotics to prevent coliform diarrhea in weaned pigs. *Animal*, *14*(1), 95–107. https://doi.org/10.1017/S1751731119002143

Girard, M., Lehtimäki, A., Bee, G., Dohme-Meier, F., Karonen, M., & Salminen, J. P. (2020). Changes in Feed Proanthocyanidin Profiles during Silage Production and Digestion by Lamb. *Molecules 2020, Vol. 25, Page 5887*, *25*(24), 5887. https://doi.org/10.3390/MOLECULES25245887

Gupta, S., & Abu-Ghannam, N. (2011). Bioactive potential and possible health effects of edible brown seaweeds. *Trends in Food Science & Technology*, *22*(6), 315–326. https://doi.org/10.1016/J.TIFS.2011.03.011

Hernes, P. J., & Hedges, J. I. (2004). *Tannin signatures of barks, needles, leaves, cones, and wood at the molecular level*. https://doi.org/10.1016/j.gca.2003.09.015

Hesekamp, D., Pahl, M. H., Hesekamp, Dipl.-I. D., & Pahl, M. H. (1996). Curing effects on viscosity of reactive epoxy resin adhesives. *Rheologica Acta 1996 35:4*, *35*(4), 321–328. https://doi.org/10.1007/BF00403532

Hoong, Y. B., Paridah, M. T., Luqman, C. A., Koh, M. P., & Loh, Y. F. (2009). Fortification of sulfited tannin from the bark of Acacia mangium with phenol–formaldehyde for use as plywood adhesive. *Industrial Crops and Products*, *30*(3), 416–421. https://doi.org/10.1016/J.INDCROP.2009.07.012

IEA. (2021). *Key World Energy Statistics 2021*. https://www.iea.org/reports/key-world-energy-statistics-2021/final-consumption. 04/04/2022

Ismayati, M., Nakagawa-izumi, A., & Ohi, H. (2017a). Structural elucidation of condensed tannin from the bark waste of Acacia crassicarpa plantation wood in Indonesia. *Journal of Wood Science*, *63*(4), 350–359. https://doi.org/10.1007/S10086-017-1633-4

Jansone, Z., Muizniece, I., & Blumberga, D. (2017). Analysis of wood bark use opportunities. *Energy Procedia*, *128*, 268–274. https://doi.org/10.1016/J.EGYPRO.2017.09.070

Jaramillo, A. F., Martinez, J. C., Flores, P., Medina, C., Rojas, D., Díaz-Gómez, A., Fuentealba, C., & Meléndrez, M. F. (2022). Condensed tannin resins extracted from Pinus radiata bark as a support matrix in carbon nanofiber-reinforced polymers. *Polymer Bulletin*, *79*(2), 743–762. https://doi.org/10.1007/S00289-020-03530-8

Kaal, J. S., Maximilian P.W., & Schmidt, M. W. I. (2012). Rapid molecular screening of black carbon (biochar) thermosequences obtained from chestnut wood and rice straw: A pyrolysis-GC/MS study. *Journal Article Accepted Version Originally*. https://doi.org/10.1016/j.biombioe.2012.05.021

Kaczmarek, B. (2020). Tannic acid with antiviral and antibacterial activity as a promising component of biomaterials—A minireview. *Materials*, *13*(14). https://doi.org/10.3390/MA13143224

Kemppainen, K., Siika-Aho, M., Pattathil, S., Giovando, S., & Kruus, K. (2014). Spruce bark as an industrial source of condensed tannins and non-cellulosic sugars. *Industrial Crops and Products*, *52*, 158–168. https://doi.org/10.1016/j.indcrop.2013.10.009

Khanbabaee, K., & van Ree, T. (2001). Tannins: Classification and Definition. *Natural Product Reports*, *18*(6), 641–649. https://doi.org/10.1039/B101061L

Krzyzowska, M., Tomaszewska, E., Ranoszek-Soliwoda, K., Bien, K., Orlowski, P., Celichowski, G., & Grobelny, J. (2017). Tannic acid modification of metal nanoparticles: possibility for new antiviral applications. *Nanostructures for Oral Medicine*, 335–363. https://doi.org/10.1016/B978-0-323-47720-8.00013-4

Kuruppu, K. A. D. U. M., & Karunanayake, L. (2019). Synthesis and characterization of tannin based porous cation exchange resins from cassia auriculata (Ranawara). *Vidyodaya Journal of Science*, *22*(2), 17–31. https://doi.org/10.31357/VJS.V22I2.4386

Liao, J., Brosse, N., Pizzi, A., & Hoppe, S. (2019). Dynamically cross-linked tannin as a reinforcement of polypropylene and UV protection properties. *Polymers*, *11*(1). https://doi.org/10.3390/POLYM11010102

Lisperguer, J., Saravia, Y., & Vergara, E. (2016). Structure and thermal behavior of tannins from acacia dealbata bark and their reactivity toward formaldehyde. *Journal of the Chilean Chemical Society*, *61*(4), 3188–3190. https://doi.org/10.4067/S0717-97072016000400007

Liu, L.-Y., Patankar, S. C., Chandra, R. P., Sathitsuksanoh, N., Saddler, J. N., & Renneckar, S. (2020). Valorization of bark using ethanol–water organosolv treatment: isolation and characterization of crude lignin. *ACS Sustainable Chemistry & Engineering*, *8*(12), 4745–4754. https://doi.org/10.1021/ACSSUSCHEMENG.9B06692

Liu, R., Smeds, A., Wang, L., Pranovich, A., Hemming, J., Willför, S., Zhang, H., & Xu, C. (2021). Fractionation of lignin with decreased heterogeneity: based on a detailed characteristics study of sequentially extracted softwood kraft lignin. *ACS Sustainable Chemistry and Engineering*, *9*(41), 13862–13873. https://doi.org/10.1021/ACSSUSCHEMENG.1C04725

Makino, R., Ohara, S., & Hashida, K. (2011a). Radical scavenging characteristics of condensed tannins from barks of various tree species compared with quebracho wood tannin. *Holzforschung*, *65*(5), 651–657. https://doi.org/10.1515/HF.2011.086/MACHINEREADABLECITATION/RIS

Makino, R., Ohara, S., & Hashida, K. (2011b). Radical scavenging characteristics of condensed tannins from barks of various tree species compared with quebracho wood tannin. *Holzforschung*, *65*(5), 651–657. https://doi.org/10.1515/HF.2011.086/MACHINEREADABLECITATION/RIS

Malinda, K., Sutanto, H., & Darmawan, A. (2017). Characterization and antioxidant activity of gallic acid derivative. *AIP Conference Proceedings*, *1904*(1), 020030. https://doi.org/10.1063/1.5011887

Mannelli, F., Daghio, M., Alves, S. P., Bessa, R. J. B., Minieri, S., Giovannetti, L., Conte, G., Mele, M., Messini, A., Rapaccini, S., Viti, C., & Buccioni, A. (2019). Effects of chestnut tannin extract, vescalagin and gallic acid on the dimethyl acetals profile and microbial community composition in rumen liquor: An in vitro study. *Microorganisms*, *7*(7). https://doi.org/10.3390/MICROORGANISMS7070202

Furlan, C.M.; Motta, L.B.; Santos, D.Y.A.C. (2010). Tannins: What do they represent in plant life? In tannins: types, foods containing, and nutrition; Chapter, 10; Petridis, G.K., Ed.; Nova Science Publishers, Inc.: Harpak, NY, USA, 2010; ISBN 978-1-61761-127-8

Martins, P., Barbehenn, R. v, & Constabel, C. P. (2011). *Tannins in plant-herbivore interactions*. https://doi.org/10.1016/j.phytochem.2011.01.040

Mazri, S., Benotmane, B., Hachemi, M., Pranovich, A., Willför, S., & Smeds, A. (2021). Chemical characterization of sapwood and heartwood of Fraxinus angustifolia growing in Algeria. *Journal of Wood Chemistry and Technology*, *42*(1), 26–36. https://doi.org/10.1080/02773813.2021.2004165

McInnes, A. G., Ragan, M. A., Smith, D. G., & Walter, J. A. (1984). High-molecular-weight phloroglucinol-based tannins from bown algae: structural variants. *Eleventh International Seaweed Symposium*, 597–602. https://doi.org/10.1007/978-94-009-6560-7_124

Mittal, K. L. (2021). *Progress in Adhesion and Adhesives. Volume 6* (Vol. 6). Wiley.

Mole, S. (1993). The systematic distribution of tannins in the leaves of angiosperms: A tool for ecological studies. *Biochemical Systematics and Ecology*, *21*(8), 833–846. https://doi.org/10.1016/0305-1978(93)90096-A

Molino, S., Casanova, N. A., Rufián Henares, J. Á., & Fernandez Miyakawa, M. E. (2020). Natural tannin wood extracts as a potential food ingredient in the food industry. *Journal of Agricultural and Food Chemistry*, *68*(10), 2836–2848.

https://doi.org/10.1021/ACS.JAFC.9B00590/ASSET/IMAGES/MEDIUM/JF-2019-005909_0003.GIF

Mueller-Harvey, I. (2001). Analysis of hydrolysable tannins. *Animal Feed Science and Technology*, *91*(1–2), 3–20. https://doi.org/10.1016/S0377-8401(01)00227-9

Nagesh, P. K. B., Chowdhury, P., Hatami, E., Jain, S., Dan, N., Kashyap, V. K., Chauhan, S. C., Jaggi, M., & Yallapu, M. M. (2020). Tannic acid inhibits lipid metabolism and induce ROS in prostate cancer cells. *Scientific Reports 2020 10:1*, *10*(1), 1–15. https://doi.org/10.1038/s41598-020-57932-9

Niemetz, R., & Gross, G. G. (2005). Enzymology of gallotannin and ellagitannin biosynthesis. *Phytochemistry*, *66*(17), 2001–2011. https://doi.org/10.1016/J.PHYTOCHEM.2005.01.009

Normand, M. le, Edlund, U., Holmbom, B., & Ek, M. (2012). Hot-water extraction and characterization of spruce bark non-cellulosic polysaccharides. *Nordic Pulp and Paper Research Journal*, *27*(1), 18–23. https://doi.org/10.3183/NPPRJ-2012-27-01-P018-023/HTML

Ohara, S., Yasuta, Y., & Ohi, H. (2003). Structure elucidation of condensed tannins from barks by pyrolysis/gas chromatography. *Holzforschung*, *57*(2), 145–149. https://doi.org/10.1515/HF.2003.023

Okuda, T., & Ito, H. (2011). Tannins of constant structure in medicinal and food plants—hydrolyzable tannins and polyphenols related to tannins. *Molecules 2011, Vol. 16, Pages 2191-2217*, *16*(3), 2191–2217. https://doi.org/10.3390/MOLECULES16032191

Okuda, T., Yoshida, T., & Hatano, T. (1990). Oligomeric hydrolyzable tannins, a new class of plant polyphenols. *Heterocycles*, *30*(2), 1195–1218. https://doi.org/10.3987/REV-89-SR5

ÖRSA, F., & HOLMBOM, B. (1994). A convenient method for the determination of wood extractives in papermaking process waters and effluents. *Journal of Pulp and Paper Science*, *20*(12).

Pagani, M., Liu, Z., Lariviere, J., & Ravelo, A. C. (2009). High earth-system climate sensitivity determined from pliocene carbon dioxide concentrations. *Nature Geoscience 2010 3:1*, *3*(1), 27–30. https://doi.org/10.1038/ngeo724

Peña, C., Martin, M. D., Tejado, A., Labidi, J., Echeverria, J. M., & Mondragon, I. (2006). Curing of phenolic resins modified with chestnut tannin extract. *Journal of Applied Polymer Science*, *101*(3), 2034–2039. https://doi.org/10.1002/APP.23769

Petchidurai, G., Nagoth, J. A., John, M. S., Sahayaraj, K., Murugesan, N., & Pucciarelli, S. (2019). Standardization and quantification of total tannins, condensed tannin and soluble phlorotannins extracted from thirty-two drifted coastal macroalgae using high performance liquid chromatography. *Bioresource Technology Reports*, *7*, 100273. https://doi.org/10.1016/J.BITEB.2019.100273

Ping, L., Brosse, N., Chrusciel, L., Navarrete, P., & Pizzi, A. (2011). Extraction of condensed tannins from grape pomace for use as wood adhesives. *Industrial Crops and Products*, *33*(1), 253–257. https://doi.org/10.1016/J.INDCROP.2010.10.007

Pizzi, A. (1994a). Advanced wood adhesives technology. *Advanced Wood Adhesives Technology*, 156–165. https://doi.org/10.1201/9781482293548

Pizzi, A. (1994b). Advanced wood adhesives technology. *Advanced Wood Adhesives Technology*, 149–162. https://doi.org/10.1201/9781482293548

Pizzi, A. (2012). Recent developments in eco-efficient bio-based adhesives for wood bonding: opportunities and issues. *20*(8), 829–846. https://doi.org/10.1163/156856106777638635

Pizzi, A. (2017). Phenolic resin adhesives. In *Handbook of Adhesive Technology, Third Edition*. CRC Press. https://doi.org/10.1201/9781315120942

Pizzi, A., & Scharfetter, H. O. (1978). The chemistry and development of tannin-based adhesives for exterior plywood. *Journal of Applied Polymer Science*, *22*(6), 1745–1761. https://doi.org/10.1002/APP.1978.070220623

Rahman, A.-, Choudhary, M. Iqbal., & Perry, George. (2014). *Recent Advances in Medicinal Chemistry. Volume 1* (Vol. 1).

Sameni, J., Krigstin, S., Rosa, D. dos S., Leao, A., & Sain, M. (2014b). Thermal characteristics of lignin residue from industrial processes. *BioResources*, *9*(1), 725–737. https://doi.org/10.15376/BIORES.9.1.725-737

Sarika, P. R., Nancarrow, P., Khansaheb, A., & Ibrahim, T. (2020). Bio-based alternatives to phenol and formaldehyde for the production of resins. *Polymers 2020, Vol. 12, Page 2237*, *12*(10), 2237. https://doi.org/10.3390/POLYM12102237

Shahat, A. A., & Marzouk, M. S. (2013). Tannins and related compounds from medicinal plants of africa. *Medicinal Plant Research in Africa: Pharmacology and Chemistry*, 479–555. https://doi.org/10.1016/B978-0-12-405927-6.00013-8

Shahidi, F., & Ho, C.-T. (2005). Phenolics in food and natural health products: An Overview. https://pubs.acs.org/sharingguidelines

Smeriglio, A., Barreca, D., Bellocco, E., & Trombetta, D. (2017). Proanthocyanidins and hydrolysable tannins: occurrence, dietary intake and pharmacological effects. *British Journal of Pharmacology*, *174*(11), 1244–1262. https://doi.org/10.1111/BPH.13630

Soldado, D., Bessa, R. J. B., & Jerónimo, E. (2021). Condensed tannins as antioxidants in ruminants-effectiveness and action mechanisms to improve animal antioxidant status and oxidative stability of products. *11*, 3243. https://doi.org/10.3390/ani11113243

Speirs, J., McGlade, C., & Slade, R. (2015). Uncertainty in the availability of natural resources: Fossil fuels, critical metals and biomass. *Energy Policy*, *87*, 654–664. https://doi.org/10.1016/J.ENPOL.2015.02.031

Sundberg, A., Sundberg, K., Lillandt, C., & Holmbom, B. (1996). Determination of hemicelluloses and pectins in wood and pulp fibres by acid methanolysis and gas chromatography. *Nordic Pulp and Paper Research Journal*, *11*(4), 216–219. https://doi.org/10.3183/NPPRJ-1996-11-04-P216-219/MACHINEREADABLECITATION/RIS

TAPPI T 211 om-02. (2002). *Ash in wood, pulp, paper and paperboard combustion at 525 ℃*.https://www.tappi.org/content/sarg/t211.pdf.

Timell, T. E. (1975). *Proceedings of the Eighth Cellulose Conference. I. Teil - Wood Chemicals - A future Challenge. Applied Polymer Symposia 28,345-347.* https://opac.ncl.res.in/cgi-bin/koha/opac-detail.pl?biblionumber=12125&query_desc=au%3A%22Timell%2CT.E._Ed%22

Tondi, G., & Petutschnigg, A. (2015). Middle infrared (ATR FT-MIR) characterization of industrial tannin extracts. *Industrial Crops and Products*, *65*, 422–428. https://doi.org/10.1016/J.INDCROP.2014.11.005

Varila, T., Brännström, H., Kilpeläinen, P., Hellström, J., Romar, H., Nurmi, J., & Lassi, U. (2020). From Norway Spruce Bark to Carbon Foams : Characterization, and Applications. *BioResources*, *15*(2), 3651–3666. https://doi.org/10.15376/BIORES.15.2.3651-3666

Venter, P. B., Senekal, N. D., Amra-Jordaan, M., Bonnet, S. L., & van der Westhuizen, J. H. (2012). Analysis of commercial proanthocyanidins. Part 2: An electrospray mass spectrometry investigation into the chemical composition of sulfited quebracho (Schinopsis lorentzii and Schinopsis balansae) heartwood extract. *Phytochemistry*, *78*, 156–169. https://doi.org/10.1016/J.PHYTOCHEM.2012.01.027

Venter, P. B., Sisa, M., van der Merwe, M. J., Bonnet, S. L., & van der Westhuizen, J. H. (2012). Analysis of commercial proanthocyanidins. Part 1: The chemical composition of quebracho (Schinopsis lorentzii and Schinopsis balansae) heartwood extract. *Phytochemistry*, *73*, 95–105. https://doi.org/10.1016/J.PHYTOCHEM.2011.10.006

Wang, L., Lagerquist, L., Zhang, Y., Koppolu, R., Tirri, T., Sulaeva, I., Schoultz, S. von, Vähäsalo, L., Pranovich, A., Rosenau, T., Eklund, P. C., Willför, S., Xu, C., & Wang, X. (2020). Tailored thermosetting wood adhesive based on well-defined hardwood lignin fractions. *ACS Sustainable Chemistry and Engineering*, *8*(35), 13517–13526. https://doi.org/10.1021/ACSSUSCHEMENG.0C05408/ASSET/IMAGES/LARGE/SC0C05408_0004.JPEG

Willför, S., Pranovich, A., Tamminen, T., Puls, J., Laine, C., Suurnäkki, A., Saake, B., Uotila, K., Simolin, H., Hemming, J., & Holmbom, B. (2009). Carbohydrate analysis of plant materials with uronic acid-containing polysaccharides–A comparison between different hydrolysis and subsequent chromatographic analytical techniques. *Industrial Crops and Products*, *29*(2–3), 571–580. https://doi.org/10.1016/J.INDCROP.2008.11.003

WYATT. (2022). *SEC-MALS for Absolute Molar Mass and Size Measurements*. https://www.wyatt.com/solutions/techniques/sec-mals-molar-mass-size-multi-angle-light-scattering.html?gclid=Cj0KCQjw2_OWBhDqARIsAAUNTTGzdS1J2g2nESwyrFLFsUHbfsHELNvPQZeYJOlSU6rMCt2AIe_mEf8aAgaeEALw_wcB. 24/07/2022

Xindi Zhang, Hongyue Wang, Qianyun Jia, Jiaqing Cao, & Xiangrong Zhang. (2021). Extraction and application of tannin in the medical, food and chemical industries. *Journal of Polyphenols*, 62–75. http://jpolyph.syphu.edu.cn/EN/Y2021/V3/I1/62

Xu, W., Pranovich, A., Uppstu, P., Wang, X., Kronlund, D., Hemming, J., Öblom, H., Moritz, N., Preis, M., Sandler, N., Willför, S., & Xu, C. (2018). Novel biorenewable composite of wood polysaccharide and polylactic acid for three dimensional printing. *Carbohydrate Polymers*, *187*, 51–58. https://doi.org/10.1016/J.CARBPOL.2018.01.069

Xu, Y., Guo, L., Zhang, H., Zhai, H., & Ren, H. (2019). Research status, industrial application demand and prospects of phenolic resin. *RSC Advances*, *9*(50), 28924–28935. https://doi.org/10.1039/C9RA06487G

Yamada, H., Hirokane, T., Ikeuchi, K., & Wakamori, S. (2017). *Fundamental Methods in Ellagitannin Synthesis*. https://doi.org/10.1177/1934578X1701200846.

Yamada, H., Wakamori, S., Hirokane, T., Ikeuchi, K., & Matsumoto, S. (2018). Structural Revisions in Natural Ellagitannins. *Molecules 2018, Vol. 23, Page 1901*, *23*(8), 1901. https://doi.org/10.3390/MOLECULES23081901

Yuan, T. Q., Sun, S. N., Xu, F., & Sun, R. C. (2011). Characterization of lignin structures and lignin-carbohydrate complex (LCC) linkages by quantitative ^{13}C and 2D HSQC NMR spectroscopy. *Journal of Agricultural and Food Chemistry*, *59*(19), 10604–10614. https://doi.org/10.1021/JF2031549/ASSET/IMAGES/JF-2011-031549_M003.GIF

Zhao, Y., Yan, N., & Feng, M. W. (2013). Biobased phenol formaldehyde resins derived from beetle-infested pine barks - Structure and composition. *ACS Sustainable Chemistry and Engineering*, *1*(1), 91–101. https://doi.org/10.1021/SC3000459/ASSET/IMAGES/LARGE/SC-2012-000459_0008.JPEG

Zhao, Z., & Umemura, K. (2014). Investigation of a new natural particleboard adhesive composed of tannin and sucrose. *Journal of Wood Science*, *60*(4), 269–277. https://doi.org/10.1007/S10086-014-1405-3/FIGURES/13

Zhou, X., & Du, G. (2019). Applications of tannin resin adhesives in the wood industry. *Tannins - structural properties, biological properties and current knowledge*. https://doi.org/10.5772/INTECHOPEN.86424

Appendix

Appendix I: DSC spectra of crude tannins

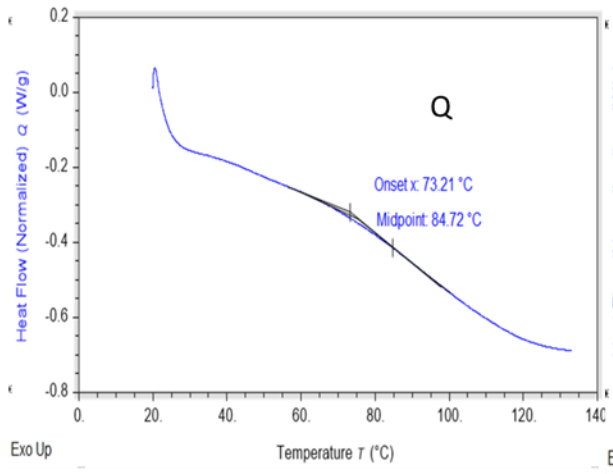

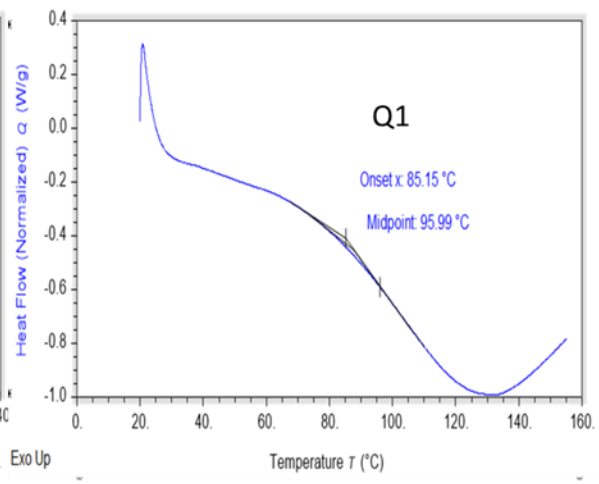

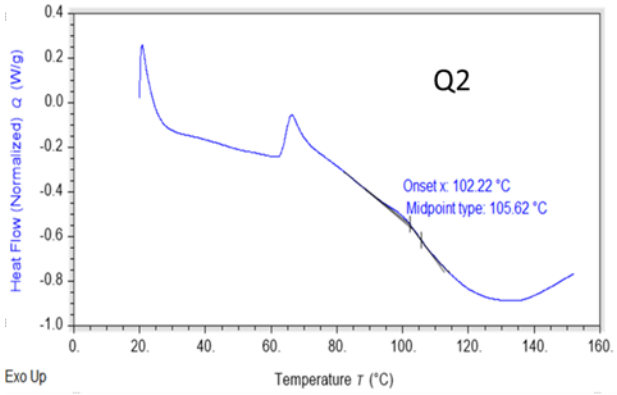

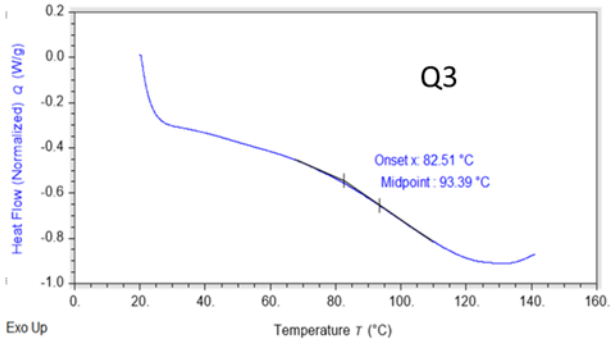

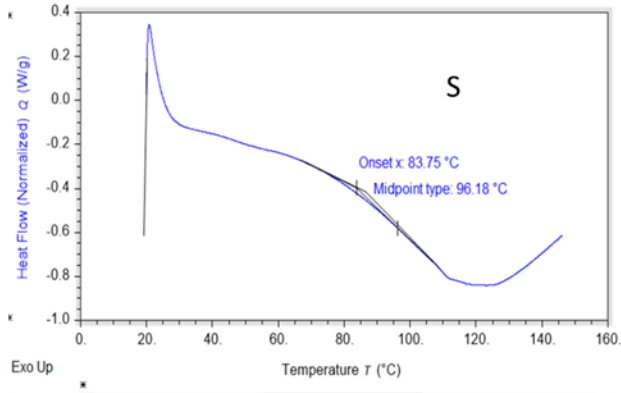

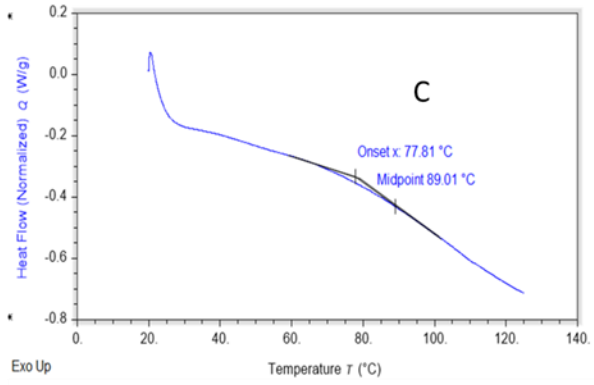

Appendix II: Result of short-column GC.

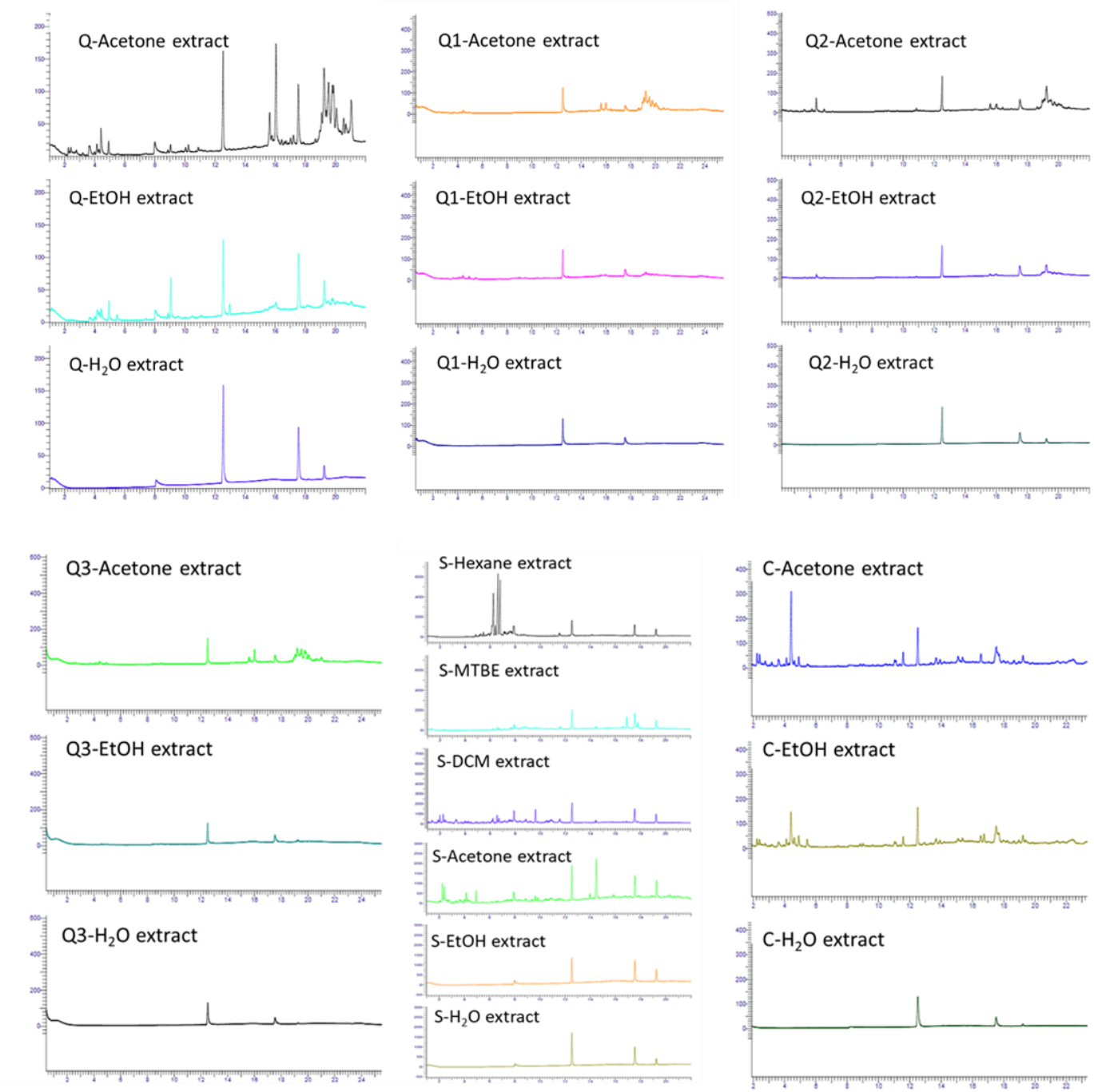

Appendix III: GC-MS result of acetone extract after alkaline hydrolysis

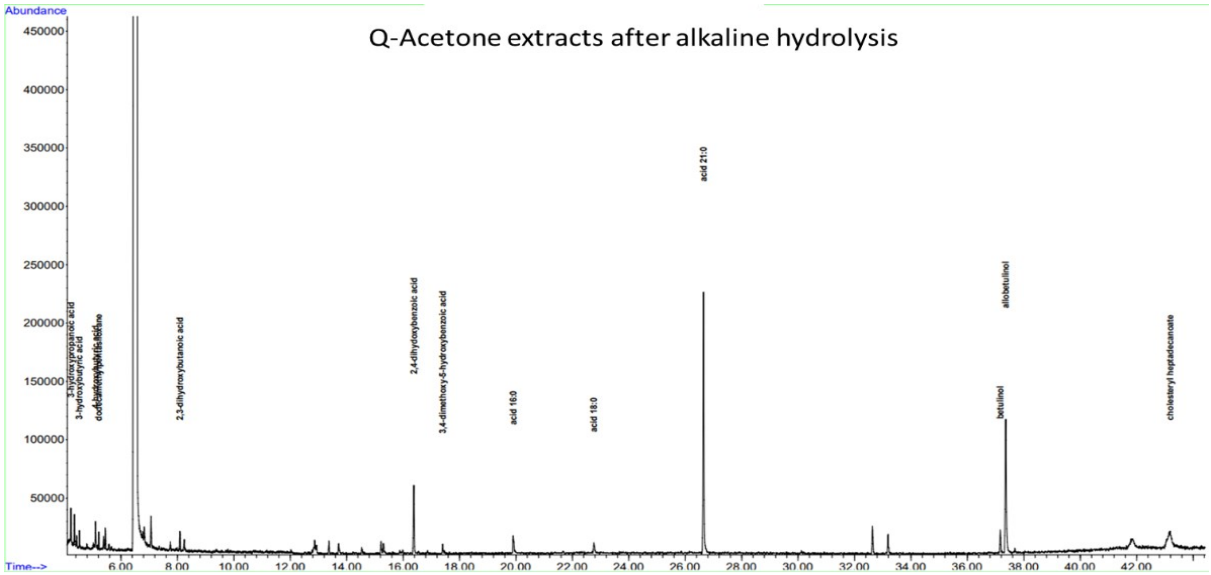

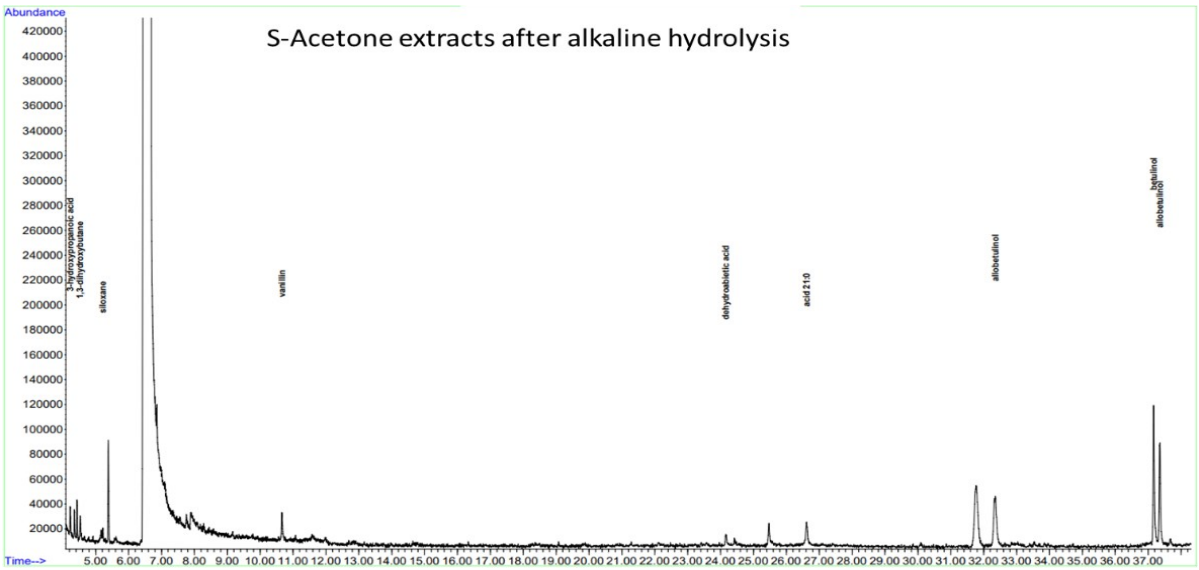

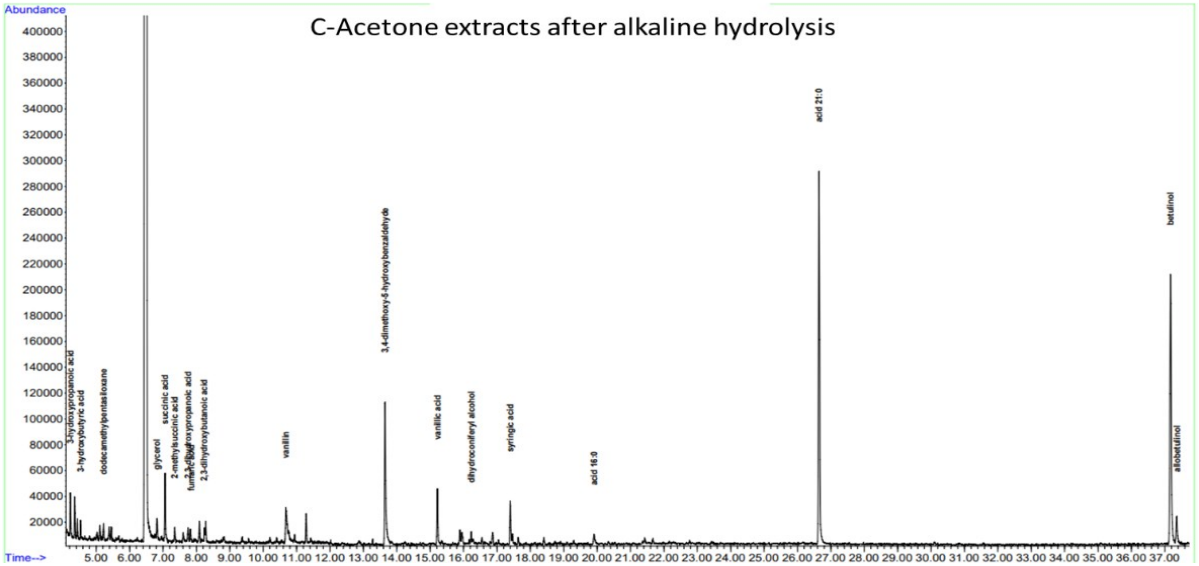

Appendix IV: List of identified volatile compounds from long column GC

Table IV- 1: *Components analyzed by long column GC in acetone and EtOH extract of* Q tannin.

Compounds	Classified	Acetone extract [mg/g]	EtOH extract [mg/g]
1-syringylglycerol	Alcohols	0.10	-
3,4,5-trihydroxybenzoic acid	Acids	8.87	1.35
3,4dihydroxybenzaldehyde	Aldehydes	0.05	-
3,4dihydroxybenzoic	Acids	0.41	0.06
3,5,4´-trithydroxy-3´-methoxy-dihydrosti	Others	-	0.01
8,15-isopimaradien-18-oic acid	Acids	-	0.01
abietatetraenoic acid	Acids	0.08	0.11
acid 18:0	Acids	0.06	-
acid 18:1	Acids	0.12	0.02
acid 18:2	Acids	0.15	0.05
arabinose-1,5-lactone	Sugars	0.03	-
astringin (glucoside)	Sugars	0.18	0.08
catechin	Others	1.21	-
deoxyhexose	Sugars	0.77	0.03
disaccharide	Sugars	1.20	0.72
fructopyranose	Sugars	4.74	0.94
glycerol	Alcohols	0.17	-
hexose	Sugars	5.78	3.01
HMR	Others	0.72	0.17
inositol	Alcohols	0.13	0.57
levopimaric acid	Acids	0.04	-
pentitol	Alcohols	0.20	0.08
pentose	Sugars	12.42	3.39
pinoresinol	Others	0.13	0.04
pyrogallol	Others	0.09	0.01
resorcinol	Others	0.16	0.04
rhamnopyranose	Sugars	1.63	0.04
threose	Sugars	0.12	-
trehalose	Sugars	1.30	2.63
xylulose	Sugars	0.17	0.02
Total		***41.03***	***13.38***

Table IV- 2: *Components analyzed by long column GC in acetone and EtOH extract of* Q1 tannin.

Compounds	Classified	Acetone extract [mg/g]	EtOH extract [mg/g]
acid 18:0	Acids	0.11	-
acid 18:1	Acids	0.19	-
acid 18:2	Acids	0.09	-
acid 18:3	Acids	0.04	-
catechol	Others	0.15	-
cis-abienol	Others	0.02	-
fructofuranose	Sugars	1.56	0.54
gallic acids	Acids	6.83	0.97
glycerol	Alcohols	0.62	-
glyoxalic hydrate	Aldehydes	0.28	-
hexitol	Alcohols	-	0.18
hexopyranose	Sugars	-	0.49
hexose	Sugars	3.71	2.44
inositol	Alcohols	-	0.06
myo-insitol	Alcohols	-	0.43
pentitol	Sugars	0.39	0.10
pentonic acid,1,5-lactone	Acids	0.16	-
pentose	Sugars	2.89	0.83
pyrogallol	Others	1.09	-
resorcinol	Others	0.99	-
rhamnopyranose	Sugars	0.01	0.22
rhamnose	Sugars	1.15	-
rhamnopyranose	Sugars	0.31	-
x-hydrohy-dehydroabietic acid	Acids	0.03	-
Total		***20.62***	***6.26***

Table IV- 3: *Components analyzed by long column GC in acetone and EtOH extract of* Q2 tannin.

Compounds	Classified	Acetone extract [mg/g]	EtOH extract [mg/g]
3,4-dihydroxybenzonic acids	Acids	0.04	-
3,4dihydroxybenzoic	Acids	-	0.20
arabinonic acid, gama.-lactone	Acids	-	0.05
catechol	Others	0.01	-
erythritol	Sugars	0.03	-
fructpyranose	Sugars	0.05	0.73
gallic acids	Acids	0.64	4.46
hexitol	Sugars	-	0.25
hexose	Sugars	0.32	2.60
inositol	Alcohols	-	0.09
myo-inositol	Alcohols	0.03	0.47
pentitol	Sugars	-	0.25
pentono-1-4-lactone	Others	0.01	-
pentose	Sugars	0.27	1.81
pyrogallol	Others	0.33	0.35
resorcinol	Others	0.13	-
rhamnopyranose	Sugars	0.06	0.20
Total		***1.92***	***11.46***

Table IV- 4: *Components analyzed by long column GC in acetone and EtOH extract of* Q3 tannins.

Compounds	Classified	Acetone extract [mg/g]	EtOH extract [mg/g]
2,3-dihydroxypropanoic acid	Acids	-	0.79
acid 18:0	Acids	0.19	-
acid 18:1	Acids	0.12	-
acid 18:3	Acids	0.17	-
cis-abienol	Alcohols	0.05	-
fructpyranose	Sugars	1.30	-
gallic acids	Acids	8.73	0.51
glycerol	Alcohols	1.39	0.13
hexose	Sugars	8.88	0.33
inositol	Alcohols	0.06	-
myo-inositol	Alcohols	-	0.12
pentitol	Sugars	-	0.03
pentose	Sugars	8.48	0.05
quinic acid	Acids	-	0.19
resorcinol	Others	1.55	0.17
rhamnopyanose	Sugars	2.08	-
Total		***33.00***	***2.32***

Table IV- 5: *Components analyzed by long column GC in hexane, MTBE, DCM, and acetone extract of* S tannin.

Compounds	Classified	Hexane extract [mg/g]	MTBE extract [mg/g]	DCM extract [mg/g]	Acetone extract [mg/g]
1,2-diguaiacyll-1ethanone	Others	-	-	0.02	0.22
1,3-(bis-guaicayl)-1-2, propandiol	Alcohols	-	-	0.06	-
1-guaiacylglycerol	Alcohols	-	-	0.04	-
1-monolinoleylglycerol	Alcohols	-	-	0.03	-
16-hydroxy-dehydroabietic acid	Acids	1.16	0.05	0.03	-
3,4-dihydroxybezaidehyde	Aldehydes	-	0.01	0.16	0.29
3,5,3´,4´-tetrahydroxystilbene	Others	-	-	0.03	1.23
3,5,4¨-trimethoxystilbene	Others	0.16	0.03	-	-
3,5,4´-trithydroxy-3´-methoxy-dihydrosti	Others	-	-	0.09	0.55
3-acetoxy labda-8((17), 13[16], 14-trieno	Others	0.32	-	-	-
3-hydroxybenzoic acid	Acids	-	-	0.04	0.11

3-hydroxy labda-8((17), 13[16], 14-trieno	Others	-	0.01	-	-
3-methoxy-4-hydroxycinamaldehyde	Aldehydes	-	-	0.02	0.06
4,4´-dihydroxy-3,3´-dimethoxystilbebe	Others	-	-	0.06	-
4-hydroxybenzaldehyde	Aldehydes	-	-	0.02	-
7-hydroxy—dehydroabietic acid	Acids	0.92	0.06	-	-
7-oxodehydroabietic acid	Acids	-	0.03	0.06	0.18
8,15-isopimaradien-18-oic acid	Acids	-	-	-	0.30
Hexose	Sugars	-	0.05	0.24	4.52
abietatetraenoic acid	Acids	1.24	0.01	0.08	0.92
abietic acid	Acids	12.74	0.04	0.08	0.22
acid 14:0	Acids	0.04	-	-	-
acid 16:0	Acids	0.72	-	0.06	-
acid 16:1	Acids	0.11	-	-	-
acid 17:0	Acids	0.43	-	0.02	0.10
acid 18:0	Acids	0.54	-	0.01	0.14
acid 18:1	Acids	1.51	0.02	0.08	0.04
acid 18:2	Acids	1.34	-	0.06	0.01
acid 18:3	Acids	0.34	-	0.02	-
acid 20:3	Acids	0.09	-	-	-
acid 24:0	Acids	0.31	-	-	-
acis 12:0	Acids	-	-	-	-
astringin	Sugars	-	0.11	-	-
acid 18:2	Acids	1.34	-	0.06	0.01
acid 18:3	Acids	0.34	-	0.02	-
acid 20:3	Acids	0.09	-	-	-
acid 24:0	Acids	0.31	-	-	-
campesterol	Alcohols	0.18	-	0.01	0.19
cis-abienol	Alcohols	0.69	-	0.02	0.04
dehydroabietic acid	Acids	18.74	0.18	0.27	0.57
dehydroabietol	Alcohols	-	-	0.02	-
delta-13-(trans)-neoabienol	Others	0.49	-	0.02	0.03
deoxyhexose	Sugars	-	-	-	1.34
ethyl d-glucopyranoside	Sugars	-	0.01	-	-
ethyl hexopyranoside	Sugars	-	-	0.06	0.72
gallic acids	Acids	-	-	-	0.39
glucopyranose,3,6-di-o-methyl	Sugars	-	-	0.03	0.09
glycerol	Alcohols	-	-	0.04	0.25
guaiacylglyoxylic acid	Acids	-	-	0.03	0.11
heptadecanoic acid	Acids	0.30	-	0.01	0.05
hexitol	Sugars	-	-	-	0.11
hexonic acid	Acids	-	-	0.05	0.49

hexopyranose	Sugars	-	-	-	4.34
HMR	Others	-	-	0.11	0.91
iso-abienol	Others	0.17	-	-	-
isopimaric acid	Acids	10.76	0.08	0.15	-
isopimarol	Alcohols	-	-	0.03	0.07
lariciresinol	Alcohols	-	-	0.06	0.47
levoglucosan	Sugars	-	-	-	-
levopimaric acid	Acids	0.04	-	-	-
manool	Alcohols	0.32	-	0.01	0.05
methyldehydroabietate	Others	0.31	-	-	-
neoabietic acid	Acids	0.37	-	-	-
p-hydroxyphenyl glycerol	Alchols	-	-	0.01	0.61
palustric acid	Acids	0.65	0.01	-	-
pentonic acid	Acids	-	-	-	0.05
pentose	Sugars	-	0.17	0.77	13.88
pimaric acid	Acids	1.22	0.01	0.02	-
pinoresinol	Alcohols	-	-	0.23	0.91
pintol	Alcohols	-	-	0.01	0.65
rhamnopyranose	Sugars	-	-	0.04	0.62
rhamnose	Sugars	-	-	0.05	-
sandaracopimaric acid	Acids	2.70	0.03	0.06	0.13
secoisolariciresinol	Alcohols	-	-	0.05	0.39
sitosterol	Alcohols	0.89	-	-	-
succinic acid	Acids	-	-	-	0.33
vanillin	Aldehydes	-	-	0.20	0.11
x-hydrohy-dehydroabietic acid	Acids	0.08	0.06	0.06	0.47
x-hydroxy-18-norabietatriene	Others	0.23	-	-	-
x-hydroxy-dehydroabietic acid	Acids	-	-	0.05	0.24
Total		***62.19***	***0.97***	***3.86***	***37.51***

Table IV- 6: *Components analyzed by long column GC in acetone and EtOH extract of* C tannin.

Compounds	Classified	Acetone extract[mg/g]	EtOH extract[mg/g]
disaccharide	Sugars	2.10	4.38
ellagic acids	Acids	1.70	3.20
fructofuranose	Sugars	0.51	1.14
fructopyranose	Sugars	1.22	2.48
gallic acids	Acids	12.83	17.47
hexonic acids,1,4-lactone	Acids	0.07	-
hexose	Sugars	3.66	10.06
hexitol	Sugars	0.11	0.39
inositol	Alcohols	0.75	3.45
myo-inositol	Alcohols	0.41	3.33
pentitol	Sugars	0.25	1.30
pentose	Sugars	5.85	9.80
rhamnopyranose	Sugars	0.61	0.54
rhamnose	Sugars	-	1.23
xylulose	Sugars	0.07	-
Total		***30.14***	***58.77***